Final Report

RAC Project #1384

Development and Investigations into Particle Beam-Mass Spectrometry

Ian D. Brindle

Professor of Chemistry

Brock University

St. Catharines, Ontario

L2S 3A1

Telephone 905-688-5550, Ext. 3545
Fax 905-682-9020

Liaison Officer: Dr. V. Taguchi
Laboratory Services Division
Ontario Ministry of Environment and Energy

Summary

A particle beam has been developed which can be interfaced with a sector mass spectrometer. The instrumentation has been used to investigate the determination of polynuclear aromatic hydrocarbons (PAHs). In addition, fast-atom bombardment was investigated for the determination of the important pesticide benomyl and for a study into the formation of (sodium oxalate)$^-$ and (potassium oxalate)$^-$: on pairs. As part of our study on benomyl, we also discovered a technique which allows stable standards of benomyl to be prepared. It has been difficult to determine benomyl heretofor because of its instability in organic solvents and in water around pH7.

In the first report, we described the construction of the ultra-sonic particle beam generator. This report describes, in detail, the results of our investigations described above.

Some work is continuing and will be written up in the MSc thesis of Xiao He. A copy of the thesis will be bound and forwarded to Dr. Taguchi upon completion of the project as an appendix (expected date: May, 1994).

The appendix will contain the results of Ms. He's investigations into the behaviour of azo dyes, chlorinated pesticides, and nitro-PAHs. It appears, from the results we have thus far, that nitro-PAHs undergo significant (~100% in some cases) reduction to amino compounds. The significance of this reduction process on nitro-PAHs and, perhaps, on other reducible compounds may have implications for the interpretation of the mass spectra of these compounds.

Papers arising from this work are listed below:

Raj Pal Singh, Ian D. Brindle, Timothy R.B. Jones, Jack M. Miller, and Mikio Chiba, "Fast-atom Bombardment Mass Spectrometry of Sodium and Potassium Oxalates - Mass Spectrometric Evidence for the Existence of (Sodium Oxalate)$^-$ and (Potassium Oxalate)$^-$ Ion Pairs in Aqueous Solutions," Analyst, Accepted for publication, September 24, 1993.

Raj P. Singh, Ian D. Brindle, Timothy R.B. Jones, Jack M. Miller, and Mikio Chiba, "Determination of Polycyclic Aromatic Hydrocarbons by High Performance Liquid Chromatography - Particle Beam - Mass Spectrometry", Journal of the American Society for Mass Spectrometry, **1993**, 4, 898-905.

Raj P. Singh, Ian D. Brindle, Jack M. Miller, and Mikio Chiba, "Fast Atom Bombardment Mass Spectrometric Investigation of Protonated Methyl [1-(Butylcarbamoyl)-1H-Benzamidazol-2-yl] Carbamate (Benomyl)". Rapid Communications in Mass Spectrometry, **1993**, 7, 167-171.

Raj P. Singh, Chris H. Marvin, Ian D. Brindle, C. David Hall, and Mikio Chiba, " Stability of Methyl [1-(Butylcarbamoyl)-1H-Benzamidazol-2-yl] Carbamate (Benomyl) in Hydrochloric Acid Solutions" J. Agric. & Food Chem., (short communication) **1992**, 40, 1303-1306.

Part I : Determination of Polycyclic Aromatic Hydrocarbons by High Performance Liquid Chromatography - Particle Beam - Mass Spectrometry

Abstract

In this part we report a high performance liquid chromatography-particle beam-mass spectrometric (HPLC-PB-MS) method for the determination of polycyclic aromatic hydrocarbons (PAH's). The particle beam (PB) interface consists of a concentric ultrasonic nebulizer with temperature controlled desolvation chamber and a three-stage momentum separator. The HPLC-PB-MS method showed greater sensitivity for PAH's with molecular weight greater than 178 than PAH's with molecular weights lower 178. The percent relative standard deviations for the determination of 0.5 ng chrysene, 1.0 ng dibenzo[a,h]anthracene, 1.0 ng benzo[g,h,i]perylene and 2.5 ng coronene were 20%, 2.5%, 13.7 % and 6 %, respectively. The detection limits at signal/noise = 3 were 0.2 ng for chrysene, 1.0 ng for dibenzo[a,h]anthracene, 0.5 ng for benzo[g,h,i]perylene and 1.5 ng for coronene.

Polycyclic aromatic hydrocarbons, commonly known as PAH's, are widespread in the environment [1-4]. Since several of these compounds are well known carcinogens, their determination in water, air, sediment, biota and foodstuffs is required to be made routinely. HPLC with UV and fluorescence detection [5-6] and gas chromatography-mass spectrometry (GC-MS) [7-9] are normally used for the determination of low levels of PAH's in various matrices. However, none of these methods is free from problems. The most serious problem of HPLC/UV is that it relies on a single parameter i.e., retention time, for the identification of solutes. On the other hand, GC-MS is reported to give poor sensitivity for late eluting PAH's [10]. Mass spectrometry, which allows the analyst to acquire considerable structural information, may be able to solve the problem of identification of solute, if used as a detector in combination with HPLC.

Because of the potential advantage of HPLC-MS over conventional HPLC/UV and GC-MS methods, outlined above, serious efforts have been made in recent years to interface an HPLC with the mass spectrometer [11-13]. These efforts include direct liquid introduction (DLI) [14], thermospray [15-19], electrospray [20-22], ion evaporation [13], nebulization into an atmospheric pressure chemical ionization source (APCI) [23-27], and particle beam interfaces (PB) [29-31]. The particle beam interface allows separation of the analytes from the HPLC eluent and delivers them to a conventional electron impact (EI) source, thus generating library-searchable EI spectra of the analytes. This makes particle beam mass spectrometry a valuable technique among HPLC-MS methods.

The PB interface was originally developed by Willoughby and Browner [29-30], as a helium nebulized monodisperse aerosol generating analyzer. Normally, in the PB interface, HPLC effluent is pneumatically nebulized into a desolvation chamber. Analyte molecules in the solvent stream nucleate to form sub-micrometer particles in the desolvation chamber. These particles are separated from the solvent vapour

molecules in a two- or three-stage momentum separator and are subsequently transported to the ion source of the mass spectrometer.

At the present time, a number of PB interfaces are commercially available, normally with a concentric pneumatic nebulizer system [29-36]. The sample is nebulized by helium at flow rates of 0.5 to 10 L min^{-1}. These interfaces can transport HPLC effluents of flow rates ranging from 0.1 mL min^{-1} to 1.0 mL min^{-1} to MS ion source. An ultrasonic nebulizer with controlled heating of the desolvation chamber was also developed by Ligon and Dorn [31]. In this particle beam interface, an ultrasonic nebulizer was used to nebulize HPLC effluent delivered externally at an angle to the tip of the ultrasonic horn. The dispersion gas was delivered axially through the ultrasonic nebulizer tip. A three-stage momentum separator was used to remove HPLC solvent and dispersion gas from the central particle beam. This interface was especially designed to connect an HPLC, running at high eluent flow rates (> 1.0 mL min^{-1}) , to a magnetic sector mass spectrometer.

In recent years, several papers have reported the use of PB mass spectrometry for the determination of organic compounds, especially, polar compounds such as caffeine, pesticides and pharmaceutical compounds [29-42]. However, to our knowledge, PB mass spectrometry has not been used for the determination of PAH's. Therefore, the purpose of this part was to develop a HPLC-PB-MS method for the determination of PAH's. The PB interface, used here, was a modified version of the PB interface, originally designed by Ligon and Dorn [31]. The modified interface consisted of a concentric ultrasonic nebulizer with temperature controlled desolvation chamber and a three-stage momentum separator.

Experimental

Chemicals

Acenaphthylene, acenaphthene, fluorene, phenanthrene, chrysene, dibenzo[a,h]anthracene, dibenzo[g,h,i]perylene and coronene were obtained from Aldrich Chemical Company, Inc., P.O. Box 355, Milwaukee, WIS 53201. HPLC grade ammonium acetate was from Fisher Scientific, New Jersey 07410.

Solvents

Acetonitrile and methanol were HPLC grade from Caledon Laboratories, Ltd., Georgetown, Ontario L7G 4R9, Canada. Water was distilled in glass in the laboratory.

High Performance Liquid Chromatograph

The liquid chromatograph used was a Waters 600-MS system controller with a Waters 441 UV/VIS absorbance detector. Separation of PAH's was achieved on Vydac reversed phase C-18, 5 μ, 15 cm X 4.6 mm (i.d.) column and Phenomenex Ultracarb 5 μ ODS (20) 150 x 2 mm and Ultracarb 3 μ ODS (20) 150 x 2 mm columns. The mobile phases used were acetonitrile, methanol, and methanol containing small amount of ammonium acetate. The UV detector was operated at 254 nm with detector sensitivity of 0.05 AUFS. Peaks were integrated on a Hewlett Packard HP 3396 Series II integrator. The total system was operated at ambient temperature.

Particle Beam Interface

A schematic diagram of the PB interface is shown in Figure 1. The design of the ultrasonic head, desolvation chamber, nozzle and three stage momentum

separator up to the second stage, was similar to that reported by Ligon and Dorn [31], except that the effluent from the HPLC was delivered co-axially via a silica capillary (0.075 mm i.d. and 0.34 mm o.d.) and nebulized at the exit end of the ultrasonic head by a fast, concentric flow of helium gas, at 900 mL min^{-1}. The transducer was situated in the body of ultrasonic horn (indicated by 'c' in Fig. 1). The end of silica capillary was positioned about 2 mm behind the tip of ultrasonic head (i. d. at the tip = 1 mm). The transfer tube, which included a third stage of vacuum separator, was based on the Kratos PB interface design. The two diametrically opposed pumping ports of the first stage were connected to a Welch Duo Seal Vacuum Pump with 500 L min^{-1} pumping speed. The ports of the second identical stage were connected to a Edwards High Vacuum pump with 300 L min^{-1} pumping speed. The third, and last, stage was pumped by an Edwards High Vacuum pump with 150 L min^{-1} pumping speed. The heated walls of the source provided thermal energy for instant volatilization of the particles. The ionization of the gaseous phase of volatilized particles is occurred by electron impact (EI).

Mass Spectrometer

A Kratos Concept IS double-focussing mass spectrometer (Kratos Analytical, Urmston, Manchester, UK) (E/B Configuration) employing a EI/CI source, was used for mass spectrometric analyses. The instrument was controlled by a Kratos DS 90 Data General Eclipse-based computer system. A Kratos Mach 3 data system running on a SUN SPARC station was used for further data work-up. For all studies, a nominal resolving power of 1000 was used. The standard EI-CI source, operated at temperatures 220-300 C and 6 kV accelerating potential, was used. The scan rate was 3.0 seconds per decade for full scan acquisition. SIM acquisitions were made under the same instrumental conditions as described

above using a 0.6 to 1.0 sec cycle time for the PAH groups of interests. The PB-MS system was tuned and mass calibrated with perfluorokerosene (PFK).

Results

Particle Beam Interface

Since we were going to use a magnetic sector mass spectrometer, we chose to build a nebulizing system similar to that of Ligon and Dorn [31]. However, the interface described by Ligon and Dorn [31] did not work for us as we experienced problems of signal reproducibility, apparently caused by the mis-alignment between aerosol beam, nozzle and the three-stage momentum separator. While, in theory, the Ligon and Dorn design should give satisfactory results, as constructed by our shops, the nebulizer alignment with the rest of the interface was critical. To confirm this, we constructed a clean plastic desolvation chamber to observe the spray profile of target area. The results of this experiment indicated that much of the aerosol beam was not focussed on the nozzle (as it was targeting different parts of nozzle cone) due, perhaps, to the tendency of the tangential capillary to wander when the ultrasonic horn was under power. To solve this problem, we re-designed the ultrasonic inlet to accommodate a concentric sample delivery capillary. The modified nebulizing system with concentric pneumatic ultrasonic nebulizer (Figure 1) resulted in immediate improvements in the alignment stability and signal reproducibility . Although the exact mechanism by which oscillation of the transducer is coupled to the liquid in the concentric pneumatic ultrasonic nebulizer is not known, the sensitivity of the signals clearly illustrate the function of the ultrasonic horn in the modified nebulizer. With the ultrasonic horn turned off, no signal for 20 ng chrysene was detected; whereas the same quantity gave 400,000 peak area counts with the ultrasonic horn under power. The stability of the

ultrasonic horn and the reproducibly of results suggest that the transducer, which has an energy of about 2 watt, is being cooled primarily by the expanding gas.

Response of PB-MS for Different PAH's

Figure 2 shows the relative responses of different PAH's obtained by PB-MS. The samples were injected directly into methanol streams flowing at 0.3 mL min^{-1} flow rate. It is quite obvious from Figure 2 that the sensitivity of PB-MS method was greater for PAH's with molecular weight > 178 than for PAH's with molecular weight < 178. Since the GC-MS method is reported to give relatively poor sensitivity for late eluting PAH peaks [4], the strong signals of chrysene (228), dibenzo[a,h]anthracene (278), benzo[g,h,i]perylene (276), and coronene (300), shown in Figure 2, prompted us to concentrate our efforts to develop a HPLC-PB-MS method for the determination of relatively high molecular weight PAH's.

The sensitivity of the PB interface was optimized for the solvent of the HPLC mobile phase, eluent flow rate, and source temperature. Optimization of the sensitivity of solute was normally carried out by using chrysene, since, as will be reported later, chrysene showed higher signal sensitivity than other PAH's.

Effect of Solvent of the Mobile Phase on Chrysene Signal

For HPLC separation of PAH's, normally, acetonitrile and methanol solvents were used in the mobile phase. The sensitivity of the chrysene signal was compared, using mobile phase solvents acetonitrile and methanol under direct flow injection (without a column) conditions. The representative mass chromatograms of chrysene in acetonitrile and methanol solvents are shown in Figure 3. Because methanol provided higher sensitivity for chrysene signal compared to acetonitrile, under identical operating conditions, methanol was used as the mobile phase in all the determinations reported in this paper.

Effect of Eluent Flow Rate on Chrysene Signal and Selection of HPLC Column

Since the dispersion gas, helium, was used at a fixed flow rate of 0.9 L min^{-1}, the sensitivity of the chrysene signal was optimized by changing the eluent flow rate. The results of these experiments revealed that the sensitivity of the chrysene signal between flow rates 100 - 300 µL min^{-1} remained apparently constant (peak area counts = 1.2 - 1.5 X 10^6). However, the sensitivity of the chrysene signal decreased substantially at the eluent flow rates higher than 300 µL min^{-1}. The signal counts decreased from 1.3 x 10^6 at a flow rate of 300 µL min^{-1} to 0.3 x 10^6 at a flow rate of 400 µL min^{-1}. Therefore, to increase the sensitivity, minibore columns (2 mm internal diameter (i.d.)) were used for the separation and determination of PAH's because of their favorable flow rates and faster speed (faster elution behavior) compared to conventional (4.6 mm i.d.) HPLC columns. Figure 4 shows the comparison of chromatograms, depicting the separation of chrysene, dibenzo[a,h] anthracene, benzo[g,h,i]perylene, and coronene, on a 2 mm i.d. column (with 0.3 mL min^{-1} flow rate) and 4.6 mm i.d. column (with flow rate 1.0 mL min^{-1}). It is clear from Figure 4 that the 2 mm i.d. column not only showed a faster separation of PAH's but also showed high sensitivity for all four PAH's, compared to the 4.6 mm i.d. column.

Effect of Source Temperature on Chrysene and Coronene Signals

Figure 5 shows the effect of MS source temperature on intensity of chrysene (m/z = 228) and coronene (m/z = 300) signals. Although source temperature did not have any effect on the sensitivity of the chrysene signal, a higher sensitivity and better peak shape for coronene was obtained at a temperature close to 280 C, apparently due to the lower volatility of coronene (m.p. = 428 C) than chrysene (m.p. = 255 C). Therefore, determinations involving coronene and other high molecular weight PAH's were made at a source temperature of 275-280 C.

Separation and Determination of Chrysene, Dibenzo[a,h]anthracene and Benzo[g,h,i]perylene by Full Scan Acquisition

Since the HPLC-PB-MS system showed good sensitivity for PAH' with molecular weights greater than 178, efforts were made to develop suitable conditions for their determination by full scan acquisition method. Figure 6 shows the effect of methanol flow rate on the intensity of chrysene, dibenzo[a,h]anthracene and benzo[g,h,i]perylene signals. As shown in Figure 6, the effect of eluent flow rate through the column on the intensity of the signals of PAH's appears to be different from the effect observed when the column was by-passed. In fact, the intensity of signals increased with the increase in eluent flow rate through the column, due perhaps to relatively sharper elution of PAH's at high flow rates than at low flow rates.

Figure 7 shows the total ion current mass chromatogram for the separation of 20 ng each of chrysene, dibenzo[a,h]anthracene and benzo[g,h,i]perylene. Peak 1 is due to an impurity of mass 178. Peaks 2, 3, and 4 are due to chrysene, dibenzo[a,h]anthracene and benzo[g,h,i]perylene, respectively. The mass chromatogram was not smoothed and showed the typical noise level. The spectrum of peak 2 (Figure 8) shows a clear molecular ion at m/z 228. The spectrum matched favorably with the library spectrum of chrysene (lower spectrum, Figure 8). This confirms that no degradation of chrysene has occurred when passed through the particle beam interface and that the fragmentation pattern is consistent with the molecular structure and reference EI spectrum of chrysene. Peaks 3 and 4 also generated high quality spectra for dibenzo[a,h]anthracene and benzo[g,h,i]perylene. These results suggest that the quality of EI spectra obtained for PAH's, after their determination by HPLC -PB-MS, are of sufficiently good for identification of these compounds by searching the library.

The detection limits (3 x noise) by full scan acquisition for chrysene, dibenzo[a,h]anthracene and benzo[g,h,i]perylene were estimated at 2.0 ng, 4.0 ng and 2.0 ng, respectively.

Effect of Ammonium Acetate in the Eluent on Sensitivity

It has been reported that addition of small amounts of ammonium acetate in the eluent produced substantial enhancement in the signals of some analytes during their determination by HPLC-PB-MS [27, 34]. Consequently, the effect of ammonium acetate in methanol on the signal intensity of chrysene was investigated. The results of these experiments showed that addition of a small amount of ammonium acetate (at 0.05 g per 100 mL) in methanol enhanced the signal of chrysene by approximately 2.5 times. Ammonium acetate in amounts larger than 0.05 g per 100 mL, however, showed no further enhancement of the chrysene signal.

Figure 9 shows the effect of ammonium acetate on signal sensitivities of chrysene, dibenzo[a,h]anthracene, benzo[g,h,i]perylene peak, and coronene. Again it is clear from the mass chromatograms that addition of 0.05 g / 100 mL ammonium acetate in methanol substantially enhanced the signal of all four PAH's.

Although enhancement in the signal of analytes by the addition of ammonium acetate in the eluent is not clearly understood, it is commonly believed that ammonium acetate may enhance the rate of nucleation process of solutes to form sub-micrometer particles, which can be transported to MS ion source.

Separation and Determination of Chrysene, Dibenzo[a,h]anthracene, Benzo[g,h,i]perylene and Coronene by Selected Ion Monitoring

The determination of chrysene, dibenzo[a,h]anthracene, benzo[g,h,i]perylene and coronene was also investigated by selected ion monitoring. Figure 10 shows the

single ion monitoring trace of a mixture containing 0.5 ng chrysene, 1.0 ng of dibenzo[a,h]anthracene and benzo[g,h,i]perylene and 2.5 ng of coronene. On the basis of three consecutive injections, as shown in Figure 14, we have calculated the reproducibility of the determination of these PAH's and their signal to noise ratio. The percent relative standard deviations calculated for chrysene, dibenzo[a,h]anthracene, benzo[g,h,i]perylene and coronene were respectively, 20%, 2.5%, 13.7 % and 6 %. The signal to noise ratios were 10 for chrysene, 2.5 for dibenzo[a,h]anthracene, 6 for benzo[g,h,i]perylene and 4.5 for coronene. On the basis of these data, the estimated detection limits were as follows: 200.0 pg for chrysene, 1.0 ng for dibenzo[a,h]anthracene, 500.0 pg for benzo[g,h,i]perylene and 2.0 ng for coronene.

The last chromatogram in Figure 10 shows the trace of single ion monitoring of the same mixture used in first three chromatograms (i.e., the mixture containing 0.5 ng (10 μL of 50 ppb) chrysene, 1.0 ng (10 μL of 100 ppb) of dibenzo[a,h]anthracene and benzo[g,h,i]perylene, and 2.5 ng (10 μL of 250 ppb) of coronene) but in 90% tap water and 10% acetonitrile instead in 100% acetonitrile.

Calibration

Figure 11 shows the calibration graphs for chrysene, dibenzo[a,h]anthracene and benzo[g,h,i]perylene. The plots of area counts of the signals against the concentrations of chrysene, dibenzo[a,h]anthracene and benzo[g,h,i]perylene generated straight line calibrations, over the range of concentrations investigated. The straight line calibrations suggest that the HPLC-PB-MS method reported here can be used for quantitative determination of PAH's.

Discussion

Although ultrasonic heads have been used for a long time for nebulizing effluents [42], Ligon and Dorn [31] were the first to use it in a particle beam interface. However, in our device, it was extremely difficult to keep good alignment between aerosol beam, nozzle, and three stage momentum separator when HPLC effluent was delivered tangentially to the ultrasonic tip, in the manner described by Ligon, and Dorn [30]. With the concentric ultrasonic nebulizer, however, the alignment problem is eliminated.

From the literature [29-36], it is clear that the main limitation of the PB method is its poor sensitivity. In this paper we have shown that HPLC-PB-MS method can detect ng amounts of high molecular weight PAH's. The sensitivity of the PAH's can be related to the intensity of their EI spectra as well as to their high transfer rate into the MS ion source. The transfer rate for chrysene was estimated at approximately 40 % based on the solid probe-EI and PB-MS-EI determinations. The detection limit obtained by the method described here for chrysene is comparable to HPLC with fluorescent detection [43].

Since a direct comparison of detection limit for chrysene or other PAH's with other PB interfaces was not possible, we determined the detection limits for carbaryl, which had previously been published. Using a Hewlett-Packard 59980A PB interface, Pleasance *et al.* [27] have reported a detection limit of 10 ng for carbaryl under SIM acquisition conditions. Using the system described in this paper, detection of about 1 ng carbaryl is possible under SIM conditions. Hence the PB interface with a concentric pneumatic ultrasonic nebulizer, described in this work, is more sensitive compared to a commercially available PB interface with a concentric pneumatic nebulizer. This may be due to a better transfer rate of solutes

through this PB interface than others, as very low transfer rates for some solutes through commercially available PB interface are reported in the literature [44].

In conclusion, the HPLC-PB-MS method reported here has revealed high sensitivity for PAH's. The high sensitivity of the method for PAHs with molecular weights > 178 can be exploited in developing a HPLC-PB-MS method, complementary to the popular GC-MS method, for the determination of high molecular weight PAH's.

Acknowledgements

We thank the Ontario Ministry of the Environment and Energy for funding this work under the Research Advisory Committee (Grant 1384). The authors are also thankful to John Rustenberg, Meinhart Benkel, Jim Ross and Tony Biernacki of the Technical Services Shops of Brock University for the machining and electronics of the particle beam interface. The Natural Science and Engineering Research Council of Canada (NSERC) is thanked for an equipment grant for the purchase of Kratos mass spectrometer.

References

1. Uthe, J.F.; Canadian Chem. News, August 1991, 25-27.
2. Christensen, E. R.; Zhang, X.; Environ. Sci. Technol. 1993, 27, 139-146.
3. Tan, Y. L.; Quanci, J. F.; Borys, R. D.; Quancy, M. J.; Atmospheric Environment, 1992, 26A, 1177-1181.
4. Brindle, I. D.; Li, X-F.; J. Chromatogr. 1990, 498, 11-24.
5. Ogan, K.; Katz, E.; Slavin W.; Anal. Chem. 1979, 51, 1315-1320.
6. Wise, S. A.; Benner, B. A.; Byrd, G. D.; Chesler, S. N.; Rebbert, R. E.; Schantz, M. M.; Anal. Chem. 1988, 60, 887-894.
7. Robbat, A., Jr.; Liu, T-Y; Abrahm, B. M.; Anal. Chem. 1992, 64, 1477-1483.
8. Lee, M. L.; Novotny, M.; Bartle, K. D.; Anal Chem. 1976, 48, 405-416.
9. Lee, M. L.; Novotny, M.; Bartle, K. D.; Anal Chem. 1976, 48, 1566-1572.
10. Nowicki, H.G.; Kieda, C.A.; Bassett, D.O. in 'Polynuclear Aromatic Hydrocarbons: Chemicals and Biological Effects', Bjorseth, A. and Dennis, A.J., Eds, Battelle Press, Columbus, OH, 1980; pp. 75-87.
11. Covey, T. R.; Lee, E. D.; Bruins, A. P.; Henion, J. D.; Anal. Chem. 1986, 58, 1451A-1461A.
12. Arpino, P. J.; J. Chromatogr. 1985, 325, 3-11.
13. Arpino, P. J.; Guiochon, G.; Anal. Chem. 1979, 51, 682A-701A.
14. Tsuda, T.; Keller, G.; Stan, H-J.; Anal. Chem. 1985, 57, 2280-2282.
15. Blakley, C. R.; Vestal, M. L.; Anal. Chem. 1983, 55, 750-754.
16. Hayward, M.J.; Snodgrass, J.T.; Thomson, M.L.; Rapid Commun. Mass Spectrom. 1993, 7, 85-91.
17. Abian, J.; Stone, A.; Marrow, M.G.; Creer, M.H.; Fink, L.M.; Lay, J.O., Jr.; Rapid Commun. Mass Spectrom. 1992, 6, 684-689.

18. Bean, M.F.; Pallante-Morell, S.L.; Dulik, D.M.; Fenselau, C.; Anal. Chem. 1990, 62, 121-124.
19. Barcelo, D.; Org. Mass Spectrom. 1989, 24, 898-902.
20. Arpino, P.; Mass Spectrometry Reviews, 1992, 11, 3-40.
21. Whitehouse, C. M.; Dreyer, R. N.; Yamashita, M.; Fenn, J.B.; Anal. Chem. 1985, 57, 675-679.
22. Lin, H-Y; Voyksner, R.D.; Anal. Chem. 1993, 65, 451-458.
23. Lee, E.D.; Henion, J.D.; Rapid Commun. Mass Spectrom. 1992, 6, 727-733.
24. Covey, T. R.; Lee, E. D.; Henion, J. D.; Anal. Chem. 1986, 58, 2453-2460.
25. Horning, E.C.; Carroll, D.I.; Dzidic, I.; Heagle, K.D.; Horning, M.G.; Stillwell, R.N.; J. Chromatogr. Sci. 1974, 12, 725-729.
26. Deorg, D.R.; Bajic, S.; Rapid Commun. Mass Spectrom. 1992, 6, 663-666.
27. Pleasance, S.; Anacleto, J.F.; Bailey, M.R.; North, D.H.; J. Am. Soc. Mass Spectrom. 1992, 3, 378-397.
28. Henion, J.D.; Thomson, B.A.; Dawson, P.H.; Anal. Chem. 1982, 54, 451-456.
29. Browner, R. F.; Winkler, P. C.; Perkins, D. D.; Abby, L. E.; Microchem. J. 1986, 34, 15-24.
30. Winkler, P. C.; Perkins, D. D., Williums, W. K.; Browner, R. F.; Anal. Chem. 1988, 60, 489-493.
31. Ligon, W. V., Jr.; Dorn, S. B.; Anal. Chem. 1990, 62, 2573-2580.
32. Deorge, D.R., Burger, M.W.; Bajic, S.; Anal. Chem. 1992, 64, 1212-1216.
33. Behymer, T.D.; Bellar, T.A.; Budde, W.L.; Anal. Chem. 1992, 62, 1686-1690.
34. Kim, I.S.; Sasinos, F.I.; Stephens, R.D.; Brown, M.A.; J. Agric. Food Chem. 1990, 38, 1223-1226.
35. Deorge, D.R.; Miles, C.J.; Anal. Chem. 1991, 63, 1999-2001.
36. Hsu, J.; Anal. Chem. 1992, 64, 434-443.

37. Galimberti, R.; Lecchi, P.; Angelis, L.D.; Caruso, D.; Toia, A.V., Racagni, G.; Anal. Biochem. 1992, 201, 356-361.

38. Voyksner, R.D.; Smith, C.S.; Knox, P.C.; Biomed. Environ. Mass Spectrom. 1990, 19, 523-534.

39. Miles, C.J.; Deorge, D.R.; Bajic, S.; Arch. Environ. Contam. Toxicol. 1992, 22, 247-251.

40. Ho, J.S.; Beymer, T.D.; Budde, W.L.; Bellar, T.A.; J. Am. Soc. Mass Spectrom. 1992, 3, 662-671.

41. Donnelly Betowsky, L.; Pace, C. M.; Roby, M. R.; J. Am. Soc. Mass Spectrom. 1992, 3, 823-830.

42. Olson, K.W.; Hass, W.J. Jr.; Fassel, V.A.; Anal. Chem. 1977, 49, 632-637.

43. Method HPLC/L-X3HIDI, The Determination of Polynuclear Aromatic Hydrocarbons in Surface Water, Domestic Waters, and Industrial Wastes by HPLC, Ontario Ministry of the Environment, Rexdale, Ontario, 1988.

44. Tinke, A.P.; Van Der Hoeven, R.A.M.; Niessen, W.M.A.; Tjaden, U.R.; Vander Greef, J.; J. Chromatogr. 1991, 554, 119-124.

Figure Captions

Figure 1. Schematic diagram of particle beam interface with concentric ultrasonic pneumatic nebulizer, controlled heating of desolvation chamber and three stage momentum separator.

Figure 2. HPLC-PB-MS response for different PAH's; 152 = acenaphthylene, 154 = acenaphthene, 166 = fluorene, 178 = phenanthrene, 228 = chrysene, 276 = benzo[g,h,i]perylene, 278 = dibenz[a,h]anthracene, and 300 = coronene.

Figure 3. Effect of eluent (solvent) on 20 ng signal of chrysene: Signal 1 is with MeCN (injection was made at approximately 6.3 min); Signal 2 is with 100% MeOH (MeOH as eluent was started at about 30 min, injection was made at approximately 51.3 min); Flow rate = 0.3 mL min^{-1}.

Figure 4. HPLC-UV chromatograms showing the separation of 5 ng chrysene (228), 10 ng dibenz[a,h]anthracene (278), 10 ng benzo[g,h,i]perylene (276), and 25 ng coronene (300) ; Upper chromatogram with 15 cm x 2 mm, 3 μ, C-18 silica column, Lower chromatogram with 15 cm x 4.6 mm, 5 μ, C-18 silica column; Eluent =100 % MeOH; Flow rate = 0.3 mL min^{-1} for 2 mm column and 1.0 mL min^{-1} for 4.6 mm column.

Figure 5. Effect of source temperature on the sensitivity of chrysene and coronene.

Figure 6. Effect of MeOH flow rate (through the column) on the signals of masses 228, 276 and 278; Column = 15 cm x 2 mm, 5 μ, C-18 silica, eluent = 100 % methanol.

Figure 7. Total ion current mass chromatogram of 20 ng each of chrysene (228), dibenz[a,h]anthracene (278) and benzo[g,h,i]perylene (276).; Column =

15 cm x 2 mm, 5 μ, C-18 silica, eluent = 100 % methanol, flow rate = 0.5 mL min^{-1}.

Figure 8. EI mass spectrum of peak 2, 20 ng chrysene (upper) with library spectrum (lower).

Figure 9. HPLC-PB mass chromatograms showing the separation of 5 ng chrysene (228), 10 ng dibenz[a,h]anthracene (278), 10 ng benzo[g,h,i]perylene (276), and 25 ng coronene (300) ; Column = 15 cm x 2 mm, 3 μ, C-18 silica, Eluent for first chromatogram =100 % MeOH; eluent for second chromatogram = MeOH containing 0.05 % ammonium acetate, flow rate = 0.3 mL min^{-1}.

Figure 10. SIM trace of 0.5 ng chrysene (228), 1 ng dibenz[a,h]anthracene (278), 1 ng benzo[g,h,i]perylene (276), and 2.5 ng coronene (300) (First three chromatograms) ; Last (fourth) chromatogram is SIM trace of 0.5 ng chrysene (228), 1 ng dibenz[a,h]anthracene (278), 1 ng benzo[g,h,i]perylene (276), and 2.5 ng coronene (300) in 10% MeCN + 90% tap water; Column = 15 cm x 2 mm, 3 μ, C-18 silica, eluent = MeOH containing 0.05% ammonium acetate, flow rate = 0.3 mL min^{-1}.

Figure 11. Calibration graphs for chrysene (228), dibenz[a,h]anthracene (278), and benzo[g,h,i]perylene (276)

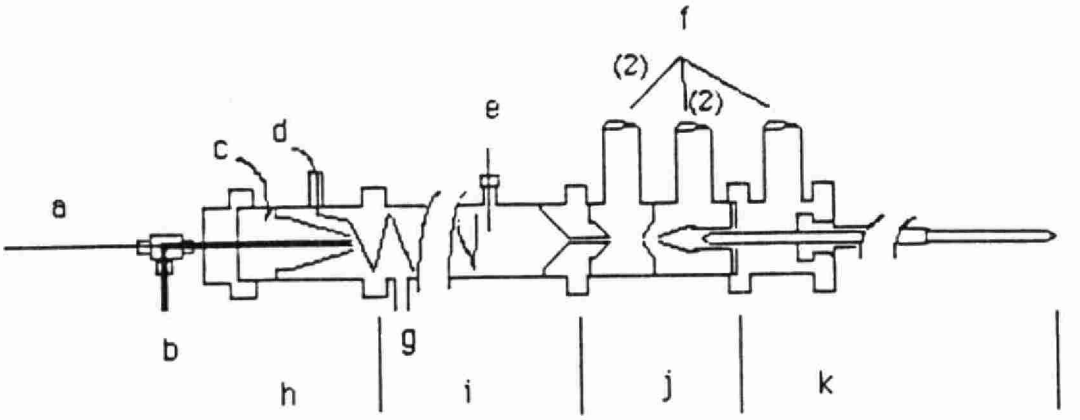

Particle Beam Schematic

a. HPLC effluent capillary
b. Helium gas inlet
c. Ultrasonic horn
d. Desolvation heater
e. Thermocouple
f. Roughing pump connections
g. Solvent waste
h. Ultrasonic jet assembly
i. Desolvation chamber
j. Skimmer stages 1 and 2
k. Final skimmer and transf

HPLC-PB-MS response for different PAH's

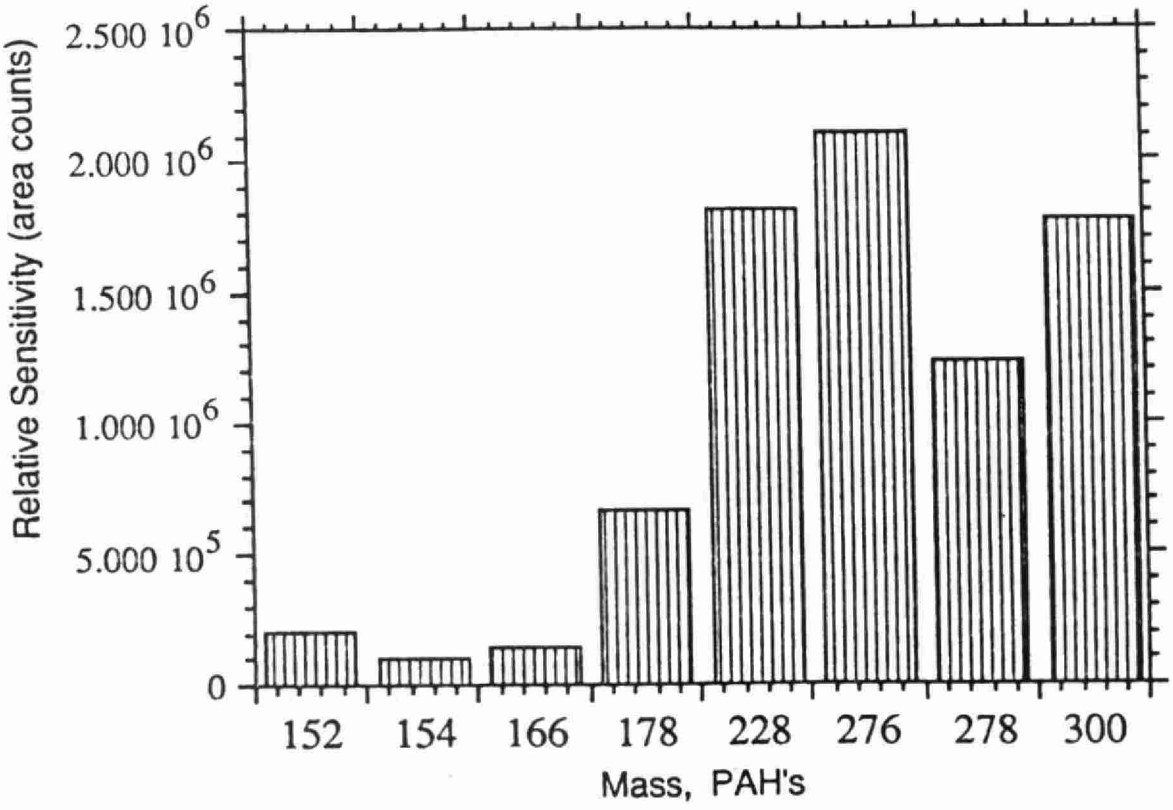

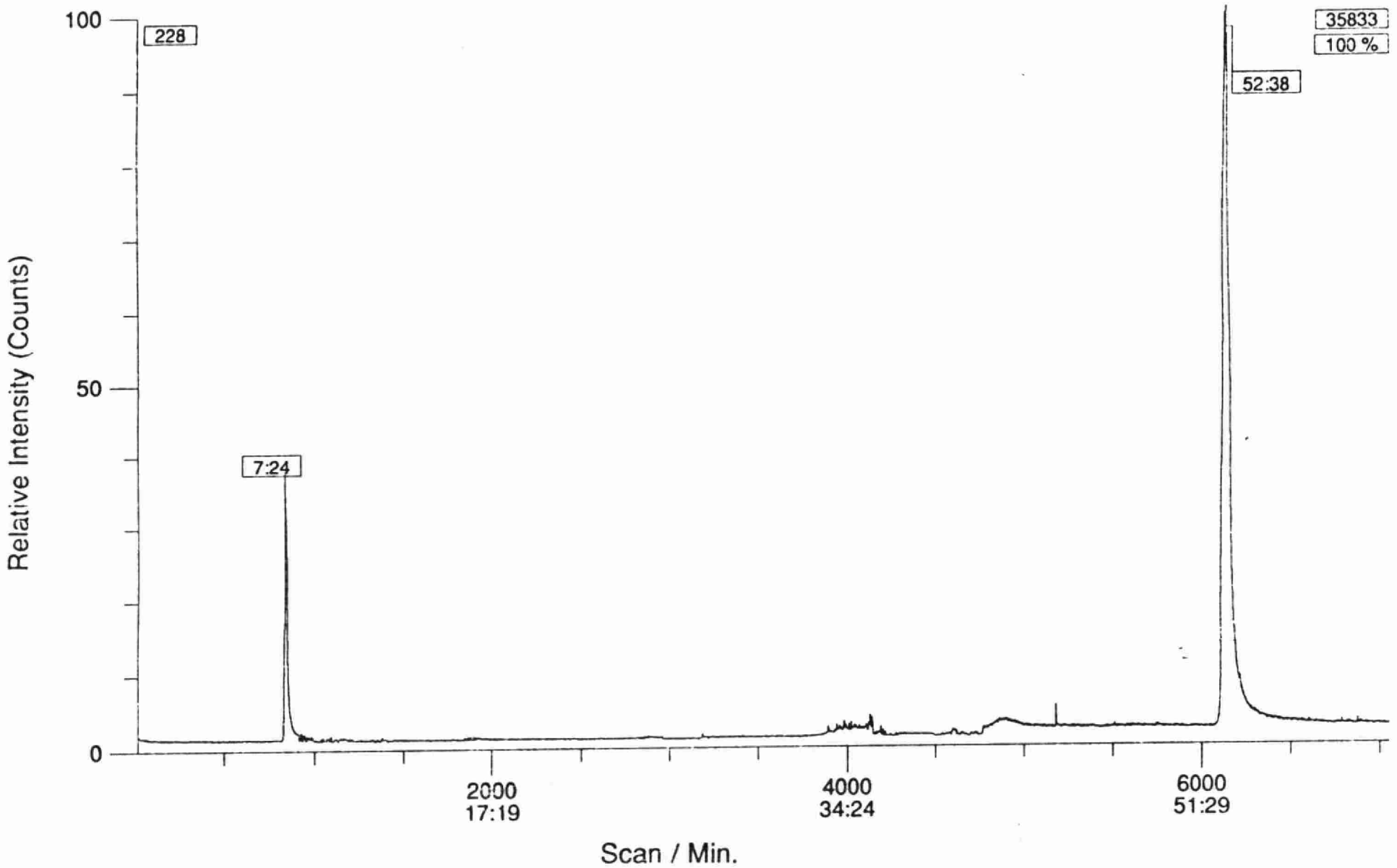

Effect of eluent (solvent) on 20 ng signal of chrysene: Signal 1 is with MeCN

; Signal 2 is with 100% MeOH

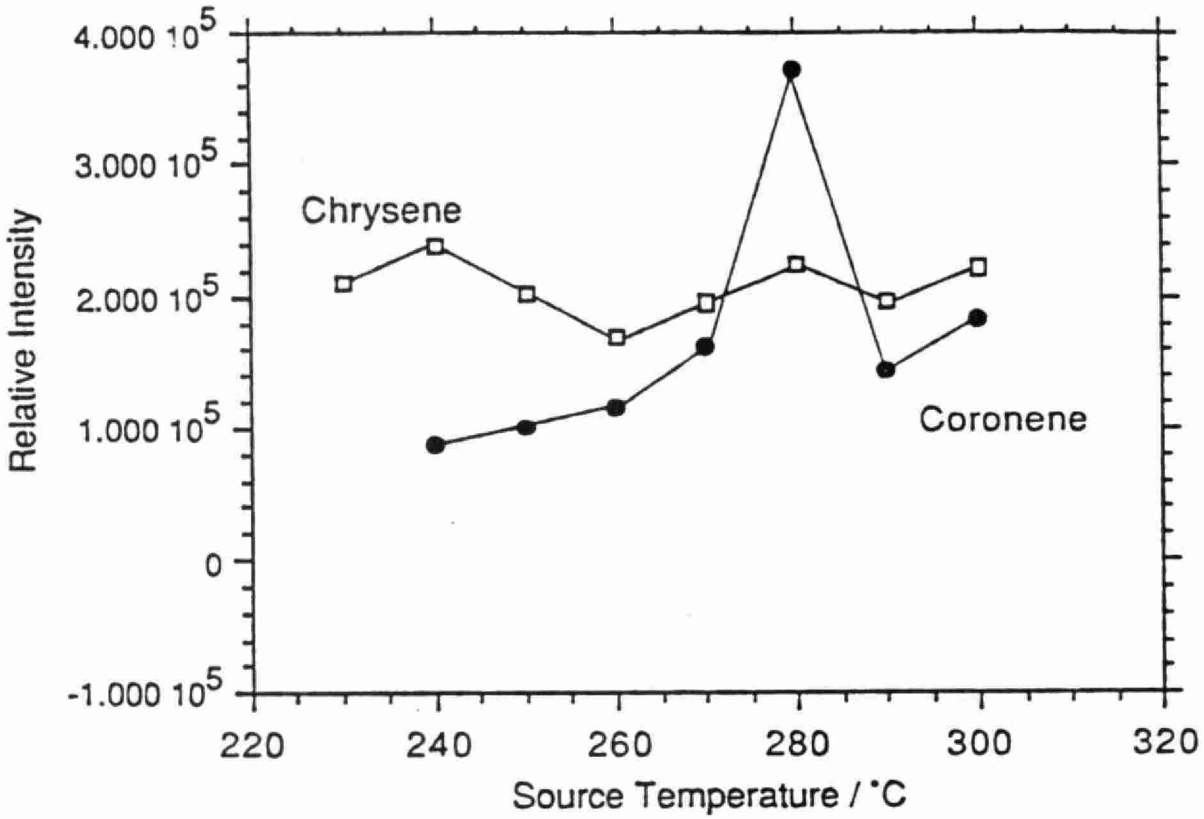
4.000 10^5
3.000 10^5
2.000 10^5
1.000 10^5
0
-1.000 10^5
Relative Intensity
Chrysene
Coronene
220
240
260
280
300
320
Source Temperature / °C

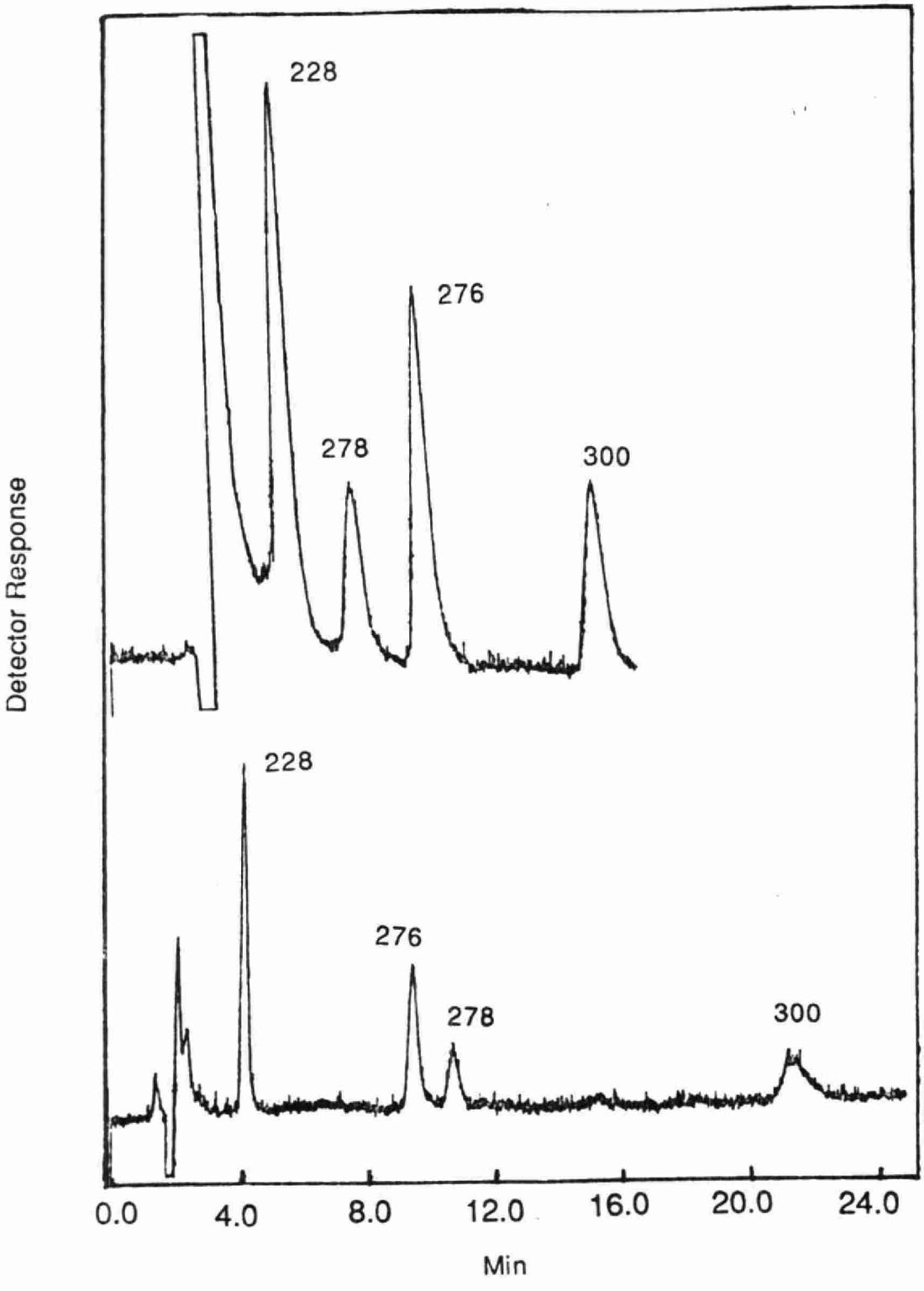

HPLC-UV chromatograms showing the separation of 5 ng chrysene (228), 10 ng dibenz[a,h]anthracene (278), 10 ng benzo[g,h,i]perylene (276), and 25 ng coronene (300) ; Upper chromatogram with 15 cm x 2 mm, 3 μ, C-18 silica column, Lower chromatogram with 15 cm x 4.6 mm, 5 μ, C-18 silica column

Effect of MeOH flow rate (through the column) on the signals of masses 228, 276 & 278

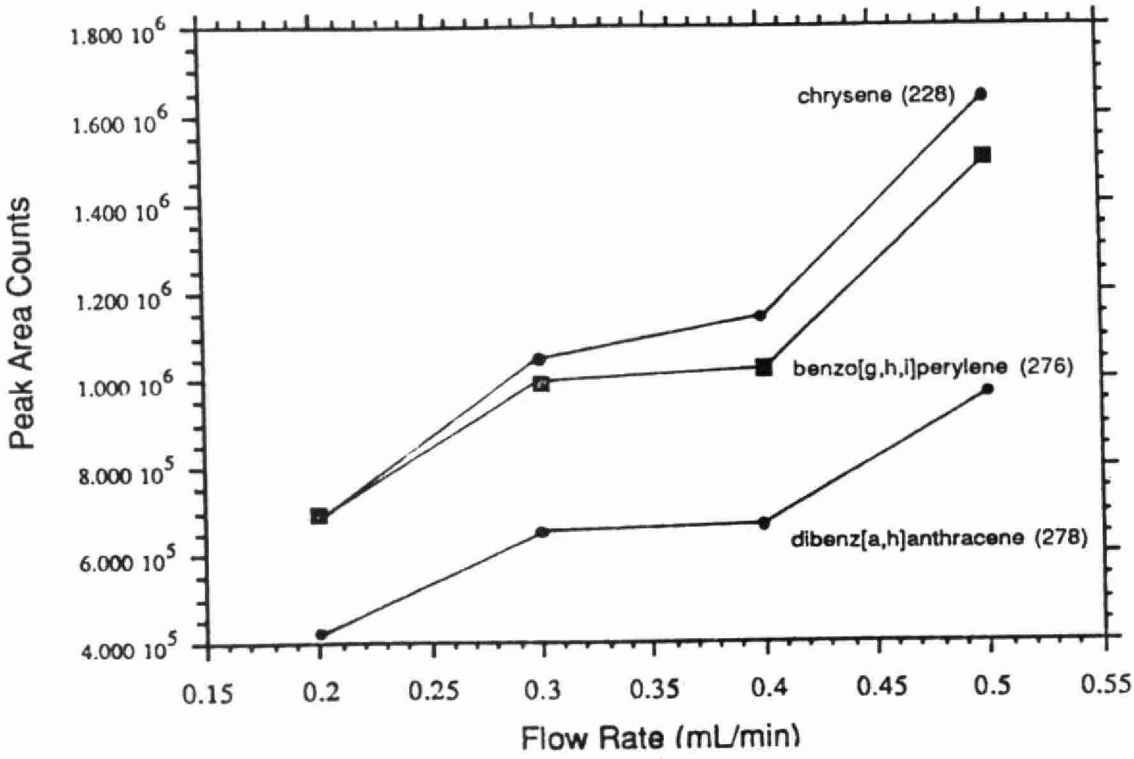

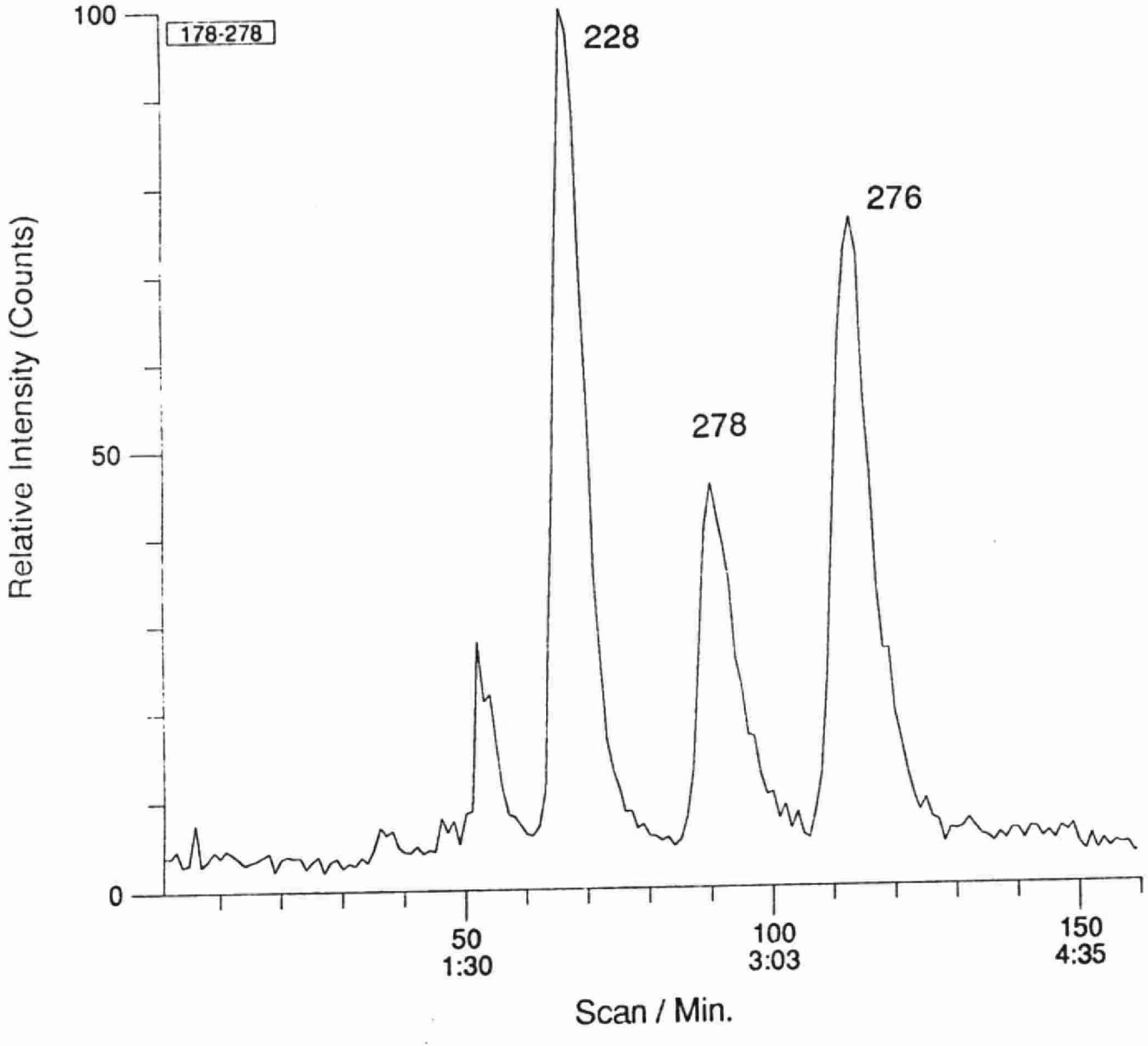

HPLC-PB mass chromatogram of 20 ng each of chrysene (228), dibenz[a,h]anthracene (278) and benzo[g,h,i]perylene (276).; Column = 15 cm x 2 mm, 5 µ, C-18 silica, eluent = 100 % methanol, flow rate = 0.5 mL/min.

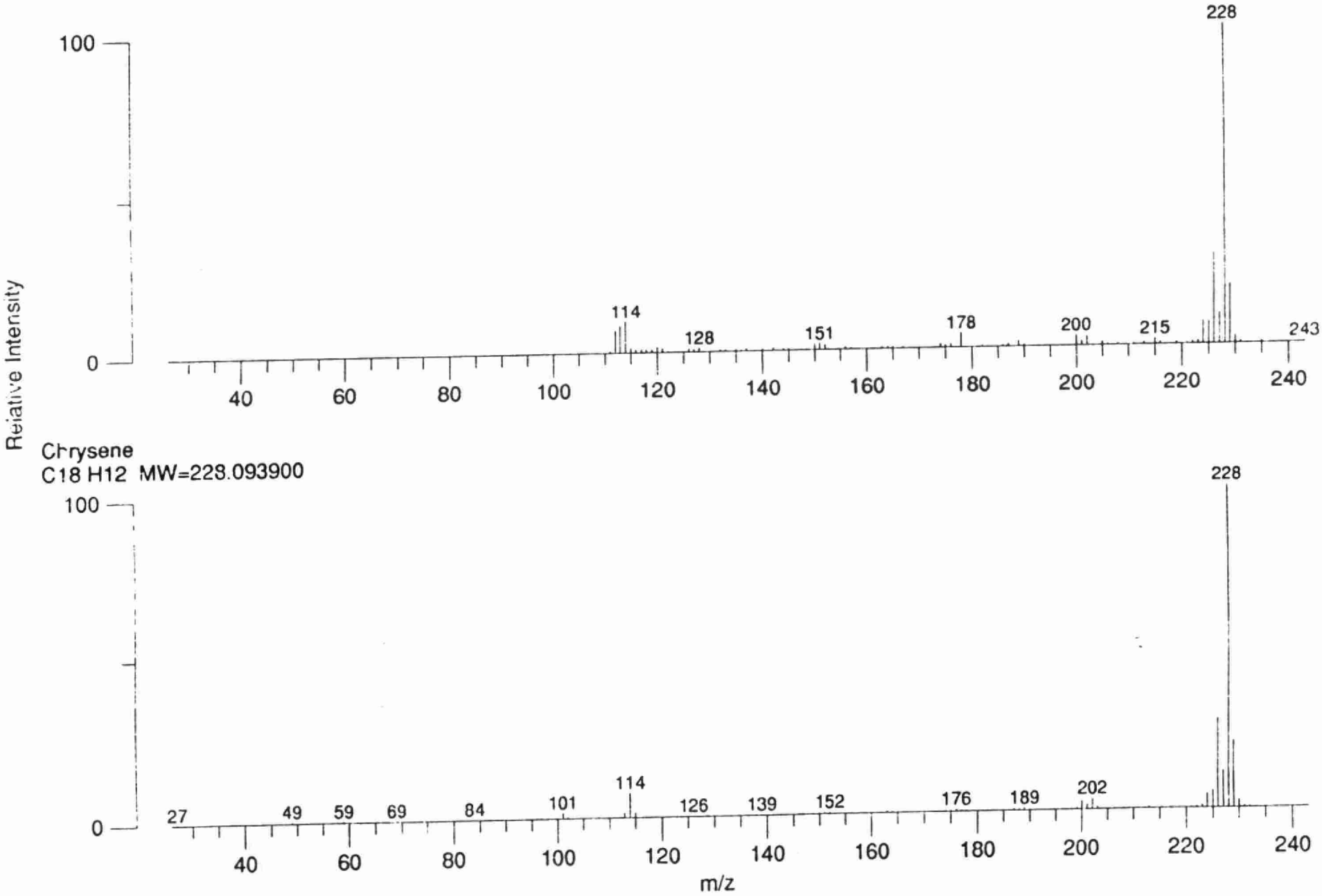

EI mass spectrum of peak 2, 20 ng chrysene (upper) with library searched

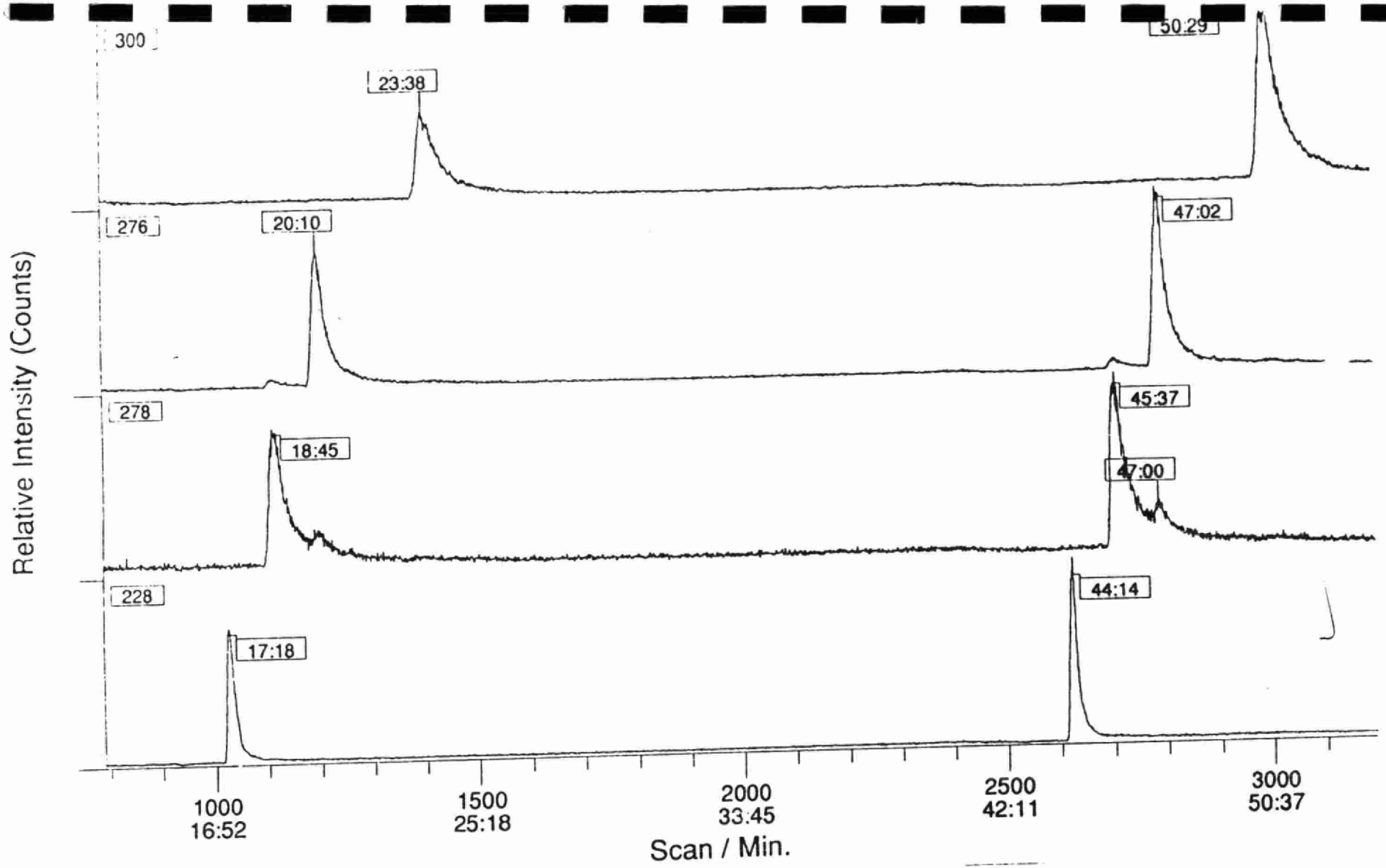

HPLC-PB mass chromatograms showing the separation of 5 ng chrysene (228), 10 ng dibenz[a,h]anthracene (278), 10 ng benzo[g,h,i]perylene (276), and 25 ng coronene (300) ; Column = 15 cm x 2 mm, 3 µ, C-18 silica, Eluent for first chromatogram =100 % MeOH; eluent for second chromatogram = MeOH containing 0.05 % ammonium acetate, flow rate = 0.3 mL/min.

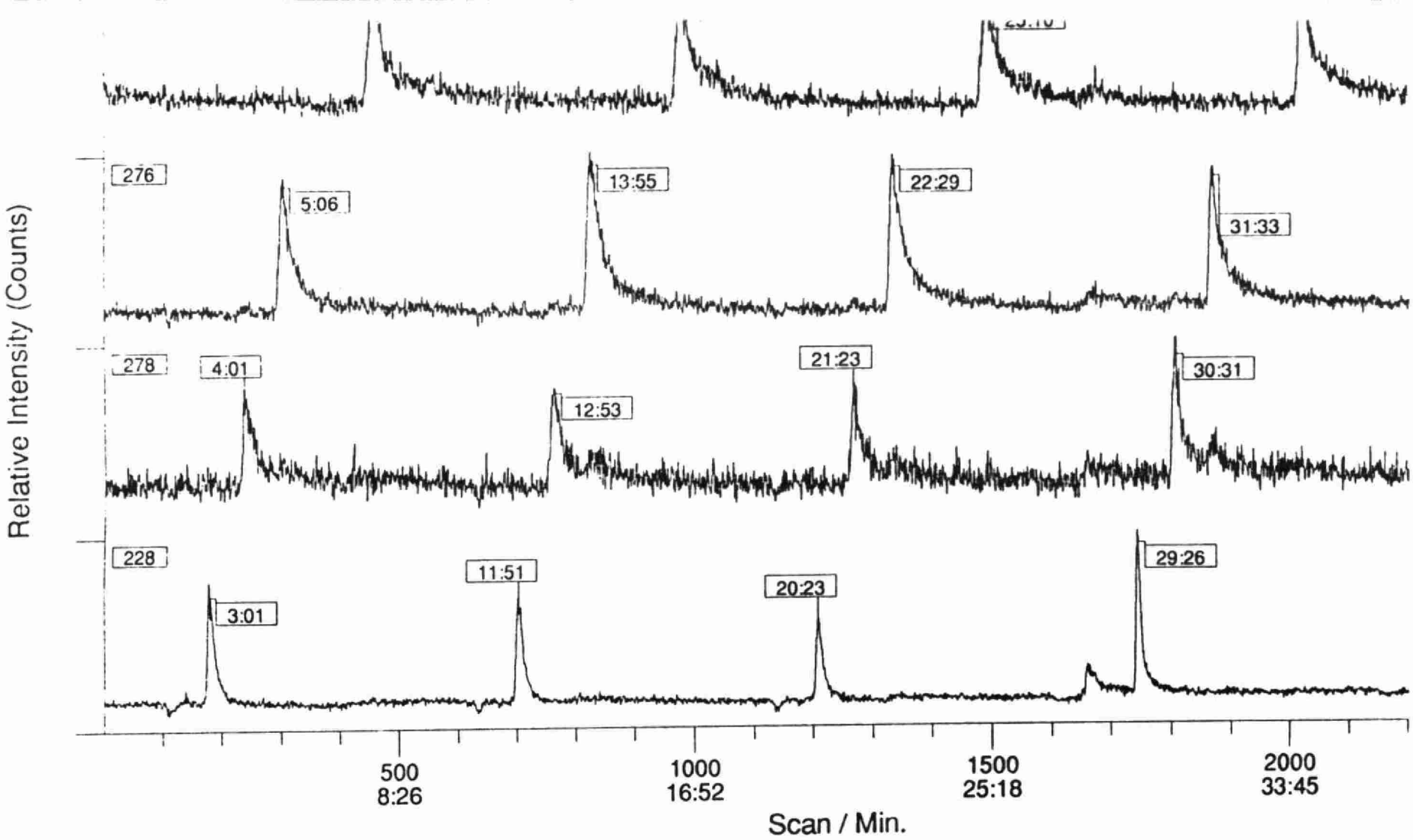

HPLC-PB mass chromatograms showing the separation of 0.5 ng chrysene (228), 1 ng dibenz[a,h]anthracene (278), 1 ng benzo[g,h,i]perylene (276), and 2.5 ng coronene (300) ; Column = 15 cm x 2 mm, 3 µ, C-18 silica, eluent = MeOH containing 0.05 % ammonium acetate, flow rate = 0.3 mL/min. First 3 chromatograms are of standard in MeCN; fourth chromatogram is of standard in 10% MeCN & 90% tap water

Calibration graphs of 228, 276 and 278

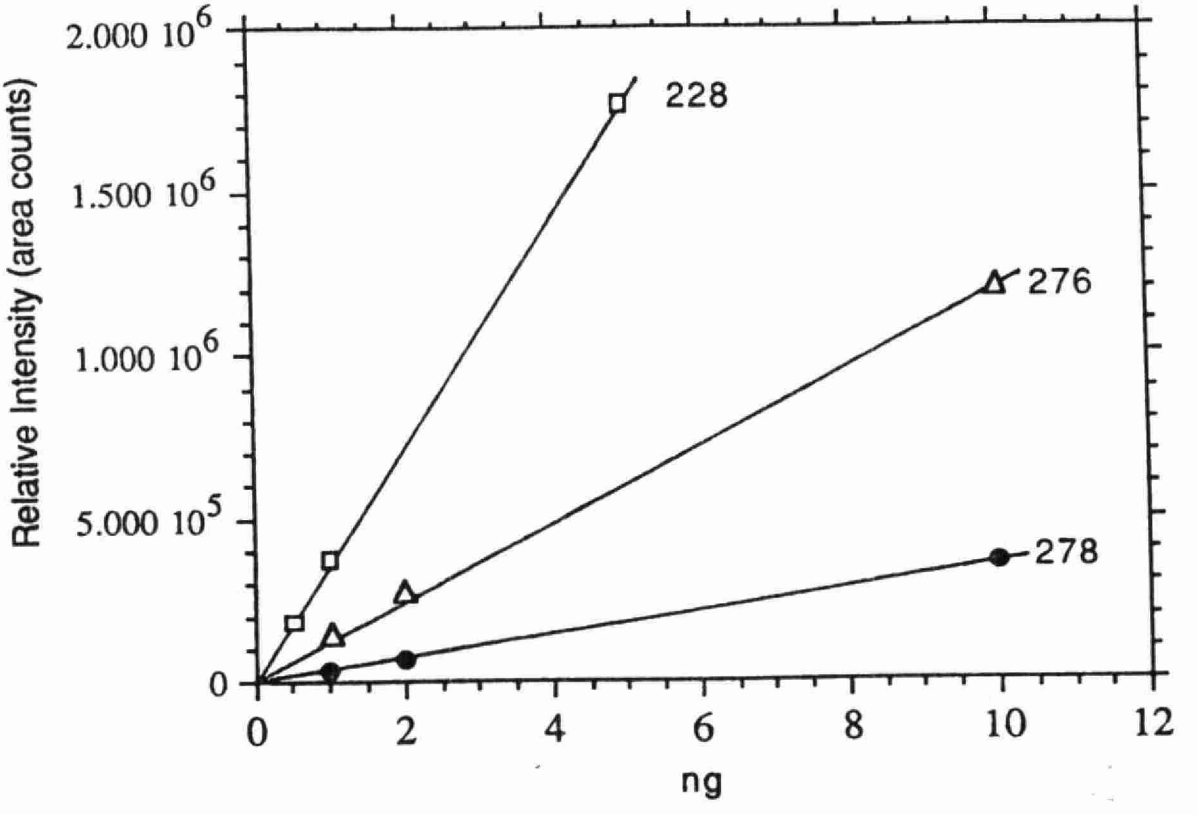

Part II: Determination of Benomyl and its Degradation Compounds by Particle Beam Mass Spectromery (PB-MS) and Fast-Atom Bombardment Mass Spectrometry (FAB-MS)

Part II A: Investigation by Particle Beam and Fast-Atom Bombardment Mass Spectrometry of the Degradation Compounds of Fungicide Benomyl Methyl [1-(Butylcarbamoyl)-1H-benzimidazol-2-yl]carbamate

Abstract

This part reports our results on the particle beam - mass spectrometric (PB-MS) and fast-atom bombardment mass spectrometric (FAB-MS) analysis of the degradation compounds of methyl [1-(Butylcarbamoyl)-1H-benzimidazol-2-yl]carbamate (benomyl) i.e., methyl 1H-benzimidazol-2-ylcarbamate (carbendazim, more commonly called MBC), 3-butyl-2,4-dioxo-s-triazino[1,2-a]benzimidazole (STB) and, 1-(2-benzimidazolyl)-3-n-butylurea (BBU), and 2-aminobenzimidazole (2-AB). Determination of these compounds is important in different matrices such as crops, soil and water and is of health and environmental importance. It is reported in this paper that PB-MS method showed good sensitivity (at 10 mg L^{-1}) for quantitative and / or qualitative determination of MBC and 2-AB. Preliminary results on FAB-MS investigation of these compounds indicated that 3-nitrobenzyl alcohol is a good matrix for the determination of these compounds by the FAB-MS technique. Very high sensitivity for the determination of 2-AB in 3-nitrobenzyl alcohol is obtained by FAB-MS method.

Introduction

Benomyl (Methyl [1-(Butylcarbamoyl)-1H-benzimidazol-2-yl]carbamate) is one of the most widely used systemic fungicides. For many years benomyl has been successfully used for the control of many plant diseases (1-6). Recently, use of benomyl was estimated at 2000,000 lbs of active ingredient per year (7). In aqueous solutions, at ambient temperature, benomyl is not stable and converts to

methyl 1H-benzimidazol-2-ylcarbamate (carbendazim, more commonly called MBC), 3-butyl-2,4-dioxo-s-triazino[1,2-a]benzimidazole (STB), 1-(2-benzimidazolyl)-3-n-butylurea (BBU), and 2-aminobenzimidazole (2-AB) depending upon the pH of the solutions as follows (8):

benomyl Æ MBC + BIC (pH = 3 to 7, k = 3.16 x 10^{-5} Sec^{-1}, BIC = butyl isocyanate)

benomyl Æ STB (pH = 13.0, k = 1.0 x 10^{-2} Sec^{-1}).

STB Æ BBU (pH = 13.0, k = 5.3 x 10^{-4} Sec^{-1})

MBC Æ 2-AB (pH = 14.0, k = 1.3 x 10^{-4} Sec^{-1}).

Although the k values for the degradation of benomyl to STB and BBU, and for MBC to 2-AB are reported at very high pHs, which may not exist in real samples, these conversions may also occur at lower pHs at degradation rates slower than mentioned here. The conversion of benomyl to 2-AB has also been reported to occur in soil and animals (9-10). Benomyl slowly converts to its stable degradation compounds, carbendazim, 2-AB, STB and / or BBU depending upon pH and the medium. Therefore, the determination of degradation compounds of benomyl in environmental water, soil extracts, and crops is important. Determination of these compounds is also of analytical importance, as in most cases benomyl is determined in the form of its stable degradation compounds MBC, 2-AB and BBU (7, 10-29). Singh and Chiba (30) and Chiba and Singh (31) developed a method to determine benomyl and MBC individually by converting benomyl to STB while MBC remained intact under those conditions.

For the determination of carbendazim, STB, BBU, and 2-AB, HPLC and GC techniques have usually been used (10, 12-31). However, methods involving mass spectrometry have not been developed for the determination of these

degradation compounds of benomyl. The only report involving mass spectrometry is by Liu et al. (7) who used a high-performance liquid chromatography / thermospray / mass spectrometry / selective ion monitoring method for the determination of MBC. This method was used for the determination of benomyl as MBC in tomatoes, peaches and apples.

Since mass spectrometry provides structural identification of the compounds, in addition to their quantification, in this paper we report the preliminary results of the analysis of carbendazim, STB, BBU, and 2-AB by particle beam - mass spectrometry (PB-MS), and fast- atom bombardment mass spectrometry (FAB-MS) in two commonly used matrices, glycerol and 3-nitrobenzyl alcohol. The particle beam interface (32-34) is one of the several interfaces (35-51) currently used to interface an HPLC with the mass spectrometer. Although particle beam / mass spectrometry does not show high sensitivity for the majority of the analytes which are analyzed by HPLC-PB-MS (52-61), its ability to generate library searchable EI spectra of analytes makes it a valuable technique among HPLC-MS methods. FAB-MS, since its development by Barber et al. (62) and Surman and Vickerman (63), has been established as a powerful analytical technique for both qualitative and quantitative determination of a number of analytes (64-68).

Experimental

Reagents

(a) MBC — Analytical standard MBC, was obtained from E.I. du Pont de Nemours and Co., Inc., Delaware. Purity of MBC was assumed to be 100%.

(b) STB and BBU — STB and BBU were prepared from benomyl as reported earlier (14). The purity of STB and BBU was tested by HPLC and assumed to be 100% in this study.

(c) 2-AB — 2-AB was obtained from Aldrich Chemical Company Inc. Milwaukee WIS.

The molecular structures of MBC, STB, BBU and 2-AB are shown in Figure 1.

(d) Solvents— Methanol and acetonitrile, used in this work were HPLC-grade reagent from Caledon Laboratories Ltd., Georgetown, Ontario.

(e) Other Reagents— Spectrophotometric grade glycerol and 3-nitrobenzyl alcohol (3-NBA) were obtained from Aldrich Chemical Company, Inc., Milwaukee, WIS.

Standard Solutions

Standard solutions of MBC, BBU and 2-AB were prepared in methanol at 100 mg L^{-1} (weighed to the nearest 0.1 mg). The 100 mg L^{-1} standard solution of STB was prepared in acetonitrile (weighed to the nearest 0.1 mg).

Particle Beam - Mass Spectrometry

The particle (PB) interface, reported earlier (69) was used. The design of the ultrasonic head, desolvation chamber, nozzle and three stage momentum separator up to the second stage, was similar to that reported by Ligon and Dorn [34], except that the effluent from the HPLC was delivered co-axially via a silica capillary and nebulized at the exit end of the ultrasonic head by a fast, concentric flow of helium gas, optimized at 900 mL min^{-1}. The end of the silica capillary was positioned about 2 mm behind the tip of ultrasonic head. The transfer tube, which

included a third stage of the vacuum separator, was based on the Kratos PB interface design. The whole PB interface was constructed in the machine shops at Brock University. The two diametrically opposed pumping ports of the first stage were connected to a 500 L min^{-1} Welch Duo Seal Vacuum Pump. The ports of the second identical stage were connected to a 300 L min^{-1} Edwards High Vacuum pump. The third, and last, stage was pumped by an Edwards High Vacuum pump with 150 L min^{-1} pumping speed. A Kratos Concept IS double-focussing mass spectrometer (Kratos Analytical, Urmston, Manchester, UK) (E/B Configuration) employing a EI/CI source, was used for mass spectrometric analyses. The instrument was controlled by a Kratos Mach 3 data system running on a SUN SPARC station. For all studies, a nominal resolving power of 1000 was used. The standard EICI source, operated at temperatures 220-300 °C and 6 kV accelerating potential, was used. The scan rate was 3.0 seconds per decade for full scan acquisition. The PB-MS system was tuned and mass calibrated with perfluorokerosene (PFK).

The liquid chromatograph used was a Waters 600-MS system controller with a 20 µL sample loop. Methanol was used as the mobile phase and pumped at a rate of 0.3 mL min^{-1}.

FAB Mass Spectrometry

A Kratos Concept IS double-focussing mass spectrometer (described above) using a fast atom bombardment (FAB) source, was operated in both positive and negative ion modes. The instrument was controlled by a Kratos DS 90 Data General Eclipse based computer system. A Kratos Mach 3 data system running on a SUN SPARC station was used for further data work-up. For all studies, a nominal resolving power of 1000 was used. The spectrometer was fitted with an

Ion Tech Saddle field atom gun and xenon was used as the fast-atom beam. The fast-atom beam energy was 7.5 keV and the density corresponding to an emission current was about 1 mA. The source was operated at room temperature and 8 kV accelerating potential. The scan rate was 10 sec per decade. Approximately one microliter solution of different compounds in glycerol and 3-nitrobenzyl alcohol was placed on the probe tip for FAB-MS determination.

Results and Discussion

Particle Beam - Mass Spectrometry

Figure 2 shows the relative responses of 100 ng each of 2-AB, MBC, STB and BBU obtained by PB-MS analysis of individual compounds. The samples were injected directly into methanol streams flowing at 0.3 mL min^{-1} flow rate (no column was used) at source temperature of 200 °C. It is clear from Figure 2 that the sensitivity of PB-MS was substantially greater for 2-AB than for other degradation compounds at 100 ng levels.

Figure 3 shows the effect of MS source temperature on sensitivity of 2-AB (m/z = 133). It is clear that sensitivity of 2-AB is enhanced at a source temperature of 250 °C. Therefore, all the studies reported below were carried out at a source temperature of 250 °C.

Figure 4 shows the mass chromatograms of different concentrations of 2-AB. The spectrum of total ion current (TIC) mass chromatogram peak of 10 mg L^{-1} solution (Figure 5) shows molecular ion at m/z 133. The spectrum matched favorably with the library spectrum of 2-aminobenzimidazole (lower spectrum, Figure 5). This confirms that no degradation of 2-AB has occurred when it is passed through the particle beam interface and that the fragmentation pattern is

consistent with the molecular structure and reference EI spectrum of 2-AB. This also suggest that 2-AB can be determined in solutions containing 10 mg L^{-1} or greater by PB-MS using full scan acquisition. This sensitivity of 2-AB is comparable with many other analytes determined by LC-PB-MS (70) and is quite sufficient for its determination, after a 1000 times concentration step (which is quite commonly attainable and often used) in real samples. PB-MS also generated similar data for MBC, as can be seen in Figures 6 and 7.

The mass spectra obtained for STB and BBU through particle beam interface also compared well with their direct EI spectra (lower spectra in Figures 8 and 9). Since reference spectra for STB and BBU were not found in the library, we report their solid probe EI spectra with their PB-MS EI spectra. It is clear from Figures 8 and 9 that PB-MS EI spectrum of BBU was very similar to its solid probe EI spectrum; however, intensities of major peaks in the PB-MS EI spectrum of STB were slightly different than in solid probe EI spectrum of STB. Despite the difference in the intensities of major peaks, we believe that the EI spectrum of STB through PB interface is good enough for its identification through library search. The EI spectra of STB and BBU obtained by solid probe, reported here, may be used as reference spectra for library searches in future studies on these compounds.

The detection limits (3 x noise) by full scan acquisition for 2-AB was estimated to be as 5 mg L^{-1}; however, only 10 mg L^{-1} 2-AB peak from TIC (total ion current) could be identified by the library search algorithm. Similar results were also obtained for the PB-MS determination of MBC.

Linear responses were obtained for 2-AB and MBC in low concentration range (5 to 20 mg L^{-1}); regression equation for 2-AB: $y = 140433x - 313543$; for MBC: $y = 312771x - 460625$; where x = mg L^{-1} and y = peak area counts (Figure 10). At a very high concentration (e.g. at 100 mg L^{-1}) MBC showed proportionally high

response; however, the response of 2-AB was out of proportion as it showed exceptionally high response at 100 mg L^{-1} concentration. This indicated a narrow range of linearity for 2-AB. Figure 10 also indicates that 2-AB response was much higher than MBC at 100 mg L^{-1} level. However, at low concentrations, the difference in the sensitivity of the two compounds was not so substantial.

In conclusion, preliminary results reported here on the PB - MS analysis of 2-AB, MBC, STB and BBU suggest that a LC-PB-MS method may be developed for the indirect determination of benomyl or for the determination of its degradation compounds. Although, as reported in the literature (51-60), the PB-MS method usually shows a poor sensitivity for most analytes, because of its advantage in structural identification of analytes by mass spectrometry, the LC-PB-MS method may find applications in the determination of benomyl and its degradation compounds in real samples.

Analysis of MBC, STB, BBU and 2-AB by FAB-MS in Glycerol and 3-Nitrobenzyl Alcohol Matrices

2-AB — Figures 11 and 12 depict the FAB-MS spectra of 2-AB in glycerol and 3-nitrobenzyl alcohol (3-NBA) matrices, respectively. In both matrices, a strong peak for the molecular ion of 2-AB i. e. $(2\text{-AB} + H)^+$ was obtained. These results suggest that 2-AB may be determined by FAB-MS with very high sensitivity. A comparison of FAB-MS spectra of 2-AB in glycerol and 3-NBA matrices shows that the FAB-MS spectrum of 2-AB was better in 3-NBA (Figure 12). In 3-NBA, peaks only related to 2-AB i. e. at m/z 134 for $(2\text{-AB} + H)^+$ ion and at m/z 267 for $[(2\text{-AB})_2 + H]^+$ were observed. Virtually no matrix peaks in the FAB-MS spectrum of 2-AB in 3-NBA were observed. The absence of matrix (3-NBA) peaks suggest that a very high sensitivity for 2-AB may be obtained in 3-NBA by FAB-MS method.

MBC — Figures 13 and 14 depict the FAB-MS spectra of MBC in glycerol and 3-NBA matrices, respectively. The peak due to the molecular ion of MBC (i.e., (MBC + H^+) at m/z = 192 was obtained in both matrices. However, in both matrices the spectra were dominated by matrix peaks suggesting relatively poor sensitivity for MBC by FAB-MS methods in glycerol and 3-NBA matrices. A comparison of FAB-MS spectra of MBC in glycerol and 3-NBA matrices shows that, once again, the 3-NBA matrix (Figure 14) may give higher sensitivity for MBC than a glycerol matrix (Figure 14).

BBU — FAB-MS spectra of BBU in glycerol and 3-NBA matrices are shown in Figures 15 and 16 respectively. It is clear from Figure 15 that the spectrum is dominated by glycerol peaks; only a small peak due to (BBU + H^+) = at m/z 233 was seen. This indicated poor sensitivity for BBU by FAB-MS method in glycerol. However, the FAB-MS spectrum of BBU in 3-NBA showed a strong peak for BBU at m/z 233. This again indicated that 3-NBA is the matrix of choice for FAB-MS determination of BBU.

STB — In a similar fashion to BBU, a better FAB-MS spectrum for STB was obtained in 3-NBA than in glycerol (Figures 17 and 18). In glycerol, the FAB-MS spectrum showed only a small peak for STB at m/z 259 (Figure 17). A relatively stronger FAB-MS STB peak was obtained in 3-NBA (Figure 18). Slightly improved sensitivity for STB in a glycerol matrix was obtained in negative FAB-MS mode (Figure 19).

In conclusion, FAB-MS results of the analysis of 2-AB, MBC, BBU and STB, reported here, suggest that 3-NBA matrix was better for all the compounds than glycerol. A very high sensitivity for 2-AB is expected by FAB-MS method in 3-NBA. The application for this finding can be extended for high sensitivity determination of 2-AB in crops, soil and water. Benomyl and MBC, normally present in samples just

after the application of benomyl formulations may also be individually determined as 2-AB by analyzing a sample twice as follows:

Analysis 1. (a) Sample + organic solvent — Conversion of benomyl + MBC to MBC

(b) MBC (from a) + Concentrated alkali — Conversion of total MBC to 2-AB.

Analysis 2. Sample + Concentrated alkali — Selective conversion of MBC to 2-AB; benomyl in this case will selectively convert to BBU.

Finally, we would like to mention that, although the results reported here are preliminary in nature, these may be very timely and useful as, due to the recent controversy regarding the use of benomyl in some states of the U.S.A., methods of characterization and determination of benomyl and its degradation compounds in crops, soil and water are greatly required (71). Du Pont has named 15 universities in U.S.A. to provide independent tests on crops damage by Benlate DF fungicide, claimed by growers (71).

Acknowledgements

We thank the Ontario Ministry of Environment and Energy for funding this work under the Research Advisory Committee (Grant 1384). The Natural Science and Engineering Research Council of Canada (NSERC) is thanked for an equipment grant for the purchase of the Kratos mass spectrometer.

REFERENCES

1. The Biological and Economical Assessment of Benomyl, United States Department of Agriculture, November 1985.
2. C.J. Delp, in H. Lyr (Editor), Modern Selective Fungicides — Properties, Applications, Mechanisms of Action, Longman Group, London, 1987, pp. 233-244.
3. M. Chiba, A.W. Bown and D. Danic, Can. J. Microbiol., *33* , 157 (1987).
4. D.J. Hall, Proc. Fla. State Hortic. Soc., *93*, 341 (1980).
5. R.S. Hammerschlag and H.D. Sisler, Pestic. Biochem. Physiol., *3*, 42 (1973).
6. W. Koller, C.R. Allan and P.E. Kolattukudy, Pestic. Biochem. Physiol., *18*, 15 (1982).
7. C.H. Liu, G.C. Mattern, X. Yu and D. Rosen, J. Agric. Food Chem., *38*, 167 (1990).
8. R. P. Singh and M. Chiba, J. Chromatgr., *643*, 249 (1993).
9. F.J. Baude, J.A. Gardiner and J.Y.C. Han, J. Agric. Food Chem., *21*, 1084 (1973).
10. J.J. Kirkland, R.F. Holt and H.L. Pease, J. Agric. Food Chem., *21*, 368 (1973).
11. P. Slade, J. Assoc. Off. Anal. Chem., *58*, 1244 (1975).
12. S. Gorbach, Pure Appl. Chem., *52*, 2569 (1980).
13. T.D. Spittler, R.A. Marafioti and L.M. Lahr, J. Chromatogr., *317*, 527 (1984).
14. G. Zweig and R. Gao, Anal. Chem., *55*, 1448 (1983).
15. R.P. Singh, I.D. Brindle, C.D. Hall and M. Chiba, J. Agric. Food Chem., *38*, 1758 (1990).
16. C.H. Marvin, I.D. Brindle, R.P. Singh, C.D. Hall and M. Chiba, *J. Chromatogr.*, *518*, 242 (1990).

17. M.Chiba, in R. Greenhalgh and T.R. Roberts (Editors), Proceedings of Sixth International Congress of Pesticide Chemistry, Ottawa, Canada, August 10-15, Blackwell Scientific Publications, London, 1986, pp. 339-340.
18. J.P. Rouchaud and J.R. Decallonne, J. Agric. Food Chem., *22*, 259 (1974).
19. H. Pyysalo, J. Agric. Food Chem., *25*, 975 (1977).
20. E.R. White and W.W. Kilgore, J. Agric. Food Chem., *20*, 1230 (1972).
21. J.J. Kirkland, J. Agric. Food Chem., *21*, 171 (1973).
22. S. Cline, A. Felsot and L. Wei, J. Agric. Food Chem., *29*, 1087 (1981).
23. J.E. Farrow, R.A. Hoodless, M. Sargent and J.A. Sidwell, Analyst (London), *102*, 752 (1977).
24. C. Sanchez-Brunete, A.D. Cal, P. Melgarejo and J.L. Tadeo, Int. J. Environ. Anal. Chem., *37*, 35 (1989).
25. U. Kiigemagi, R.D. Inman, W.M. Mellenthin and M.L. Deinzer, J. Agric. Food Chem., 39, 400 (1991).
26. C. Bicchi, F. Belliardo and L. Cantamessa, Pestic. Sci., *25*, 355 (1989).
27. M. Maeda and A. Tsuji, J. Chromatogr., *120*, 449 (1976).
28. D.J. Austin, K. Alan and I.H. Williams, Pestic. Sci., *7*, 211 (1976).
29. P. Cobras, M. Meloni, M. Perra and F.M. Pirisi, J. Chromatogr., *180*, 184 (1979).
30. R.P. Singh and M. Chiba, J. Agric. Food Chem., *33*, 63 (1985).
31. M. Chiba and R.P. Singh, J. Agric. Food Chem., *34*, 108 (1986).
32. R. F. Browner, P. C.Winkler, D. D. Perkins and L. E. Abby, Microchem. J., *34*, 15 (1986),.
33. P. C. Winkler, D. D. Perkins, W. K. Williums and R. F. Browner, Anal. Chem., *60*, 489 (1988).
34. W. V. Ligon Jr.and S. B. Dorn, Anal. Chem., *62*, 2573 (1990).

35. T. R. Covey, E. D. Lee, A. P. Bruins and J. D. Henion, Anal. Chem., *58*, 1451A, (1986).
36. P.J. Arpino, J. Chromatogr., *325*, 3 (1985).
37. P. J. Arpino and G. Guiochon, Anal. Chem., *51*, 682A (1979).
38. T. Tsuda, G. Keller and H-J. Stan, Anal. Chem., *57*, 2280 (1985).
39. C. R. Blakley and M. L. Vestal, Anal. Chem., *55*, 750 (1983).
40. M. J. Hayward, J. T. Snodgrass and M. L. Thomson, Rapid Commun. Mass Spectrom., *7*, 85 (1993).
41. J. Abian, A. Stone, A., M. G. Marrow, M. H. Creer, L. M. Fink, and J. O. Lay Jr., Rapid Commun. Mass Spectrom., *6*, 684 (1992).
42. M. F. Bean, S. L. Pallante-Morell, D. M. Dulik and C. Fenselau, Anal. Chem., *62*, 121 (1990).
43. D. Barcelo, Org. Mass Spectrom., *24*, 898 (1989).
44. P. Arpino, Mass Spectrometry Reviews, *11*, 3 (1992).
45. C. M. Whitehouse, R. N. Dreyer, M. Yamashita and J. B. Fenn, Anal. Chem., *57*, 675 (1985).
46. H-Y. Lin and R. D. Voyksner, Anal. Chem., *65*, 451 (1993).
47. E. D. Lee and J. D. Henion, Rapid Commun. Mass Spectrom., *6*, 727 (1992).
48. T. R. Covey, E. D. Lee and J. D. Henion, Anal. Chem., *58*, 2453 (1986).
49. E. C. Horning, D. I. Carroll, I. Dzidic, K. D. Heagle, M. G. Horning and R. N. Stillwell, J. Chromatogr. Sci., *12*, 725 (1974).
50. D. R. Deorg and S. Bajic, Rapid Commun. Mass Spectrom., *6*, 663 (1992).
51. S. Pleasance, J. F. Anacleto, M. R. Bailey, and D. H. North, J. Am. Soc. Mass Spectrom., *3*, 378 (1992).
52. D. R. Deorge, M. W. Burger and S. Bajic, Anal. Chem., *64*, 1212 (1992).
53. T. D. Behymer, T. A. Bellar and W. L. Budde, Anal. Chem., *62*, 1686 (1992).

54. I. S. Kim, F. I. Sasinos, R. D. Stephens and M. A. Brown, J. Agric. Food Chem., *38*, 1223 (1990).

55. D. R. Deorge and C. J. Miles, Anal. Chem., *63*, 1999 (1991).

56. J. Hsu, Anal. Chem., *64*, 434 (1992).

57. R. Galimberti, P. Lecchi, L. D. Angelis, D. Caruso, A. V. Toia and G. Racagni, Anal. Biochem., *201*, 356 (1992).

58. R. D. Voyksner, C. S. Smith and P. C. Knox, Biomed. Environ. Mass Spectrom., *19*, 523 (1990).

59. C. J. Miles, D. R. Deorge and S. Bajic, Arch. Environ. Contam. Toxicol., *22*, 247 (1992).

60. J. S. Ho, T. D. Beymer, W. L. Budde and T. A. Bellar, J. Am. Soc. Mass Spectrom., *3*, 662 (1992).

61. L. Donnelly Betowsky, C. M. Pace and M. R. Roby, J. Am. Soc. Mass Spectrom., *3*, 823 (1992).

62. M. Barber, R.S. Bordoli, R.D. Sedgwick and A.N. Tyler, J. Chem. Soc. Chem. Commun., 325 (1981).

63. D.J. Surman and J.C. Vickerman, J.Chem. Soc. Chem. Commun., 324 (1981).

64. S.A. Martin, C.E. Costello and K. Bleman, Anal. Chem., *54*, 2362 (1982).

65. R.M. Caprioli, T. Fan and J.S. Cottrell, Anal. Chem., *58*, 2949 (1986).

66. R. B. van Breeman, H. S. Schmitz and S. J. Schwartz, Anal. Chem., 65, 965 (1993).

67. K. A. Caldwell, V. M. Sada gopa Ramanujam, Zongwei Cai, M. L. Gross and R. F. Spalding, Anal. Chem., 65, 2372 (1993).

68. R.P. Singh, I.D. Brindle, T.R.B. Jones, J.M. Miller and M. Chiba, Rapid Commun. Mass Spectrom., *7*, 167 (1993).

69. R.P. Singh, I.D. Brindle, T.R.B. Jones, J.M. Miller and M. Chiba, J. Am. Soc. Mass Spectrom., *4*, 898 (1993).

70. T. A. Clark, EPA Technical Report No. EPA/600/R-92/129, August 92, US Environmental Protection Agency, Cincinnati, Ohio 45268, pp. 173-213.

71. Chemical & Engineering News, July 12, 13(1993).

Figure Captions

Figure 1. Molecular structures of MBC, STB, BBU and 2-AB.

Figure 2. Particle beam-mass-spectrometric (PB-MS) sensitivities for 2-AB (m/z = 133), MBC (m/z = 159), BBU (m/z = 232) and STB (m/z = 258).

Figure 3. Effect of source temperature on the sensitivity of 2-AB.

Figure 4. Particle beam - mass chromatograms for different concentrations of 2-AB.

Figure 5. PB-EI mass spectrum of total ion current (TIC) of 10 mg L^{-1} 2-AB (upper spectrum) with library spectrum (lower spectrum).

Figure 6. Particle beam - mass chromatograms for different concentrations of MBC.

Figure 7. PB-EI mass spectrum of total ion current (TIC) of 10 mg L^{-1} MBC (upper spectrum) with library spectrum (lower spectrum).

Figure 8. PB-EI mass spectrum of total ion current (TIC) of 100 mg L^{-1} STB (upper spectrum) with solid probe EI spectrum (lower spectrum). The abundances of peaks (m/z) in solid probe spectrum were as follows: 258 (100%); 202 (42.8%); 159 (35.6%); 104 (14.7%); 55 (27.1%).

Figure 9. PB-EI mass spectrum of total ion current (TIC) of 100 mg L^{-1} BBU (upper spectrum) with solid probe EI spectrum (lower spectrum). The abundances of peaks (m/z) in solid probe spectrum were as follows: 232 (17.0%); 160 (23.7%); 159 (28.2%); 133 (100%); 105 (12.8%) 98 (11.9%); 73 (17%); 56 (53.4%).

Figure 10. Plots of the concentrations (mg L^{-1}) of MBC and 2-AB versus peak area counts.

Figure 11. Positive ion FAB-MS spectrum of 2-AB in glycerol.

Figure 12. Positive ion FAB-MS spectrum of 2-AB in 3-NBA.

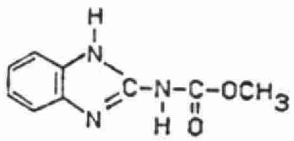

Carbendazim

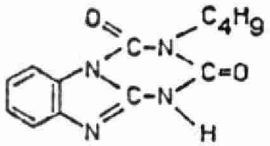

STB

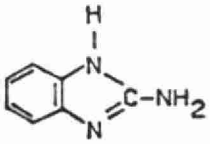

2-AB

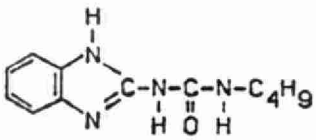

BBU

Singh et al Figure 1

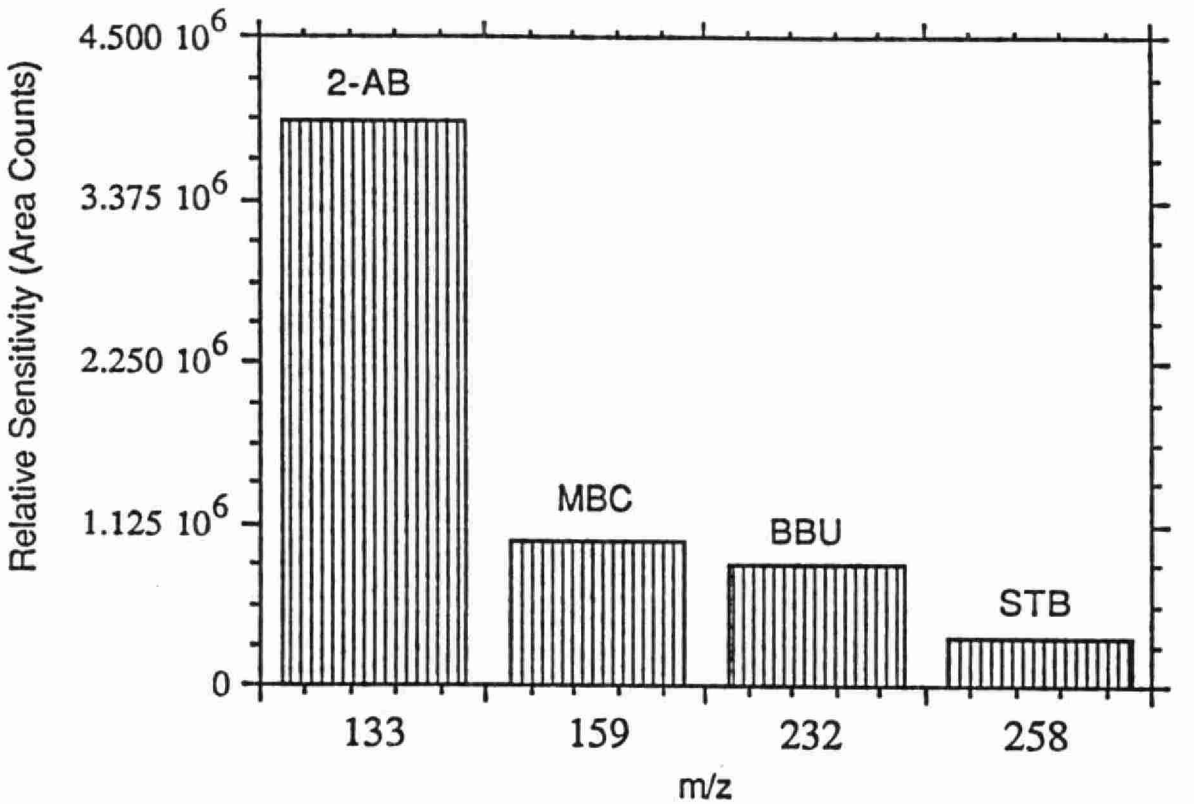
Relative Sensitivity (Area Counts)
4.500 10^6
3.375 10^6
2.250 10^6
1.125 10^6
0
2-AB
MBC
BBU
STB
133
159
232
258
m/z

Singh et al

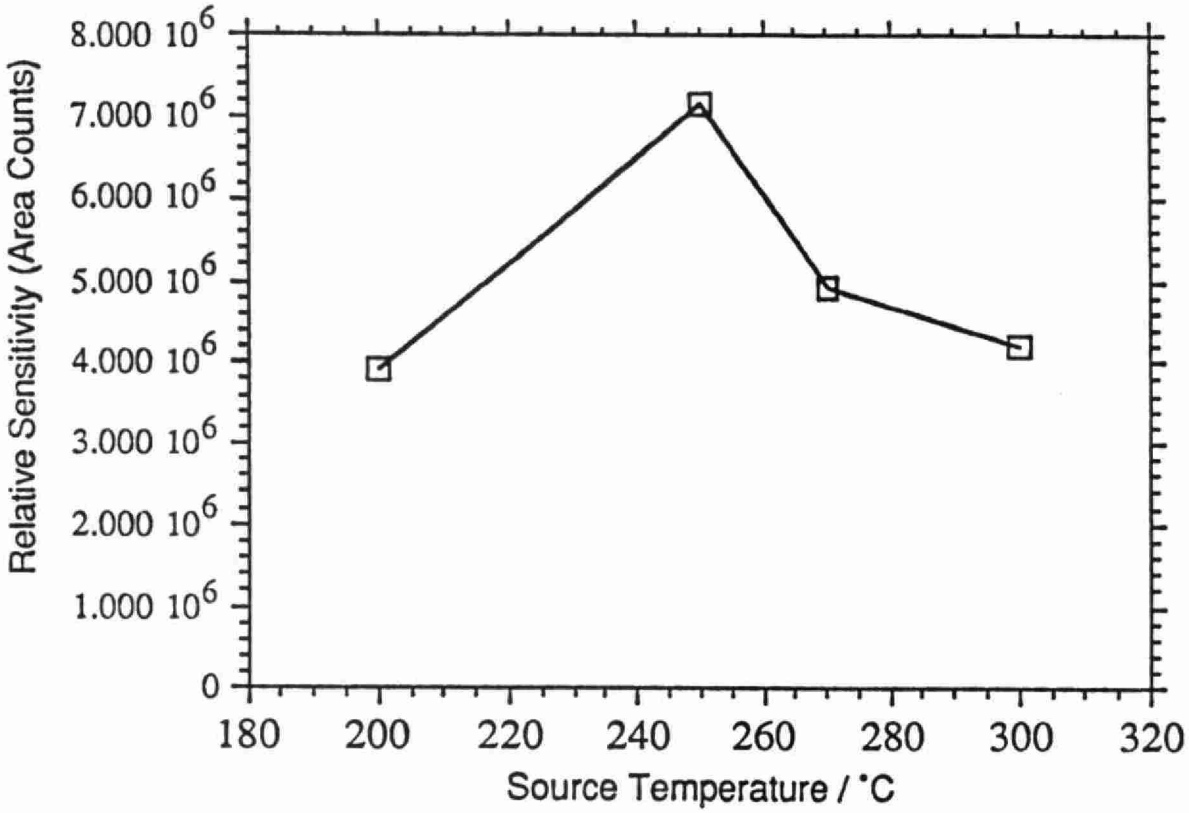

Singh etal

Figure 3

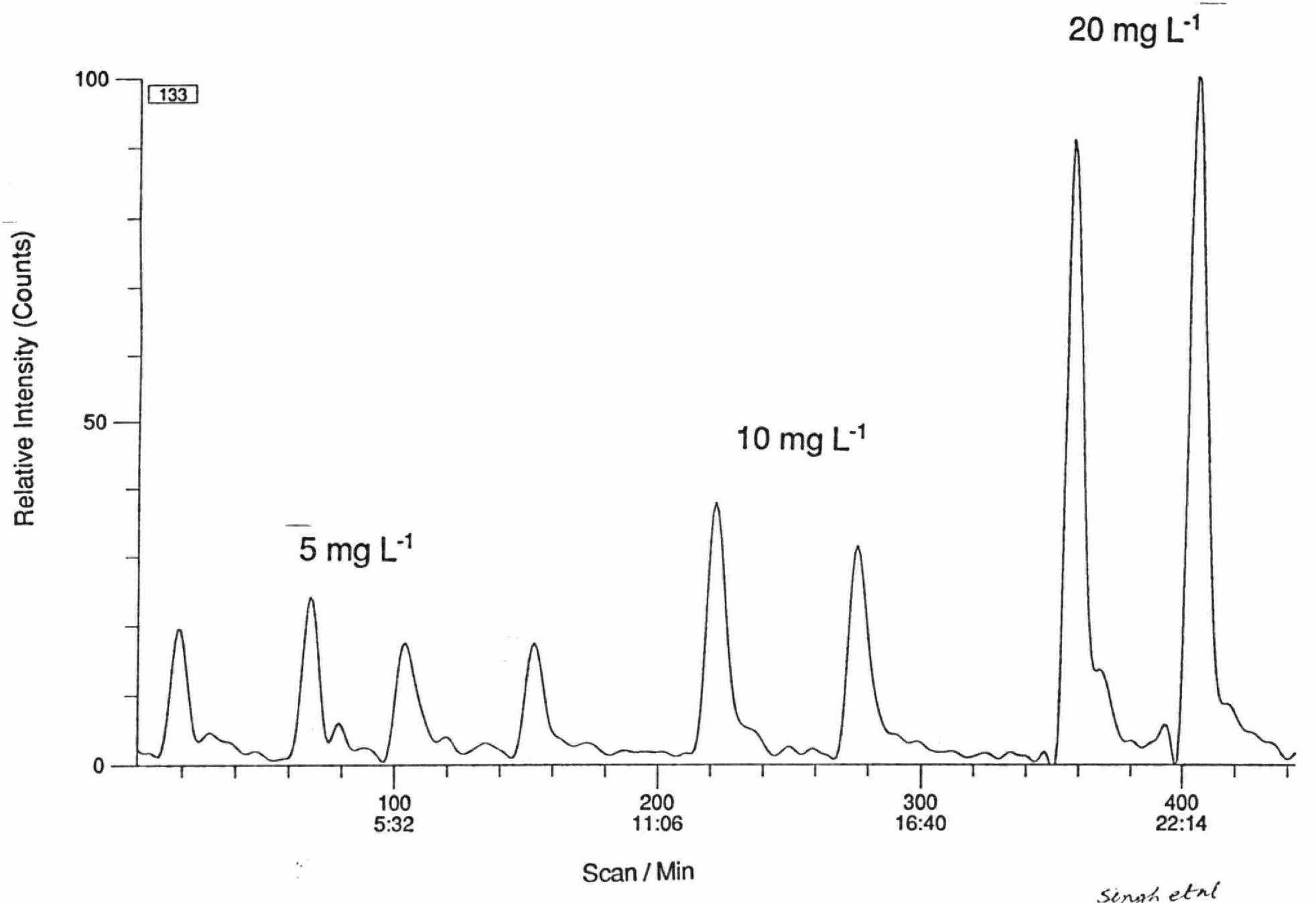
20 mg L-1
100
133
Relative Intensity (Counts)
50
10 mg L-1
5 mg L-1
0
100
5:32
200
11:06
300
16:40
400
22:14
Scan / Min

Singh et al

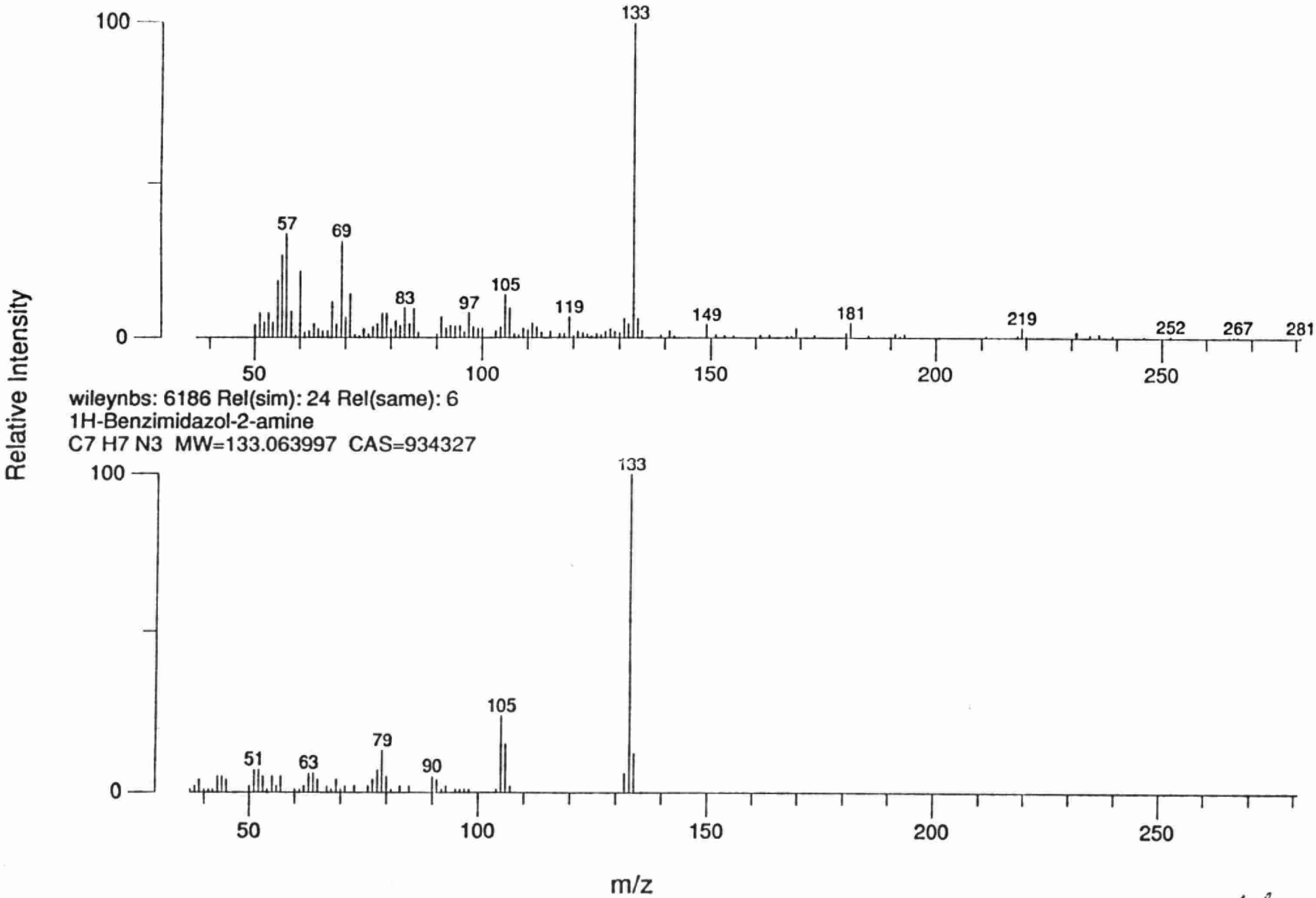
100
0
133
57
69
83
97
105
119
149
181
219
252
267
281
50
100
150
200
250
Relative Intensity
wileynbs: 6186 Rel(sim): 24 Rel(same): 6
1H-Benzimidazol-2-amine
C7 H7 N3 MW=133.063997 CAS=934327
100
0
133
105
79
51
63
90
50
100
150
200
250
m/z

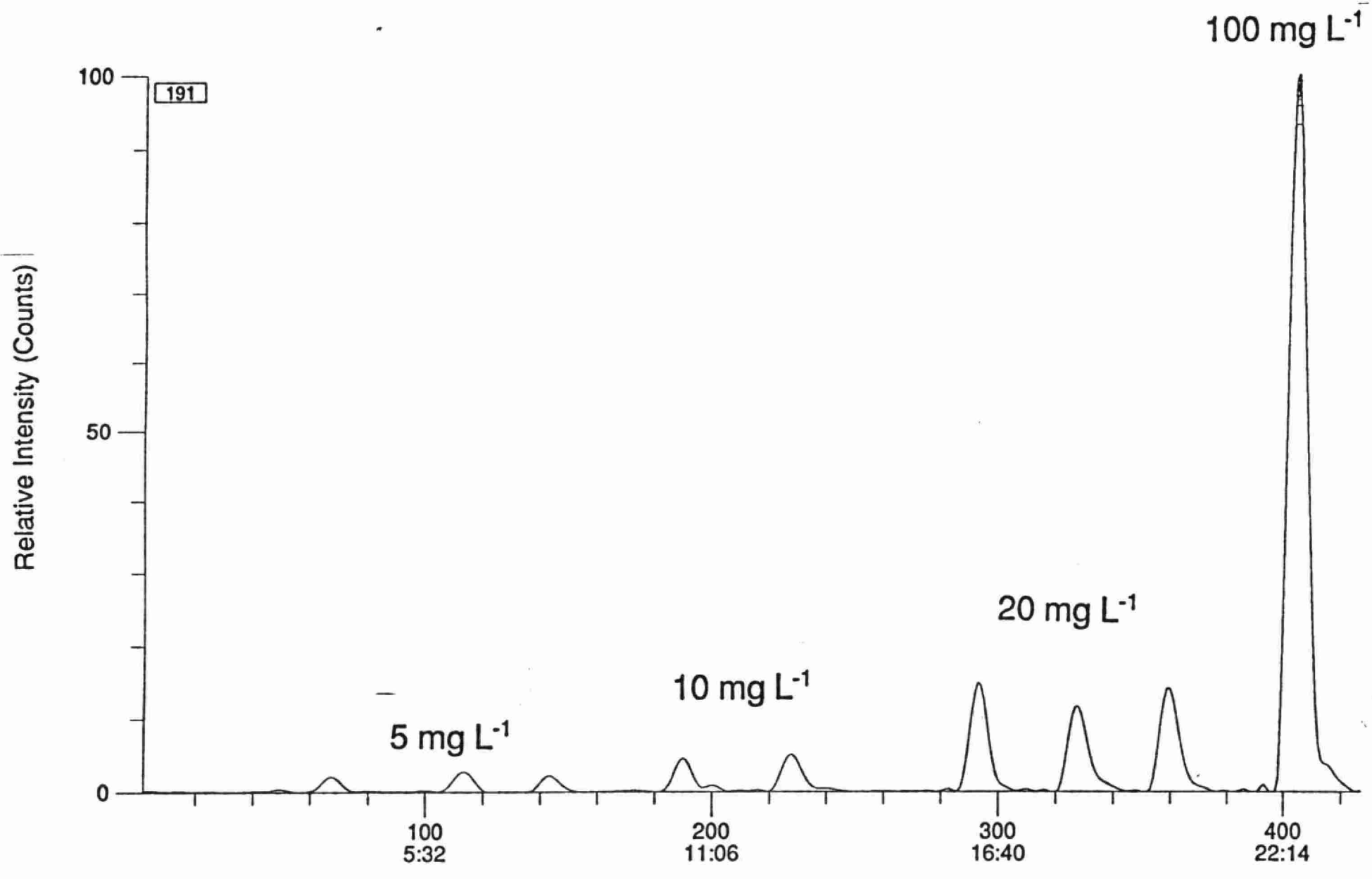

Singh et al
Figure 6

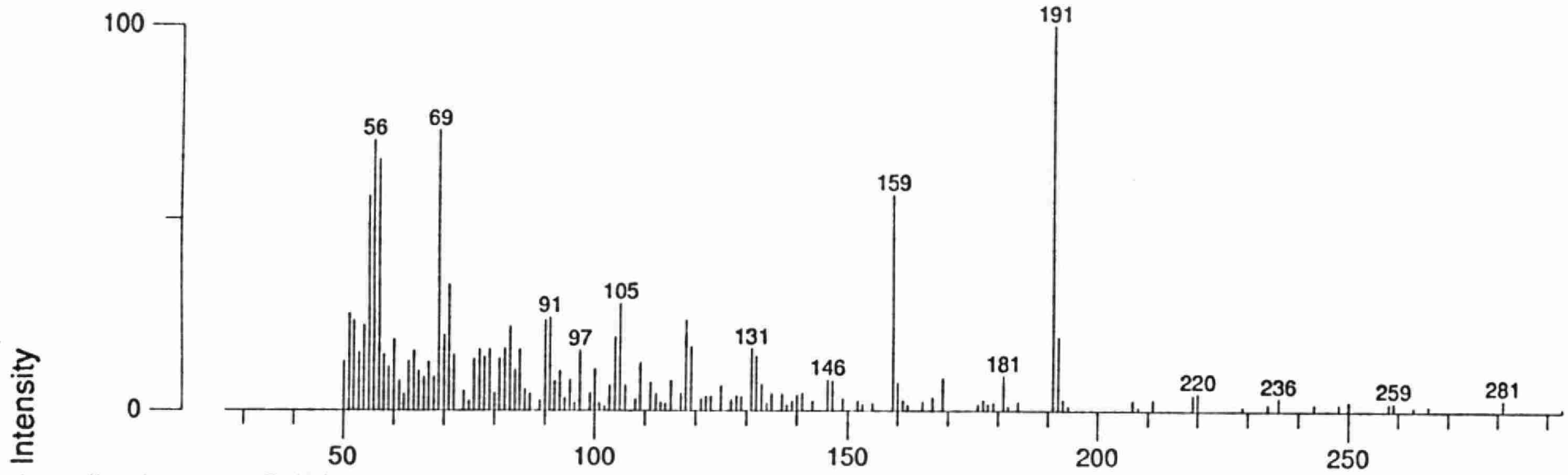

wileynbs: 20898 Rel(sim): 33 Rel(same): 10
Carbamic acid, 1H-benzimidazol-2-yl-, methyl ester
C9 H9 N3 O2 MW=191.069477 CAS=10605217

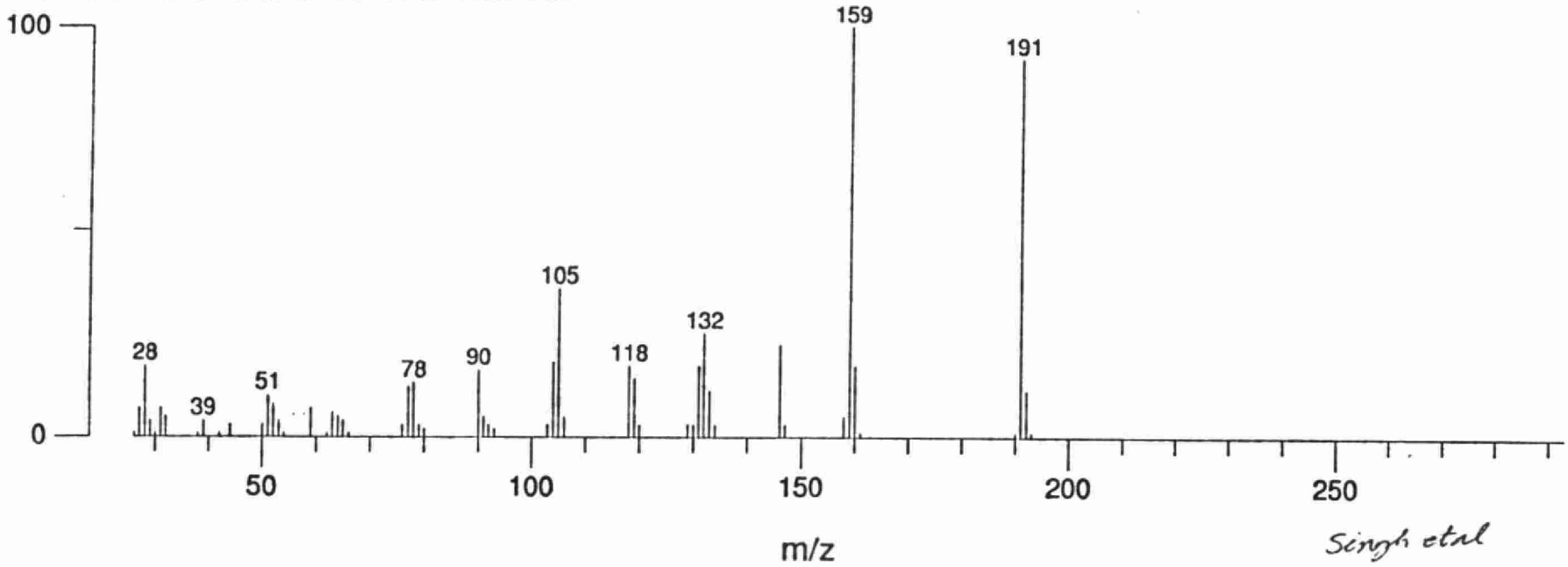

Singh et al

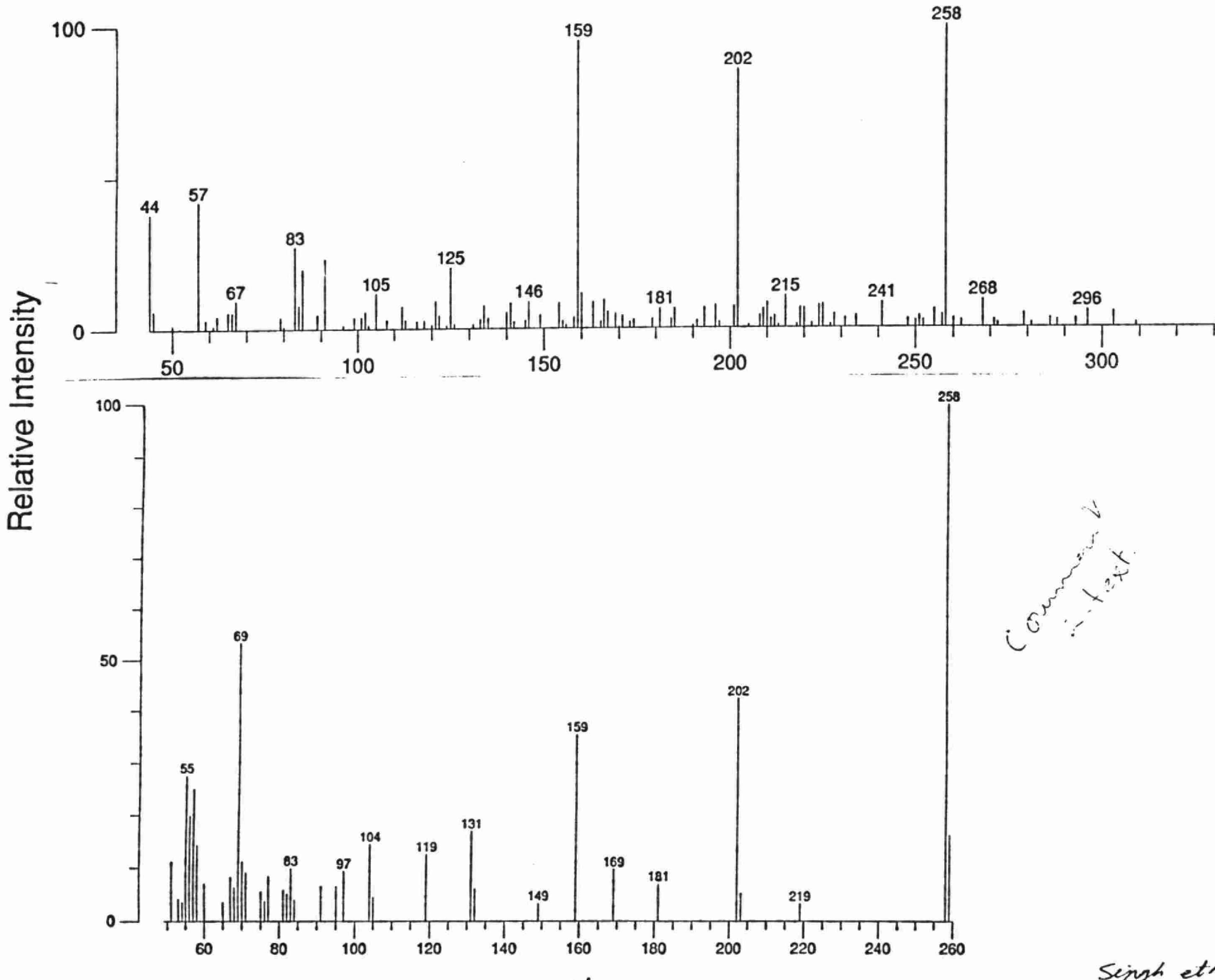

Comment in text.

Singh et al
Figure 8

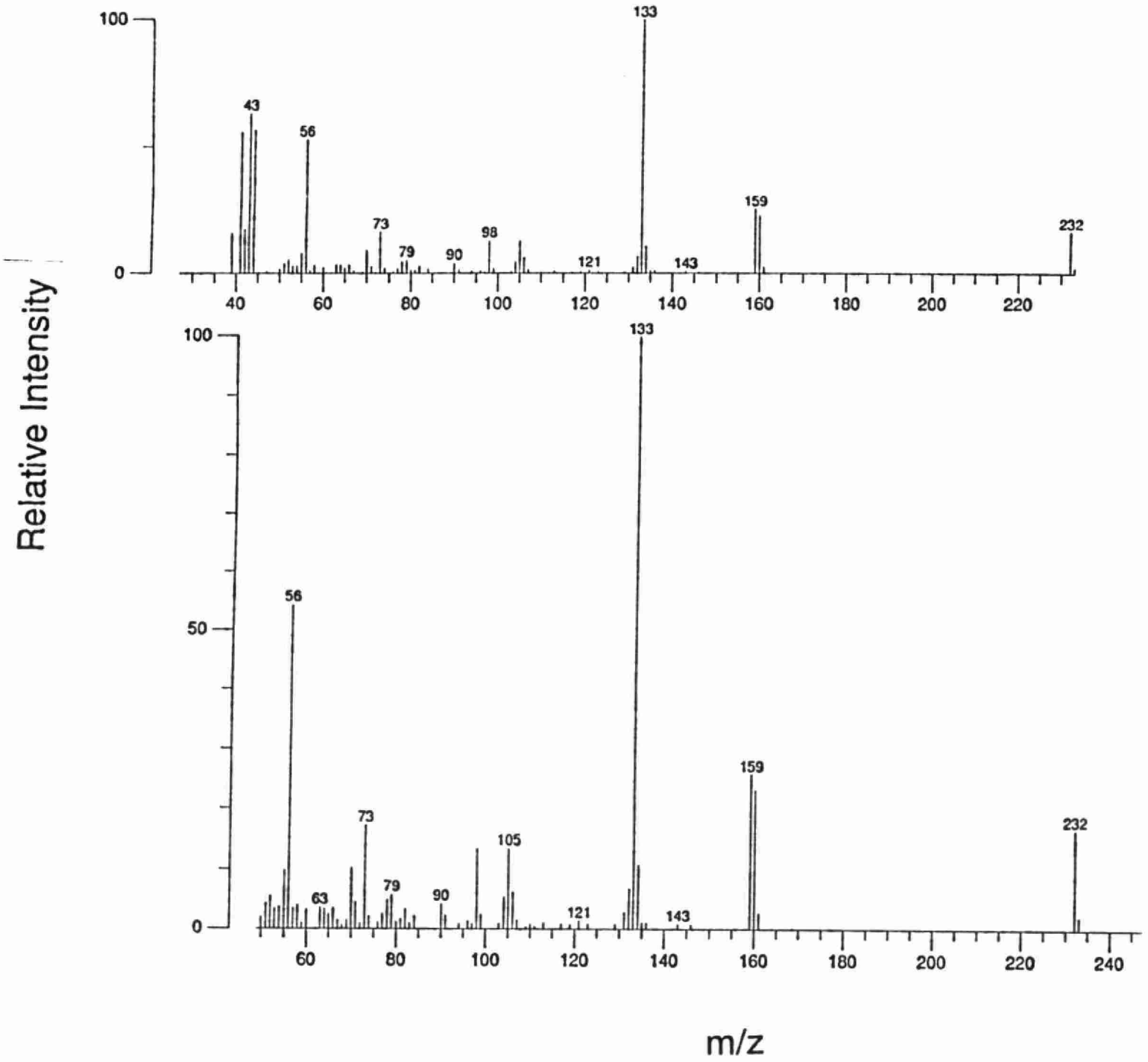
Relative Intensity
100
0
133
43
56
73
79
90
98
121
143
159
232
40
60
80
100
120
140
160
180
200
220
100
50
0
133
56
73
63
79
90
105
121
143
159
232
60
80
100
120
140
160
180
200
220
240
m/z

Singh etal

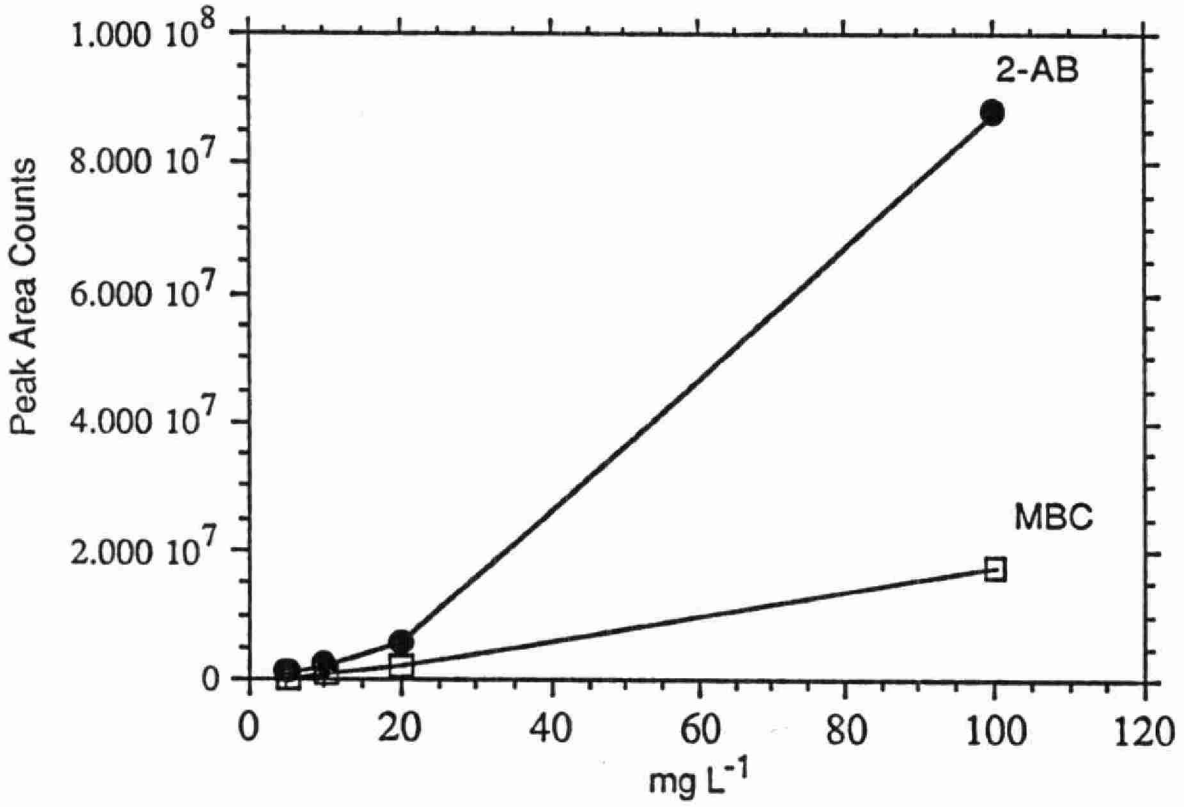

Singh et al
Figure 10

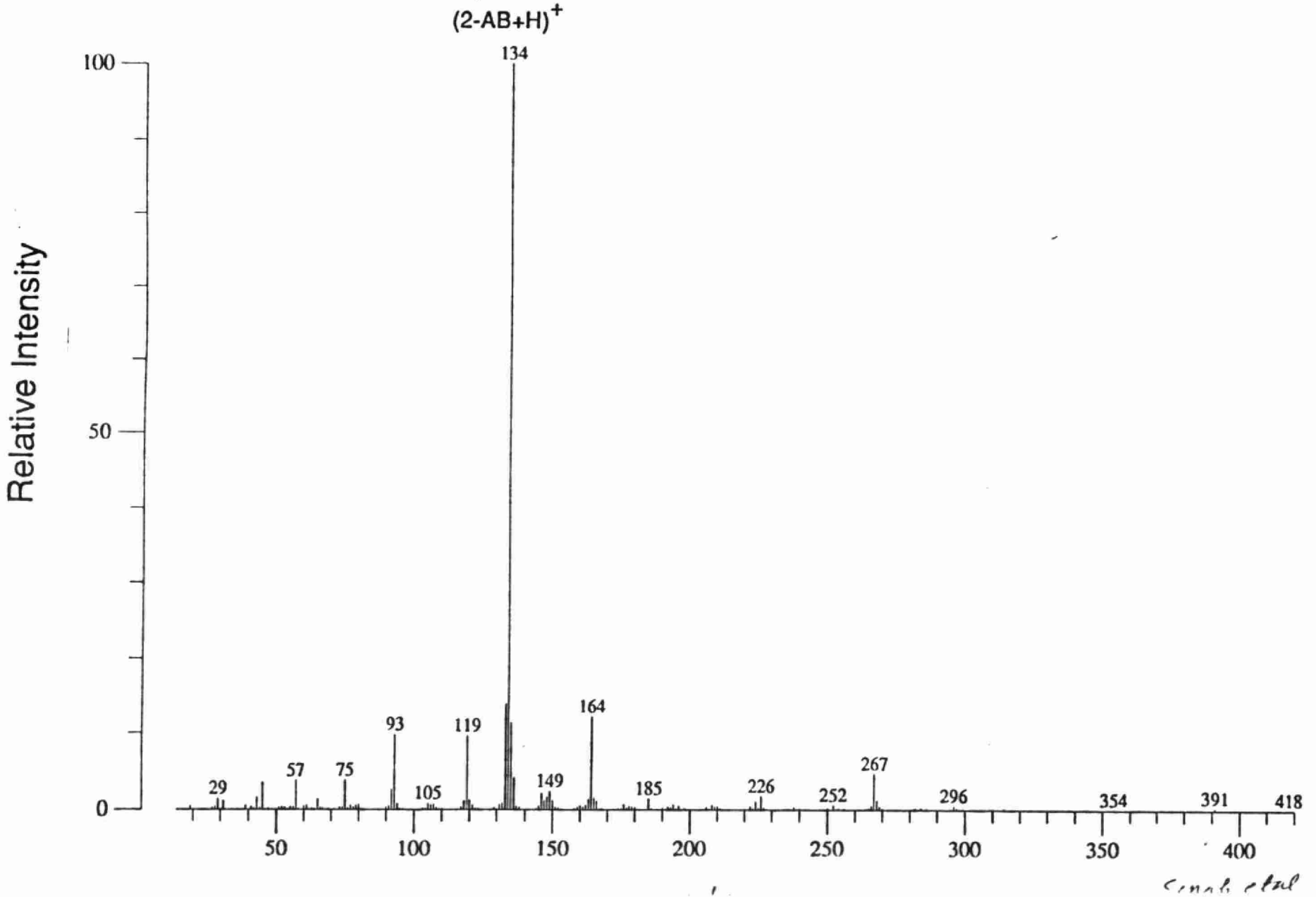
(2-AB+H)+
134
100
50
0
Relative Intensity
29
57
75
93
105
119
149
164
185
226
252
267
296
354
391
418
50
100
150
200
250
300
350
400

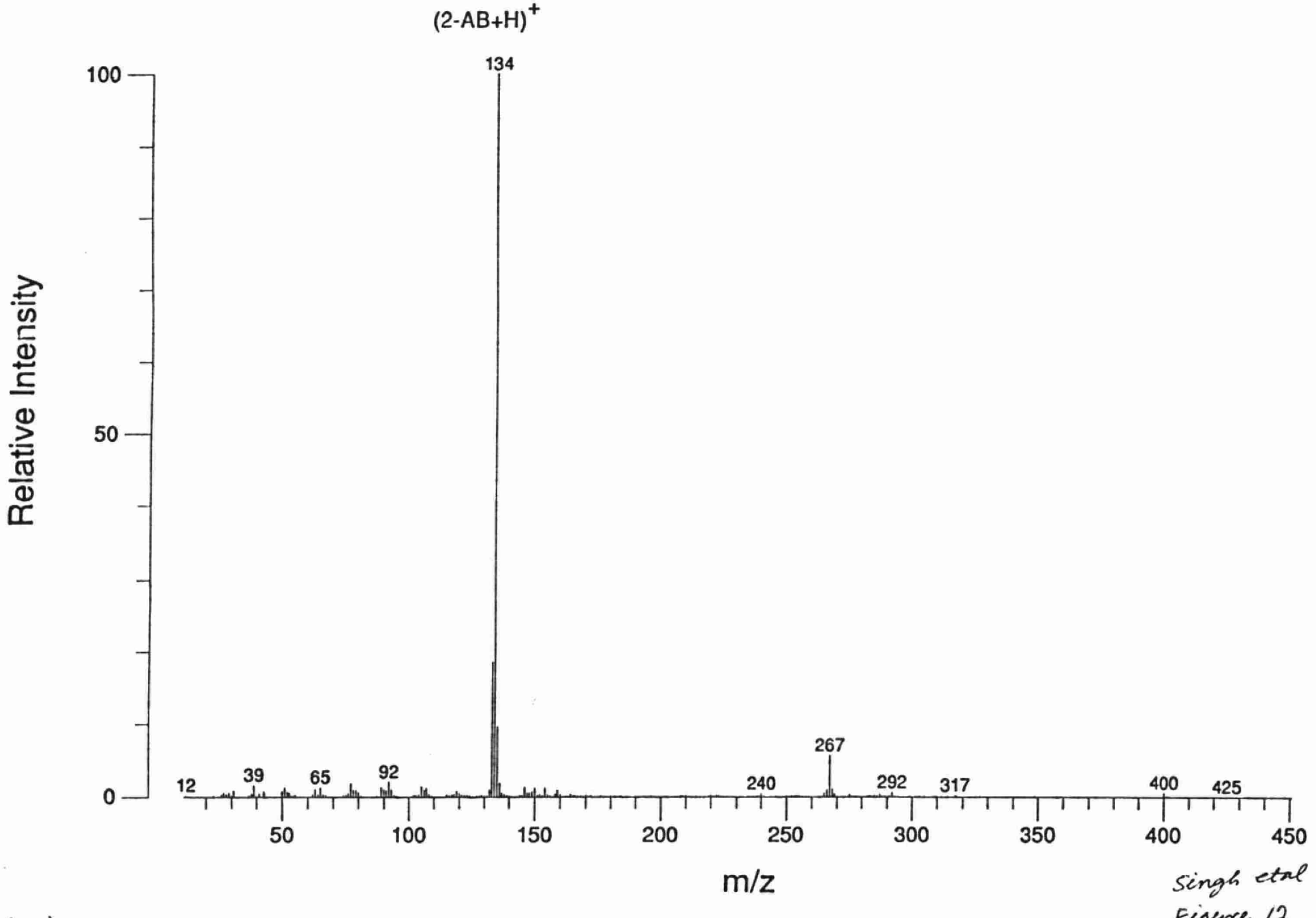

Singh et al
Figure 12

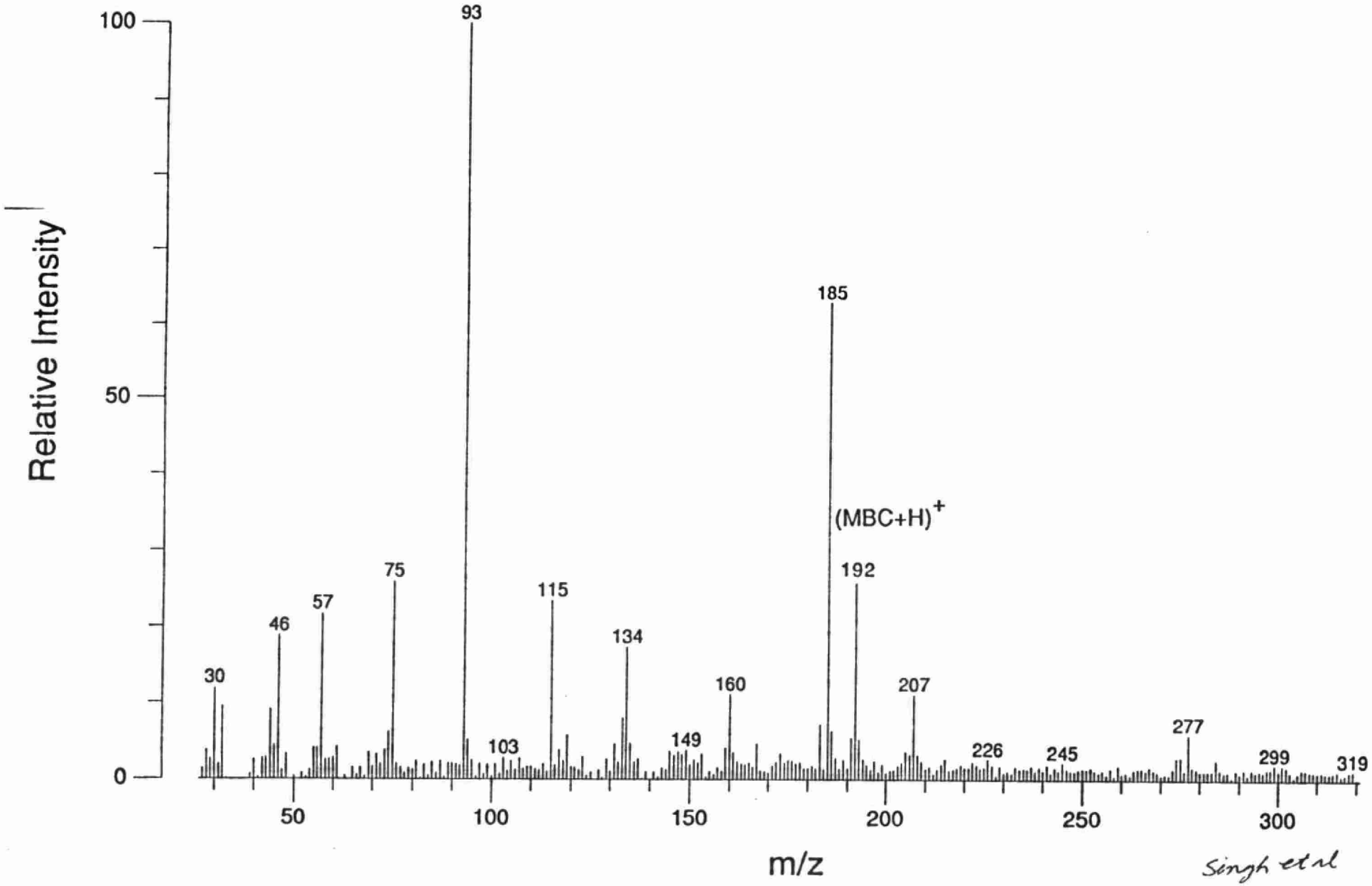
Relative Intensity
100
50
0
93
185
(MBC+H)+
192
75
115
57
46
134
30
160
207
103
149
277
226
245
299
319
50
100
150
200
250
300
m/z
Singh et al

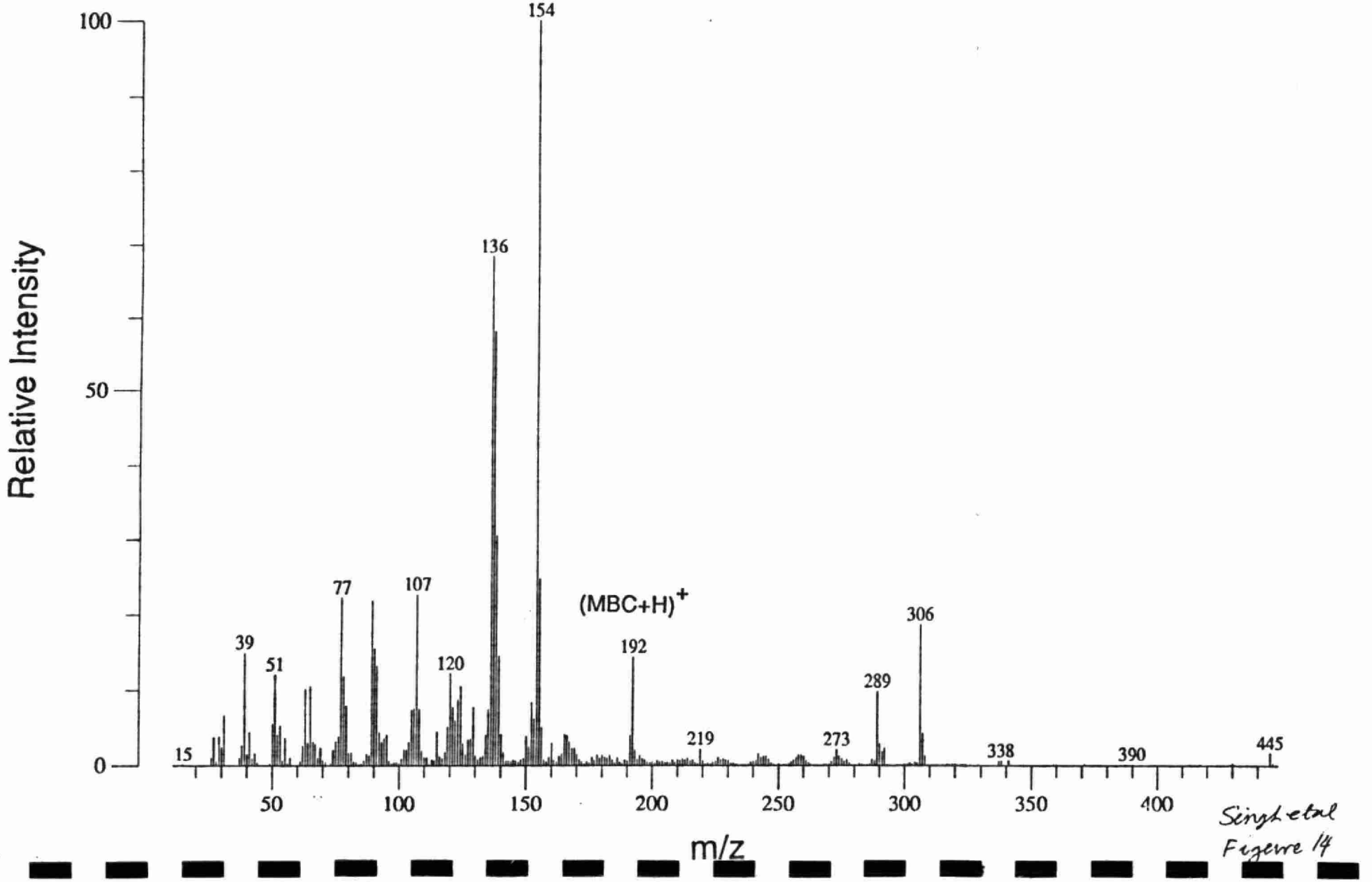

Singh et al
Figure 14

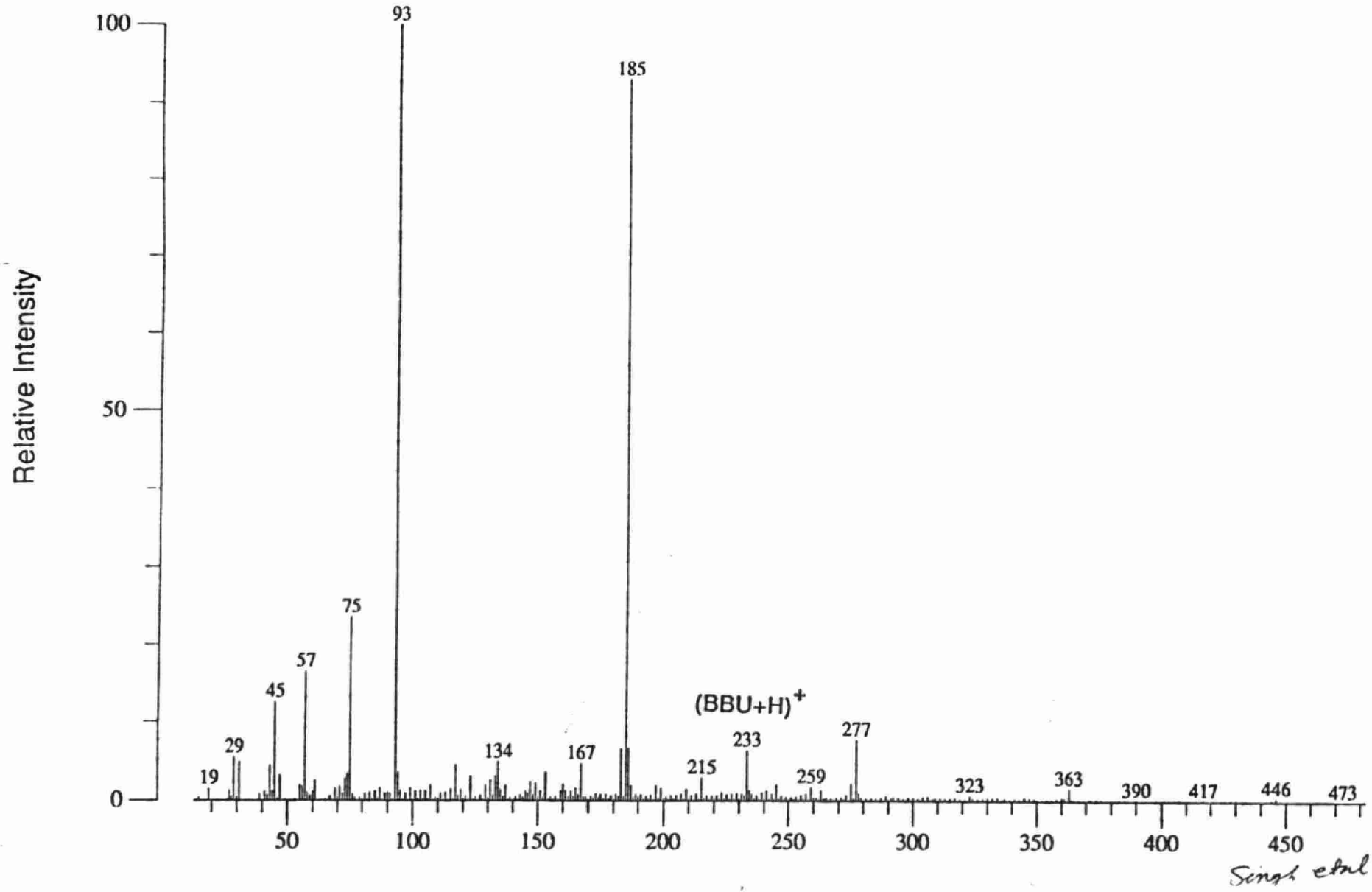
Relative Intensity
100
50
0
93
185
75
57
45
29
19
134
167
215
(BBU+H)+
233
259
277
323
363
390
417
446
473
50
100
150
200
250
300
350
400
450
Singh et al

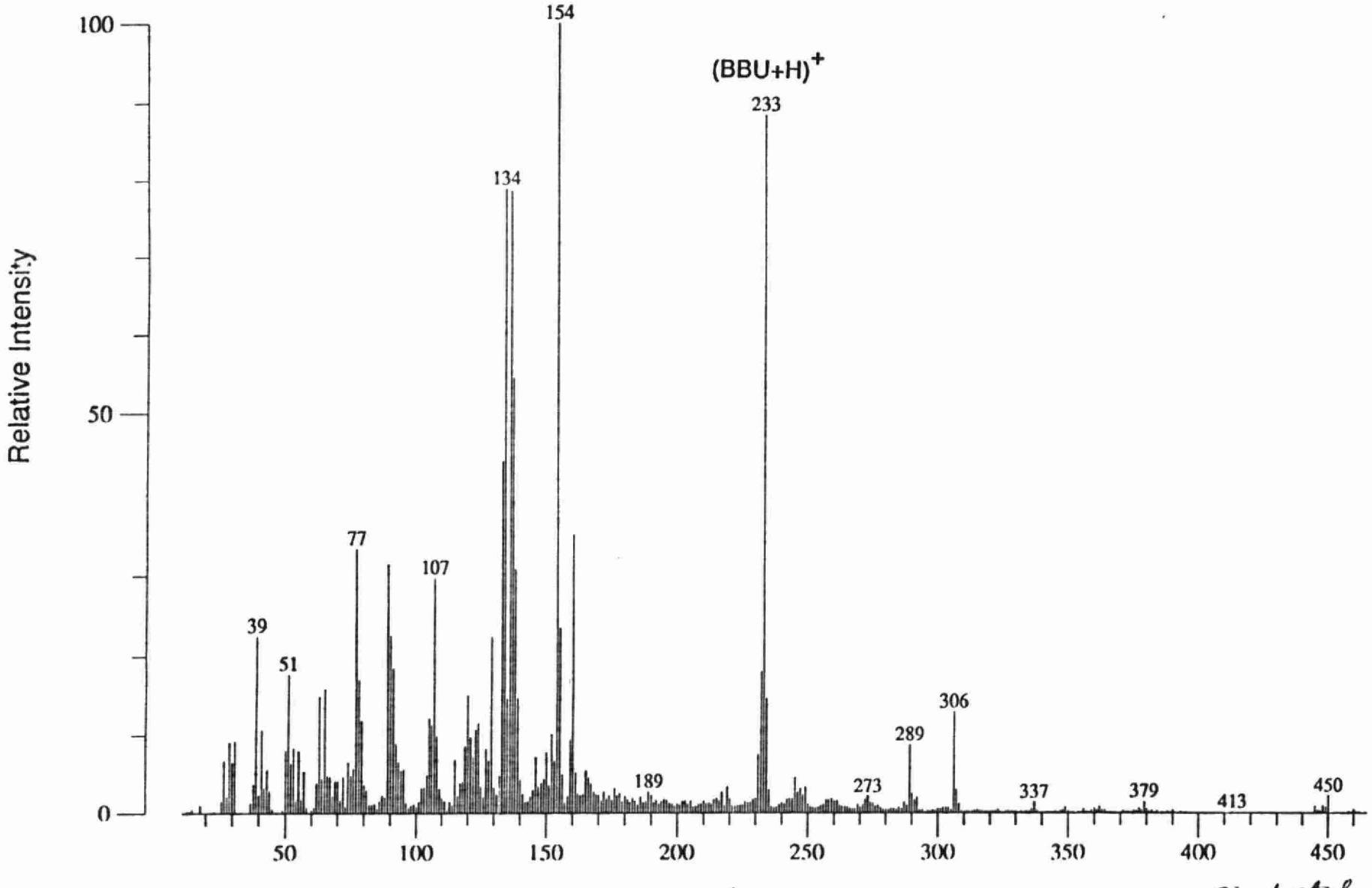
100
50
0
Relative Intensity
154
(BBU+H)+
233
134
77
107
39
51
189
273
289
306
337
379
413
450
50
100
150
200
250
300
350
400
450
m/z

Singh et al

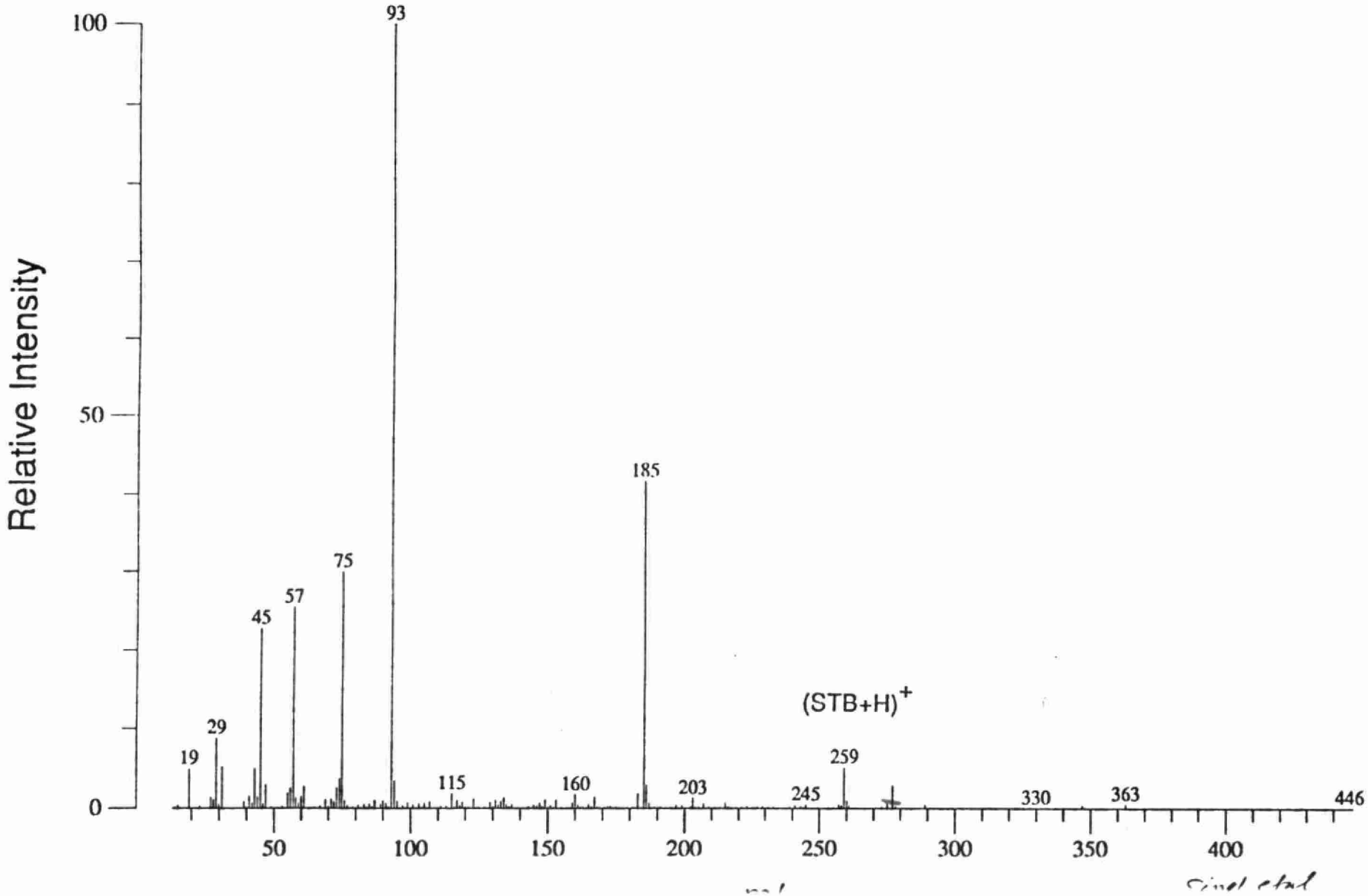
Relative Intensity
100
50
0
93
185
75
57
45
29
19
115
160
203
245
259
330
363
446
(STB+H)+
50
100
150
200
250
300
350
400

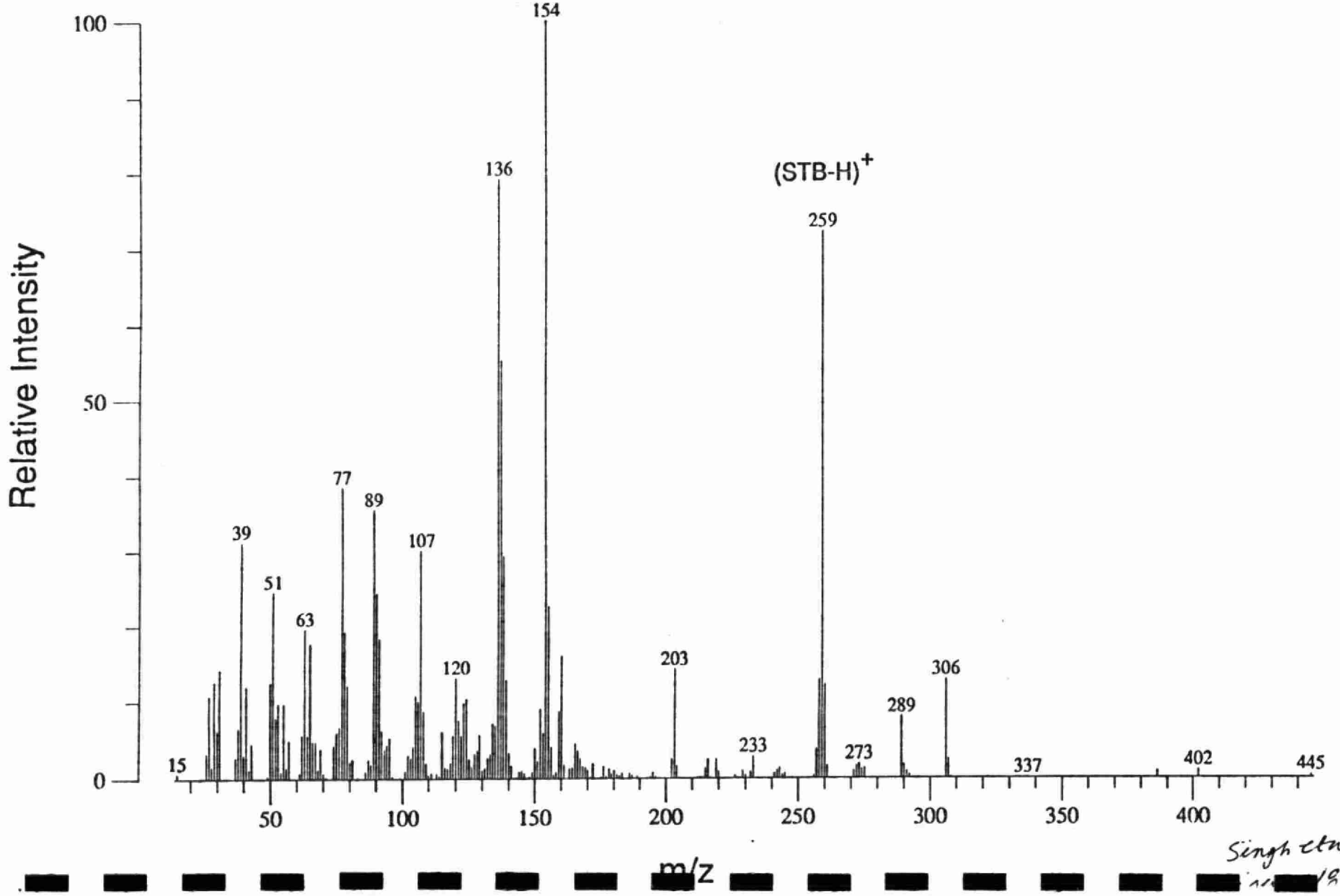
Relative Intensity
100
50
0
154
136
(STB-H)+
259
77
89
39
107
51
63
120
203
306
289
233
273
15
337
402
445
50
100
150
200
250
300
350
400
m/z

Singh et al

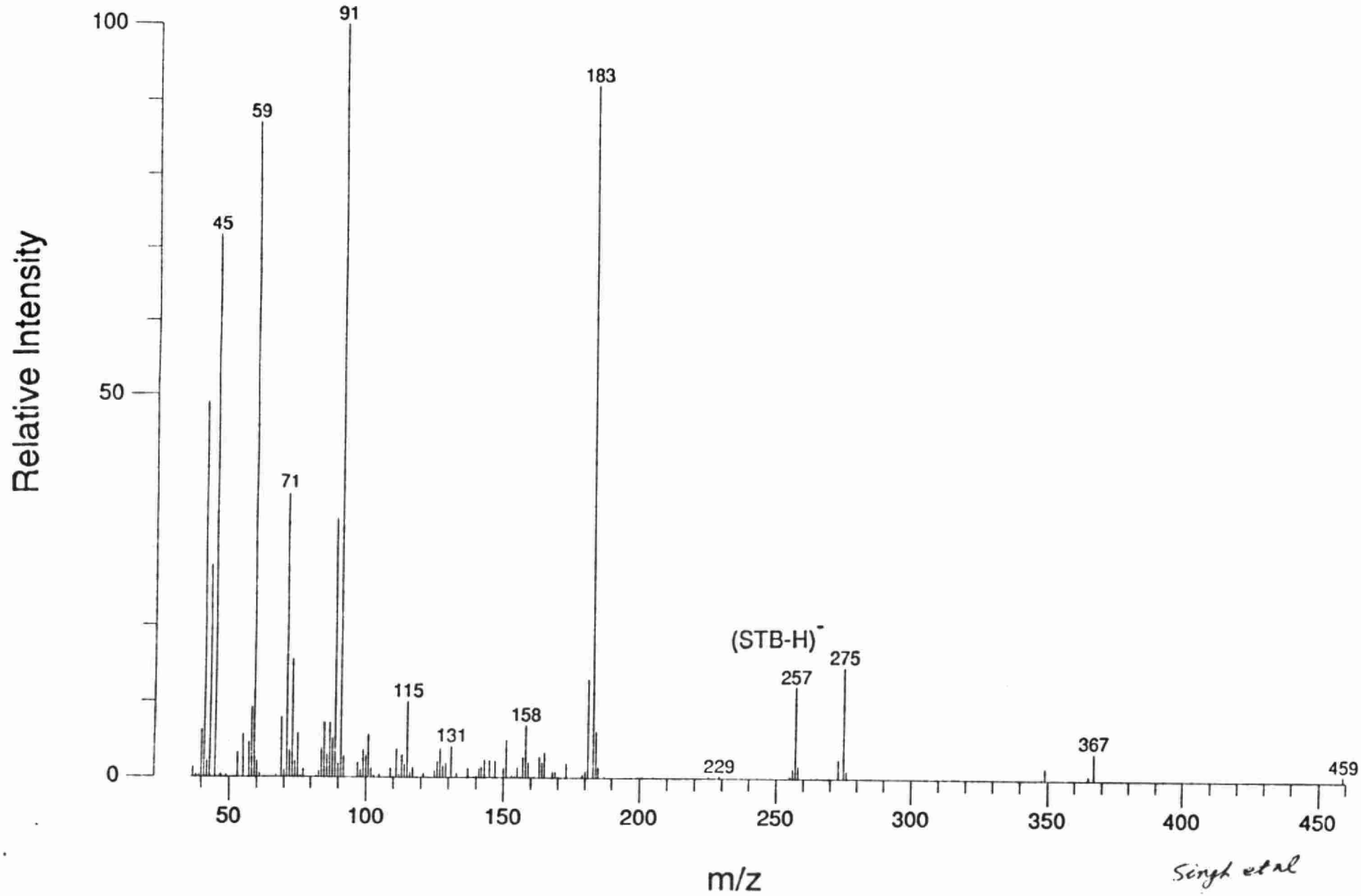
Relative Intensity
100
50
0
91
183
59
45
71
115
131
158
229
(STB-H)⁻
257
275
367
459
50
100
150
200
250
300
350
400
450
m/z
Singh et al

Part II B: Stabilization of Methyl [1-(Butylcarbamoyl)-1H-Benzimidazol-2-yl] Carbamate (Benomyl) in Hydrochloric Acid Solutions

ABSTRACT

In this part we report, for the first time, the preparation of stable stock solutions of benomyl (methyl [1-butylcarbamoyl)-1H-benzimidazol-2-yl] carbamate) in an aqueous medium. The stabilization of benomyl in acidic solutions was proven on the basis of a kinetic study of benomyl decomposition to carbendazim in different concentrations of hydrochloric acid (0.001 to 10 M) by reversed phase high performance liquid chromatography (RP-HPLC). Known amounts of benomyl can be easily dissolved and stabilized in 5 M or higher concentrations of hydrochloric acid. Determinations by RP-HPLC in hydrochloric acid solutions of 5 M or higher concentrations showed no breakdown of benomyl at room temperature for at least 14 days. The presence of benomyl in hydrochloric acid was also confirmed by mass spectrometry using fast atom bombardment (FAB). The stability of benomyl in 5-10 M hydrochloric acid also suggests that samples containing benomyl can be stabilized upon acidification. This stabilization of benomyl samples, after sampling, was not possible in the past.

INTRODUCTION

The systemic fungicide benomyl (methyl [1- (butylcarbamoyl)-1H-benzimidazol-2-yl] carbamate) has been successfully used for the control of many plant diseases for many years (Chiba et al., 1987; Delp, 1987; Hall, 1980; Hammerschlag and Sisler, 1973; Kollar et al., 1982). According to a recent report (Liu et al., 1990) the National Research Council (USA) has estimated the use of benomyl at 2,000,000 lbs of active ingredients per year. Because of its widespread use and suspected

carcinogenic activity, the determination of benomyl in various matrices, such as crops, vegetables, fruits, and water, is frequently required.

Due to its instability in water and organic solvents (Chiba and Doornbos, 1974; Chiba, 1977; Chiba and Cherniak, 1978), benomyl was determined by many workers as its stable degradation compound, carbendazim (methyl 1H-benzimidazol-2-yl-carbamate, commonly known as MBC). The determination was made by high performance liquid chromatography (HPLC) after quantitative conversion of the parent benomyl to carbendazim (Austin et al., 1976; Bradalaye and Wheeler, 1985; Gorbach, 1980; Kirkland, 1973; Kirkland et al., 1973; Spittler et al., 1984; Zweig and Gao, 1983). The major problem associated with this method is that carbendazim, that is produced from benomyl as its degradation product during the analysis, cannot be distinguished from the carbendazim which was present in the sample as the natural degradation product of benomyl. Moreover, since carbendazim is also fungitoxic, and its biological activity is different from benomyl, analytical determination of benomyl as MBC has only limited applications.

Considering the above-mentioned problems, Chiba and Singh (1986) developed an indirect reversed-phase HPLC (RP-HPLC) method for the simultaneous determination of benomyl and carbendazim in water. In this method, benomyl is determined as 3-butyl-2, 4-dioxo-s-triazino [1,2-*a*] benzimidazole (STB) after its quantitative conversion to STB at pH 13. During the treatment of benomyl (and carbendazim) with alkaline solution (pH 13), carbendazim remained mostly intact and was determined as carbendazim along with STB. Although this method can be used for the accurate determination of benomyl and carbendazim in water and other matrices, such as wettable powders, development of a RP-HPLC method for direct determination of benomyl and stabilization of benomyl samples after sampling remained highly desirable.

In recent papers (Singh et al. 1990; Marvin et al., 1990), we have shown that low concentrations of benomyl in water can be determined by a RP-HPLC method without any observable conversion of benomyl to carbendazim. However, it was not possible to prepare benomyl stock solutions of the desired strength. Stock solutions of benomyl are normally prepared in organic solvents but due to its instability in organic solvents, benomyl rapidly converts to carbendazim before aqueous solutions can be prepared by dilution with water.

Aqueous solutions of benomyl can be prepared by using an ultrasonic technique (Singh and Chiba, 1985) or with the aid of a surfactant (Chiba and Northover, 1988). These methods are rather impractical for routine HPLC analyses because it is very difficult to prepare standards containing known and desired concentration of benomyl in aqueous media. In view of the above difficulties it is quite obvious that direct determination of benomyl in aqueous media, preparation of stable stock standards of benomyl of desired concentrations in aqueous media, and stabilization of benomyl-containing samples after sampling, are desirable goals for the determination of benomyl in various types of samples.

In this paper, we report that, contrary to previously published reports (Pyysalo, 1977; Spittler et al., 1984), benomyl can be stabilized in acidic media. Standard aqueous solutions of desired concentrations of benomyl can be prepared in hydrochloric acid (HCl) and are stable over long periods of time.

MATERIALS AND METHODS

Solvents. Acetonitrile was HPLC grade from Caledon Laboratories, Ltd., Georgetown, Ontario L7G 4R9, Canada. Water was distilled in glass in the laboratory.

Chemicals. Benomyl and carbendazim analytical standards were obtained from E. I. du Pont de Nemours and Co., Inc.

Instrumentation. The liquid chromatograph used was a Perkin-Elmer Series 3 equipped with a 50 mL Rheodyne syringe loop-type injector and a Perkin-Elmer LC-55 UV detector.

HPLC Operating Conditions. A Vydac reversed phase C-18, 5 mm, 15 cm X 4.6 mm (i.d.) column was used. The UV detector was operated at 280 nm. The chart speed was 1 cm min^{-1} and the detector sensitivity was 0.05 AUFS at a recorder range of 1.0 mVFS. The total system was operated at ambient temperature.

Mobile Phase. A mixture of 45% acetonitrile and 55% water was used isocratically.

Flow Rate. The flow rate was fixed at 1.0 mL min^{-1}.

Procedure. A sample of pure benomyl was dissolved at 1130 mg L^{-1} in 10 M HCl and the kinetic rate constant of benomyl in the solution was determined by measuring the benomyl peak height with time as follows:

$$k = \frac{2.303}{\Delta t} \log \frac{C_1}{C_2}$$

where C_1 is the benomyl peak height at time t_1, C_2 is the benomyl peak height at t_2, and $\Delta t = t_2 - t_1$. Similarly, benomyl solutions were prepared in varying concentration of HCl (0.001 M - 5 M) and the kinetic rate constants were determined. The k values so calculated at different time intervals compared favorably confirming first-order rate kinetics. Since the use of the analytical column is recommended between pH 2 and 7, these benomyl solutions were diluted to an HCl concentration of 0.01 M prior to the injection of 50 mL of solution onto the analytical column.

Mass Spectrometry. Analysis of benomyl solution (in 5 M HCl) was carried out on a Kratos Concept IS double-focusing mass spectrometer (Kratos Analytical,

Urmston, Manchester, UK) using a fast atom bombardment (FAB) source, at room temperature.

RESULTS AND DISCUSSION

The results of the kinetic studies are listed in Table I. These results clearly indicate that benomyl is substantially more stable in 1.0 M HCl compared with more dilute acid concentrations. The stability of benomyl is increased with an increase in acid concentrations. Benomyl remained stable (within experimental error) in 5 and 10 M HCl solutions for at least 14 days at ambient temperatures, as can be seen in Table I. There was no difference in the peak heights of benomyl immediately after, and 14 days after, the preparation of sample solutions in 5 M and 10 M HCl. Figure 1 shows the HPLC chromatogram of a sample of benomyl prepared in 10 M HCl and kept at room temperature for 14 days. As revealed in Figure 1, a small peak corresponding to carbendazim (approximately 0.7% of the peak height of benomyl) was always present in the chromatogram, even when using the analytical standard grade benomyl. The presence of a constant level of a trace of carbendazim in the chromatogram for the maximum study period of 14 days suggests that carbendazim is present as a trace impurity in the analytical standard of benomyl.

The presence of benomyl in a 5 M HCl solution (after 14 days) was also confirmed by mass spectrometry using a FAB source. A very strong molecular ion of benomyl at mass 291 clearly indicated the presence of benomyl in acid solution.

The results discussed above also suggest that benomyl can be determined quantitatively using the HPLC conditions reported in this study. The results for the determination of benomyl in a wettable power (WP) sample compared well with those obtained using the method developed by Chiba and Singh (1986).

The above results also indicate that stable reference standard aqueous solutions of benomyl can be prepared. Benomyl in water can be stabilized by strongly

acidifying the solutions. The acidified benomyl solutions will keep for at least 14 days at room temperature, and probably for longer periods, by storing them at lower temperatures (for example at 4 °C in refrigerator). Other alkyl isocyanate homologues of benomyl (Chiba and Northover, 1988; Northover and Chiba, 1989) could also be stabilized in a similar fashion.

CONCLUSIONS

In conclusion, in this communication we report that, for the first time, the preparation of stable stock solutions of benomyl (methyl [1-butylcarbamoyl)-1H-benzimidazol-2-yl] carbamate) in an aqueous medium is possible. The stabilization of benomyl in acidic solutions was confirmed by RP-HPLC. Mass spectrometry, using a FAB source, also confirmed the stabilization of benomyl in a 5 M hydrochloric acid solution. On the basis of these investigations, known amounts of benomyl can be easily dissolved and stabilized in 5 M or higher concentrations of hydrochloric acid. This opens up a real possibility for the preparation of reference standards of benomyl in aqueous (acidic) media. The stability of benomyl in 5 to 10 M hydrochloric acid also suggests that water samples containing benomyl can be stabilized upon acidification. This stabilization of benomyl containing aqueous samples was not possible in the past.

Table I. Observed First-Order Rate Constants (k) for Benomyl Decomposition to Carbendazim at Ambient Temperatures in Varying Concentrations of Hydrochloric Acid

HCl (M)	k (s^{-1})	$t_{0.5}$ (hr)
0.001	3.6×10^{-5}	5.3
0.01	3.1×10^{-5}	6.0
0.1	1.2×10^{-5}	1.6×10
1.0	7.7×10^{-7}	2.5×10^{2}
2.5	1.3×10^{-7}	1.5×10^{3}
5.0	STABLE	
10.0	STABLE	

LITERATURE CITED

Austin, D.J.; Lord; K.A. Williams; I.H. High pressure liquid chromatography of benzimidazoles. *Pestic. Sci.* **1976**, *7*, 211.

Bardalaye, P.C.; Wheeler, W.B. Simplified method for the clean-up and reversed-phase high-performance chromatographic determination of benomyl in mangoes. *J. Chromatogr.* **1985**, *330*, 403-407.

Chiba, M. A rapid spectrophotometric method for the simultaneous determination of intact benomyl and its degradation product, methyl 2-benzimidazolecarbamate (MBC), in organic solvents and water. J. *Agric. Food Chem.* **1977**, *25*, 368-373.

Chiba, M.; Bown, A.W.; Danic, D. Inhibition of yeast respiration and fermentation by benomyl, carbendazim and other fungicidal chemicals. *Can. J. Microbiol.* **1987**, *33*, 157-161.

Chiba, M.; Cherniak, E.A. Kinetic study of reversible conversion of methyl 1-(butylcarbamoyl)-2-benzimidazolecarbamate (benomyl) to methyl 2-benzimidazolecarbamate (MBC) and n-butyl isocyanate (BIC) in organic solvents. *J. Agric. Food Chem.* **1978**, *26*, 573576.

Chiba, M.; Doornbos, F. Instability of benomyl in various conditions. *Bull. Environ. Contam. Toxicol.* **1974**, *11*, 273-274.

Chiba, M.; Northover, Efficacy of new benzimidazole fungicides against sensitive and benomyl- resistant *Botrytis cinerea. J. Phytopathol.* **1988**, *78*, 613-618.

Chiba, M.; Singh, R.P., High performance liquid chromatographic method for simultaneous determination of benomyl and carbendazim in aqueous media. *J. Agric. Food Chem.* **1986**, *34*, 108-112.

Delp, C.J. Benzimidazole and related fungicides In *Modern Selective Fungicides—Properties, Applications, Mechanisms of Action*; Lyr, H., Ed.; Longman Group UK: London, **1987**; pp 233-244

Gorbach, S. A review of methods for the residue analysis of the systemic fungicides benomyl, carbendazim, thiophanate methyl and thiabendazole. *Pure Appl. Chem.* **1980**, *52*, 2569-2590.

Hall, D.J. Comparative fungicidal activity of benomyl and its breakdown product methyl 2-benzimidazolecarbamate (MBC) on citrus. *Proc. Fla. State Hortic. Soc.* **1980**, *93*, 341-344.

Hammerschlag, R.S.; Sisler, H.D. Benomyl and methyl-2-benzimidazolecarbamate (MBC): biochemical, cytological and chemical aspects of toxicity to *Ustilago maydis Saccharomyes cerevesiae. Pestic. Biochem, Physiol.* **1973**, *3*, 42-54.

Kirkland J.J. Method for high-speed liquid chromatographic analysis of benomyl and / or metabolite residues in cow milk,urine, feces, and tissues. *J. Agric. Food Chem.* **1973**, *21*, 171-177.

Kirkland J.J.; Holt, R.F.; Pease, H.L. Determination of benomyl residues in soils and plant tissues by high-speed cation exchange liquid chromatography. *J. Agric. Food Chem.* **1973**, *21*, 368-371.

Koller, W.; Allan, C.R.; Kolattukudy, P.E. Inhibition of cutinase and prevention of fungal penetration onto plants by benomyl.—A possible protective mode of action. *Pestic. Biochem. Physiol.* **1982**, *18*, 15-25.

Liu, C.H.; Mattern, G.C.; Yu, X.; Rosen, J.D. Determination of benomyl by high performance liquid chromatography / mass spectrometry / selected ion monitoring. *J. Agric. Food Chem.* **1990**, *38*, 167-171.

Marvin, C.H.; Brindle, I.D.; Singh, R.P.; Hall, C.D.; Chiba, M. Simultaneous determination of trace concentrations of benomyl, carbendazim (MBC) and nine other pesticides in water using an automated on-line pre-concentration high-performance liquid chromatographic method. *J. Chromatogr.* **1990**, *518*, 242-249.

Northover, J.; Chiba, M. Stability of benomyl homologues and their efficacy against benomyl-resistant *Botrytis cinerea*. *J. Agric. Food Chem.*. **1989**, *37*, 1416-1421.

Pyysalo, H. A rapid gas-liquid chromatographic method for determining benomyl residues in foods. J. Agric. Food Chem. 1977, 25, 995-997.

Singh, R.P.; Brindle, I.D.; Hall, C.D.; Chiba, M. Kinetic study of the decomposition of methyl [1-(butylcarbamoyl)-1H-benzimidazol-2-yl]carbamate (benomyl) to methyl 1H-benzimidazol-2-ylcarbamate (MBC). *J. Agric. Food Chem.*. **1990**, *38*, 1758-1762.

Singh, R.P.; Chiba, M. Solubility of benomyl in water at different pHs and its conversion to methyl 2-benzimidazolecarbamate, 3-butyl-2,4-dioxo[1,2-a]-s-triazinobenzimidazole, and 1-(2-benzimidazolyl)-3-n-butylurea. *J. Agric. Food Chem.*. **1985**, *33*, 63-67.

Spittler, T.D.; Marafioti, R.A.; Lahr, L.M. Determination of benomyl and its metabolites by cation- exchange high performance liquid chromatography. *J. Chromatogr.* **1984**, *317*, 527-531.

Zweig, G.; Gao, R. Determination of benomyl by reversed-phase liquid chromatography. *Anal. Chem.* **1983**, *55*, 1448-1451.

Figure Captions

Figure 1. Reversed-phase HPLC chromatogram of a benomyl solution (1.13 μg mL^{-1}) in 0.01 M HCl. The solution was prepared just before the HPLC determination by diluting a 1130 μg mL^{-1} benomyl stock solution in 10 M HCl kept at room temperature for 14 days.

Part II C: Fast-atom Bombardment Mass Spectrometric Determination of Methyl [1-(Butylcarbamoyl)-1H-benzimidazol-2-yl]carbamate (Benomyl) in Wettable Powder Formulations

ABSTRACT

In this part we report, for the first time, a direct method for the determination of benomyl (methyl [1-(butylcarbamoyl)-1H-benzimidazol-2-yl] carbamate) in wettable powder formulations by fast-atom bombardment mass spectrometry (FAB-MS). Solutions of desired concentrations of benomyl were prepared in 5 M hydrochloric acid. The matrix compound, glycerol, was added at 10% (v/v) to these solutions for obtaining FAB mass spectra. The results of the analysis of wettable powder samples, carried out by FAB-MS, compared well ($p > 0.05$) with those obtained by reversed-phase high performance liquid chromatography (RP-HPLC).

Methyl [1-(butylcarbamoyl)-1H-benzimidazol-2-yl]carbamate (benomyl) is one of the most widely used systemic fungicides[1]. Since its introduction, benomyl has been widely used for the control of a variety of plant diseases. For plant application, benomyl is sold as wettable powder, a formulated product of benomyl with the trade name 'Benlate". These formulated products normally contain 50 or 10 % of benomyl. The amount of benomyl in these formulations is guaranteed by the vendor. However, until now, there has been no direct method for confirming the amount of benomyl in these formulations guaranteed by the vendor.

Although benomyl was introduced more than 20 years ago, analytical methods for its direct determination had not been well established. Instability of benomyl in many common organic solvents and water[2-5] has been suggested as the reason why no direct method could be developed. Among the indirect methods, used for the determination of benomyl, the most popular ones use high performance liquid

chromatography (HPLC) after its conversion into carbendazim, a well known degradation product of benomyl[6-8]. The principal drawback of these methods is the over-estimation of benomyl with a wide range of errors. The over-estimation of benomyl is due to the fact that carbendazim, which is the natural degradation product of benomyl and is present in different media with benomyl at varying concentrations, is also estimated as benomyl. Carbendazim is also a known metabolite of thiophanate-methyl, a fungicide not as widely used as benomyl but registered for use on some fruits and vegetables. Therefore, use of thiophanate-methyl may also contribute to positive error in the determination of benomyl as carbendazim. For these reasons, it has been impossible to know the accuracy of benomyl quantities, determined by the methods based on the determination of benomyl as carbendazim. Recently, some progress has been made in development of a indirect method for the determination of intact benomyl and carbendazim concentrations in water and wettable powders by high performance liquid chromatography (HPLC).[9-10] However, the need to develop a direct method of benomyl determination in wettable powder formulations, soil, crops and water has remained.

In the past, for the determination of benomyl, [9-11] HPLC has been the most popular technique. HPLC, combined with a UV/VIS detector, although a well recognized and accurate technique, is not free from limitations. The most serious limitation of HPLC lies in the identification of the solutes, based only on a single parameter i.e., retention time of the solutes.

Mass spectrometry (MS), which allows the analyst to aquire considerable structural information, may be able to solve the problem of identification of solute, if used as a detector in combination with HPLC. Recently, Liu et al., [12] have reported a HPLC-MS method for the determination of benomyl in some fruits and vegetables. However, this method too is based on the determination of

carbendazim, after quantitative conversion of benomyl to carbendazim, and is therefore not free from the problem of over-estimation of benomyl.

Indirect determination of benomyl by HPLC-MS is necessary because of its instability. Due to the thermal lability of benomyl, its molecular ion under EI-MS conditions cannot be obtained.[13,14] Fast-atom bombardment mass spectrometry (FAB-MS), [15-17] may be used for mass spectrometric analysis of many thermally labile compounds. However, to our knowledge, determination of benomyl by FAB-MS has not been reported in the literature. One of the reasons for that may be the low solubility of benomyl in glycerol (and/or other matrices), which is required for FAB-MS analysis. Since benomyl is unstable in common organic solvents and in water, it is not easy to dissolve and stabilize benomyl in a suitable matrix, required for FAB-MS determination of benomyl.

In a recent communication, [18] we have reported that benomyl can be stabilized in hydrochloric acid solutions. The stabilization and solubilization of benomyl in hydrochloric acid became possible due to its protonation at the nitrogen of benzimidazole ring. The preparation of stable solutions of benomyl in hydrochloric acid, therefore, allowed us to study the FAB-MS determination of benomyl. In this communication we report that the molecular ion of benomyl can be obtained under FAB-MS conditions. We have used this finding for the quantitative determination of benomyl (as benomyl) in wettable powder formulations. The FAB-MS method reported in this paper, therefore, may be used for the confirmation of guaranteed amount of benomyl in wettable powder formulations. These studies may lead to a more sensitive determination of benomyl by continuous flow fast-atom bombardment mass spectrometry (CF-FAB-MS).[19]

EXPERIMENTAL

Chemicals. Benomyl and carbendazim analytical standards were obtained from E. I. du Pont de Nemours and Co., Inc. Fifty percent benomyl wettable powder formulations (Benlate 50% WP) were obtained from Wilson Laboratories Inc. Dundas, Ontario. Spectrophotometric grade glycerol and a 65% by weight solution in water of 4-hydroxybenzenesulfonic acid (HSA) were obtained from Aldrich Chemical Company, Inc., Milwaukee, WIS 53233. Analytical reagent grade hydrochloric acid from BDH Inc., Toronto, Ontario was used to dissolve and stabilize benomyl.

Solvents. Acetonitrile was HPLC grade from Caledon Laboratories, Ltd., Georgetown, Ontario L7G 4R9, Canada. Water was distilled in glass in the laboratory.

Instrumentation and Procedures. A Kratos Concept IS double-focussing mass spectrometer (Kratos Analytical, Urmston, Manchester, UK) (E/B Configuration) using a fast atom bombardment (FAB) source, was used for mass spectrometric analyses. The instrument was controlled by a Kratos DS 90 Data General Eclipse based computer system. A Kratos Mach 3 data system running on a SUN SPARC station was used for further data work-up. For all studies, a nominal resolving power of 1000 was used. The spectrometer was fitted with an Ion Tech Saddle field atom gun and xenon was used as the fast-atom beam. The fast-atom beam energy was 7.5 keV and the density corresponding to an emission current was about 1 mA. The source was operated at room temperature and 8 kV accelerating potential. The scan rate was 10 sec per decade. Samples were placed on the probe tip by dissolving them in HCl and the matrix compound. Standard solutions of benomyl at 200, 400 and 640 mg/L were prepared prepared from a 1000 mg/L benomyl stock solution prepared from analytical standard grade pure benomyl in 5 M HCl. In addition to benomyl, calibrating standards also

contained 5 M HCl and 10 % glycerol. For sample preparation, 50 milligrams of 50% WP (formulations) was dissolved in 25 mL of 10 M HCl in a 50 mL volumetric flask. After adding 5 mL of glycerol the volume was made up to the mark by distilled water. One microliter volumes of benomyl standards and samples were placed on the FAB-probe tip and the intensity counts were recorded.

The quantitation of benomyl in wettable powder formulations was carried out using selected ion monitoring (SIM). SIM acquisitions were made under the same instrumental conditions as described above using a 0.5 sec cycle time for the ion groups of interests. Because the samples exhibited a surge of ion current during the first scan interval, this initial scan was discarded and data were averaged for the five subsequent intervals where ion current levels had stabilized.

The liquid chromatographs used were a Perkin-Elmer Series 3 equipped with a Rheodyne syringe loop-type injector and a Perkin-Elmer LC-55 UV detector, and Waters 600-MS system controller with a Waters 441 absorbance detector. A Vydac reversed phase C-18, 5 μ, 15 cm X 4.6 mm (i.d.) column was used for the quantitative determination of benomyl in wettable powder samples (with the Waters 600-MS liquid chromatograph). The mobile phase, consisting of a mixture of 60% acetonitrile, 35% water and 5% 0.1 mol/L ammonium acetate, was run at 1.0 mL/min. The UV detector was operated at 254 nm with detector sensitivity of 0.05 AUFS. Peaks were integrated on a Hewlett Packard HP 3396 Series II integrator. The total system was operated at ambient temperature.

Separation of carbendazim and benomyl was achieved on a W-Porex, 5μ C4 guard (30 x 4.6 mm) column. The eluent, a mixture of 25% acetonitrile, 5% pH-6.8 phosphate buffer and 70% water was run at 0.7 mL/min flow rate. These determinations were made with the Perkin Elmer system with UV detector setting at 286 nm.

RESULTS AND DISCUSSION

Analysis of Benomyl by FAB-MS in Glycerol and HSA Matrices. Fig. 1 shows a representative FAB-MS spectrum of 1 μg benomyl in 5 M HCl, containing 10% glycerol. The $(M + H)^+$ signal at m/z 291 shows the presence of the molecular ion of benomyl. The other significant peak was observed at m/z 192, which is the signal of protonated carbendazim, a fragment derived from benomyl. All other peaks in the spectrum (between m/z 192 to 291) are not due to benomyl, as metastable monitoring in the the first field-free region by means of B/E linked scans[20] showed only one fragment peak of benomyl at m/z 192.

A good mass spectrum of benomyl was also obtained in 5 M HCl containing 10% HSA (Fig. 2). However, the $(M + H)^+$ signal of benomyl in 10% HSA was slightly weaker, compared to its signal in 10% glycerol. The lower intensity of the molecular ion signal of benomyl in 10% HSA compared to the signal in 10% glycerol is quite obvious from the perusal of intensity ratios of the signals at m/z 291 to 192 in both the spectra. The m/z 291 to 192 intensity ratio is significantly higher in 10% glycerol than in 10% HSA. This can be attributed to either partial decomposition of benomyl to carbendazim in presence of 10% HSA or to the inferior matrix properties of HSA as compared to glycerol. On the basis of HPLC analysis (Fig. 3) of solutions, containing (i) benomyl in 5 M HCl, (ii) benomyl in 5 M HCl and 10% glycerol, and (iii) benomyl in 5 M HCl and 10% HSA, it was concluded that the presence of HSA and glycerol in 5 M HCl does not affect the stability of benomyl. Therefore, a weaker $(M + H)^+$ signal of benomyl in the presence of 10% HSA, compared to glycerol, can be attributed to its matrix properties. Other matrices, such as thioglycerol and 3-nitrobenzyl alcohol proved to be worse than glycerol and HSA for FAB-MS determination of benomyl.

Quantitative Determination of Benomyl in Wettable Powder Formulations. The FAB-MS results of benomyl determinations, shown in Figs. 1

and 2, reveal the possibility of identification and quantitative determination of benomyl by FAB-MS. Efforts were made, therefore, to determine, quantitatively, benomyl in wettable powder formulations containing 50 % benomyl. Thus, determination of benomyl in three wettable powder samples was performed by FAB-MS method using the selected ion monitoring (SIM) mode by monitoring the intensities of m/z 192 and 291 signals. One microliter volumes of benomyl standards were placed on the FAB-probe tip and the intensity counts were recorded to generate a calibration curve. Monitoring of both signals, at m/z 192 and 291, gave straight line responses through the origin, when signal counts were plotted against benomyl concentrations (mg/L); the linear regression coefficients for the 192 and 291 signals were 0.9996 and 0.9991, respectively. A typical calibration curve for m/z 291 signal is shown in Fig. 4.

The results of benomyl determination, carried out by the FAB-MS method, are reported in Table1. In order to check the accuracy of benomyl determination by FAB-MS method, the same samples were also analyzed by HPLC. These results are also reported in Table1. Since the calculated value of Student *t* for the mean percent bias between the two methods (FAB-MS and HPLC) is less than the critical value of *t* at the 95 % confidence interval, the null hypothesis is retained. Therefore, the bias between the two methods for the determination of benomyl in WP formulations does not differ significantly from zero.

The reproducibility of the FAB-MS method for the determination of benomyl in wettable powders was checked by analyzing a 50% formulation in triplicate. The mean and standard deviation values for benomyl were estimated at 46.7 ± 1.2 % and 45.8 ± 3.6 % by FAB-MS method at 291 and 192 signals, respectively. The coefficient of variation (CV) at 2.6 % was much smaller for FAB-MS scanning at 291 than the 7.9 % CV resulted from FAB-MS scanning of 192 signal. These results suggest that for more reliable determination of benomyl in WP formulations by FAB-

MS method, determinations should be made at the 291 signal. The results of benomyl determination in the above-mentioned WP formulation at 46.7 %, as determined by FAB-MS method at 291 signal, compared well with that obtained by the so-called STB[10] and the direct HPLC methods at 46.9 % and 47.6 %, respectively. However, direct determination of benomyl in WP formulations with structural confirmation was possible only by FAB-MS method.

Although a good comparison of analytical results of benomyl in wettable powder formulations obtained by FAB-MS and HPLC methods clearly indicated the good accuracy of the FAB-MS method, verification of the selectivity of 291 ion monitoring in wettable powder matrix was still thought desirable. This was accomplished by metastable ion monitoring of sample (wettable powder) solutions in the first field-free region by means of B/E and B^2/E linked scans.[20] The B/E spectrum of the sample solution showed only one fragment peak at m/z 192, similar to the one obtained for pure benomyl solutions. The B^2/E spectrum, on the other hand, confirmed that 192 resulted from 291 only. These studies reveal that the matrix components would not cause any mass spectral interference in the mass spectrometric determination of benomyl in WP formulations.

The exact identity of chemicals used in the preparation of WP formulations is a trade secret, yet a 50% WP formulation may contain up to 55% benomyl, 2-3 % surfactant and the rest is sugar. From the literature[21-22] it appears unlikely that surfactants and suger will produce 291 or 192 ions in their FAB-MS spectra, therefore matrix components would not interfere in FAB-MS determination of benomyl in WP samples.

We would also like to mention here that this is the first time that an HPLC method, where known standards of benomyl in aqueous medium are used to generate a calibration curve (regression line, $y = 3.998\ x - 0.001$, where x is benomyl concentration in mg/L and y is the peak height in cm; linear regression

coefficient, r = 0.9999) is reported for the direct determination of benomyl. Benomyl standards and samples (which were dissolved and stabilized in 5 M HCl) were diluted to have a pH of 2 or higher before injections. Two consecutive injections gave similar (within 2%) peak heights. This suggests that the decomposition of benomyl solutions during chromatographic analysis was not significant enough to affect the accuracy of the results. This can be explained on the basis of kinetics data on benomyl decomposition to carbendazim, that we have reported recently.[8] According to the decomposition kinetics, approximately 2% benomyl will decompose to carbendazim in 5 min in a solution containing 60% acetonitrile and 40% water. Decomposition of benomyl in pure water is slower than in mixed acetonitrile and water solutions; 2% benomyl will decompose to carbendazim in about 11 min. Since the retention time of benomyl was about 4 min, its decomposition into carbendazim within two injection times (8 min) will be about 2%, which is within the range of experimental error in HPLC determination.

Possibilities of Extending FAB-MS Method for the Determination of Low Concentrations of Benomyl in Environmental Water and Crops. The FAB-MS method, described above, worked well for the determination of benomyl in WP formulations where large concentrations of benomyl are encountered. However, benomyl concentrations in environmental water and crops are expected to be low (< 1 mg/L). In case the FAB-MS method had to be extended for the determination of benomyl in these matrices, efforts were made to ascertain the minimum detectable amount of benomyl in an aqueous sample by the FAB-MS method. Fig. 5 shows the mass spectrum of 1 ng benomyl. It is obvious from Fig. 5 that the detection limit of benomyl is controlled by the chemical noise. Reproduciblity (coefficient of variation = 17.5 % , n = 6) of benomyl signal at 291 was also poor. Therefore, under normal FAB-MS conditions, determination of low concentrations of benomyl was not possible.

The sensitivity for benomyl determinations by FAB-MS may be enhanced by using a continuous flow system, as reported in the literature.[19], and by monitoring 291 Æ 192 reaction (B/E linked scans) instead of the normal FAB scan. The expected enhancement of sensitivity of benomyl in a CF-FAB-MS system using 291 Æ 192 reaction may be explained on the basis of the mass chromatogram of benomyl, depicted in Fig. 6, and the 291 Æ 192 spectrum shown in Fig. 7. As can be seen in Fig. 6, the intensities of both ions, at m/z 192 and 291, decreased sharply after the first scan. This may be due to the depletion of glycerol (the matrix compound) from the surface of the sample solution (at the tip of the FAB probe). In CF-FAB-MS the sample is continuously being renewed on the tip of FAB probe, and therefore a constant intensity of the signal should be maintained. Fig. 7 revealed that chemical noise can be minimised by monitoring the 291 Æ 192 reaction. The determination of benomyl (at low concentrations in water and other matrices) by CF-FAB-MS with metastable ion monitoring will be investigated in our laboratory in near future.

ACKNOWLEDGEMENT

We thank the Ontario Ministry of the Environment for funding this work under the Research Advisory Committee (Grant 1384).

REFERENCES

1. C.J. Delp, in Modern Selective Fungicides — Properties, Applications, Mechanisms of Action, ed. by H. Lyr, p. 233, Longman Group UK Ltd., London, (1987).
2. J.P. Calmon and D.R. Sayag, J. Agric. Food Chem., **24**, 426 (1976)
3. G.P. Clemons and H.D. Sisler, Phytopathology, **59**, 205 (1969).
4. M. Chiba and E.A. Cherniak, J. Agric. Food Chem., **26**, 573 (1978).
5. R.P. Singh, I.D. Brindle, C.D. Hall and M. Chiba, J. Agric. Food Chem., **38**, 1758, (1990).
6. J.J. Kirkland, J. Agric. Food Chem., **21**, 171 (1973).
7. J.J. Kirkland, R.F. Holt and H.L. Pease, J. Agric. Food Chem., **21**, 368 (1973).
8. T.D. Spittler, R.A. Marafioti and L.M. Lhr, J. Chromatogr., **317**, 527 (1984).
9. R.P. Singh and M. Chiba, J. Agric. Food Chem., **33**, 63 (1985).
10. M. Chiba and R.P. Singh, J.Agric. Food Chem., **34**, 108 (1986).
11. S. Gorbach, Pure Appl. Chem., **52**, 2569 (1980).
12. C.H. Liu, G.C. Mattern, X. Yu and J.D. Rosen, J. Agric. Food Chem., **38**, 167 (1990).
13. M. Chiba and F. Doornbos, Bull. Environ. Contamn. Toxicol., **11**, 273 (1974).
14. J. Northover and M. Chiba, J. Agric. Food Chem., **37**, 1416 (1989).
15. M. Barber, R.S. Bordoli, R.D. Sedgwick and A.N. Tyler, J. Chem. Soc. Chem. Commun., 325 (1981).
16. D.J. Surman and J.C. Vickerman, J.Chem. Soc. Chem. Commun., 324 (1981).
17. S.A. Martin, C.E. Costello and K. Bleman, Anal. Chem., **54**, 2362 (1982).
18. R.P. Singh, C.H. Marvin, I.D. Brindle, C.D. Hall and M. Chiba, J. Agric. Food Chem., **40**, 1303 (1992).
19. R.M. Caprioli, T. Fan and J.S. Cottrell, Anal. Chem. **58**, 2949 (1986).
20. R.K. Boyd and J.H. Beynon, Org Mass Spectrm. 12, 163 (1977).

21. F. Ventura, J. Caixach, A. Figuras, I. Espalder, D. Fraisse and J. Rivera, Wat. Res. 23, 1191 (1989).

22. L.M. Teesch and J. Adams, Org. Mass spectrom. **27**, 931 (1992)

Table 1. Comparison of results of the determination of benomyl in wettable formulations by FAB-MS at m/z 192 (FAB-192), FAB-MS at m/z 291 (FAB-291) and HPLC techniques

Sample No	Benomyl (mg/L) as Determined				
	by HPLC (X)	by FAB-192 (Y)	Bias-1*	by FAB-291 (Z)	Bias-2**
1	485	429	+11.5	485	0.0
2	538	533	+0.9	538	0.0
3	492	499	-1.4	464	+5.7
		Mean	+3.7		+1.9
		Std Dev	6.9		3.3
		Student *t*	0.76		0.81
Student *t* at 95% confidence interval			4.3		

Bias-1* = [(X-Y)/X]100

Bias-2** = [(X-Z)/X]100

Figure Captions

Fig. 1. Positive ion FAB mass spectrum of 1 μg benomyl in 10% glycerol and 5 M HCl.

Fig. 2. Positive ion FAB mass spectrum of 1 μg benomyl in 10% 4-hydroxybenzenesulfonic acid and 5 M HCl.

Fig. 3. Chromatograms of carbendazim and benomyl (from 50% wettable powder) in different media.

Fig. 4. Calibration graph of benomyl for m/z 291 signal.

Fig. 5. Positive ion FAB mass spectrum of 1 ng benomyl in 10% glycerol and 5 M HCl.

Fig. 6. Positive ion FAB mass chromatograms of 1 μg benomyl in 10% glycerol and 5 M HCl.

Fig. 7. Normal B/E linked scan of 10 mg/L benomyl.

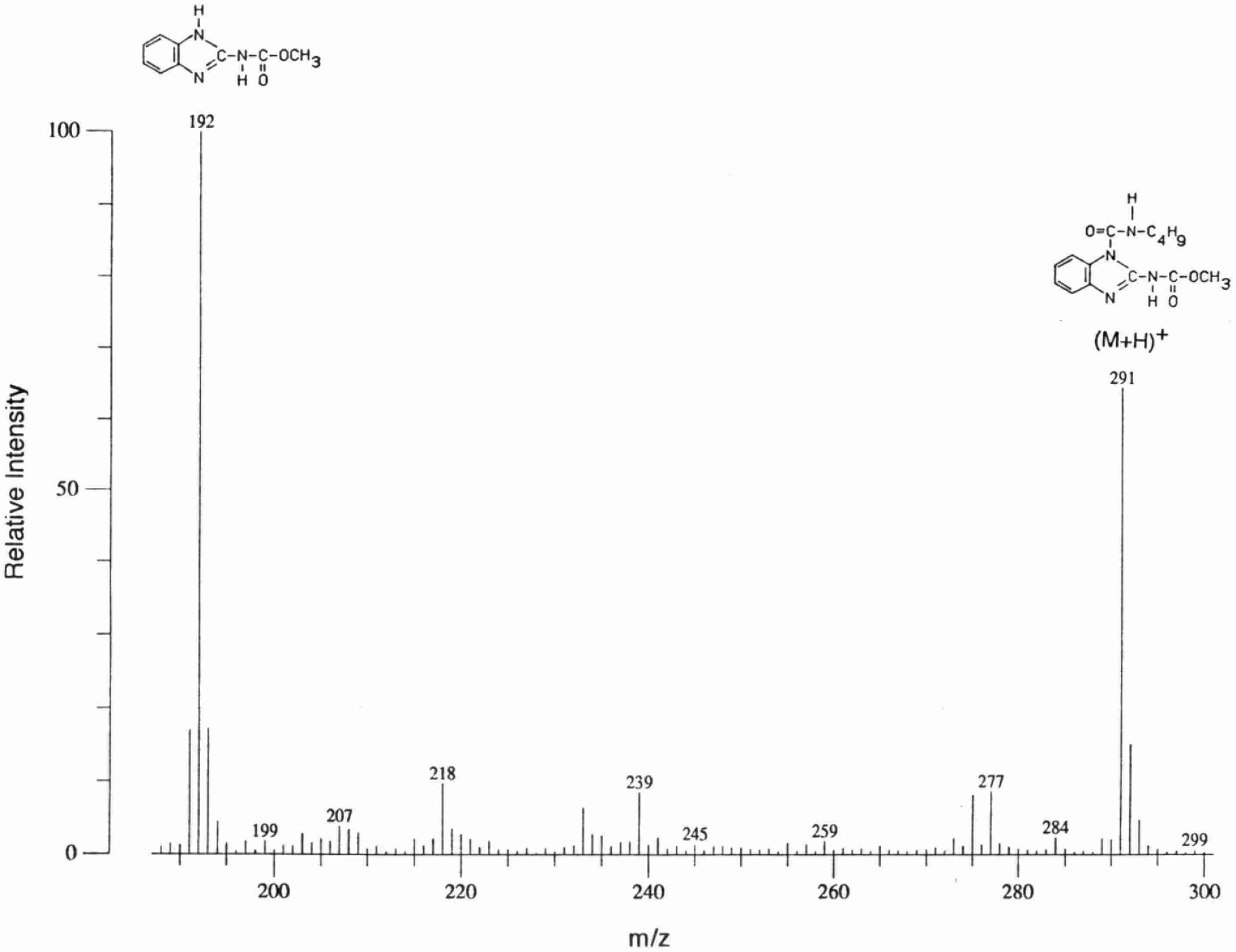
Relative Intensity
100
50
0
192
291
199
207
218
239
245
259
277
284
299
200
220
240
260
280
300
m/z
(M+H)+

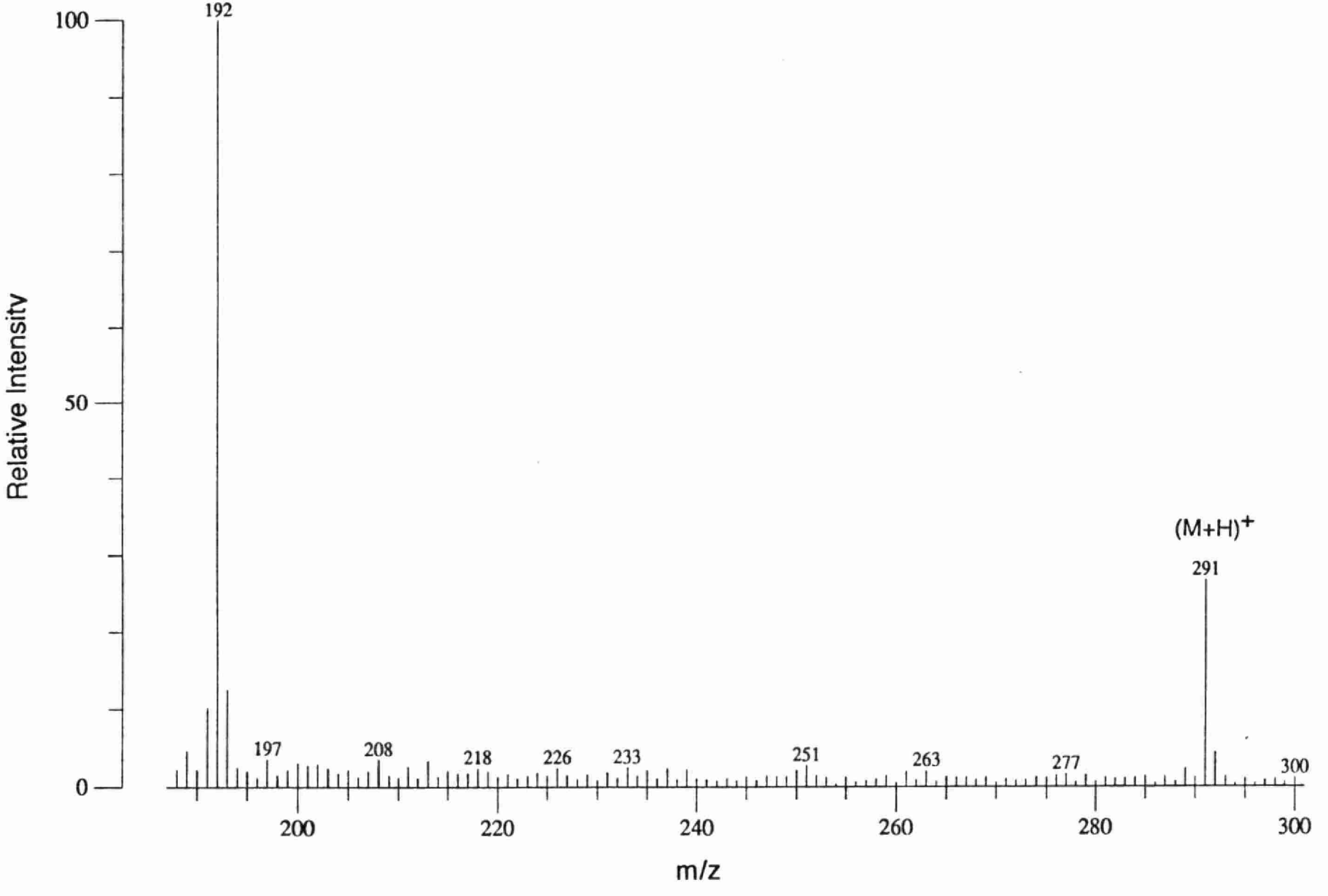
100
50
0
Relative Intensity
192
197
208
218
226
233
251
263
277
291
(M+H)+
300
200
220
240
260
280
300
m/z

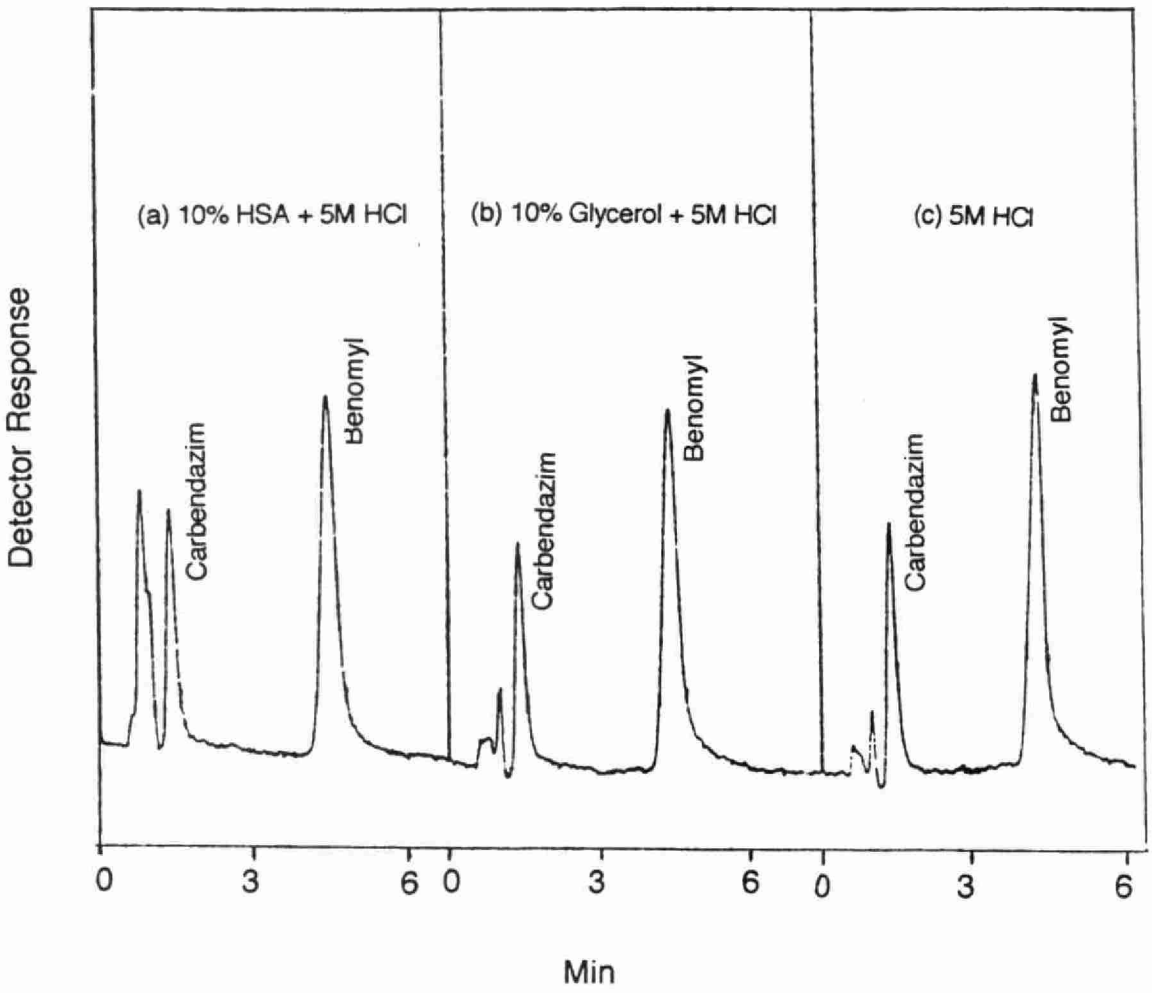
(a) 10% HSA + 5M HCl
(b) 10% Glycerol + 5M HCl
(c) 5M HCl
Carbendazim
Benomyl
Carbendazim
Benomyl
Carbendazim
Benomyl
Detector Response
0
3
6
0
3
6
0
3
6
Min

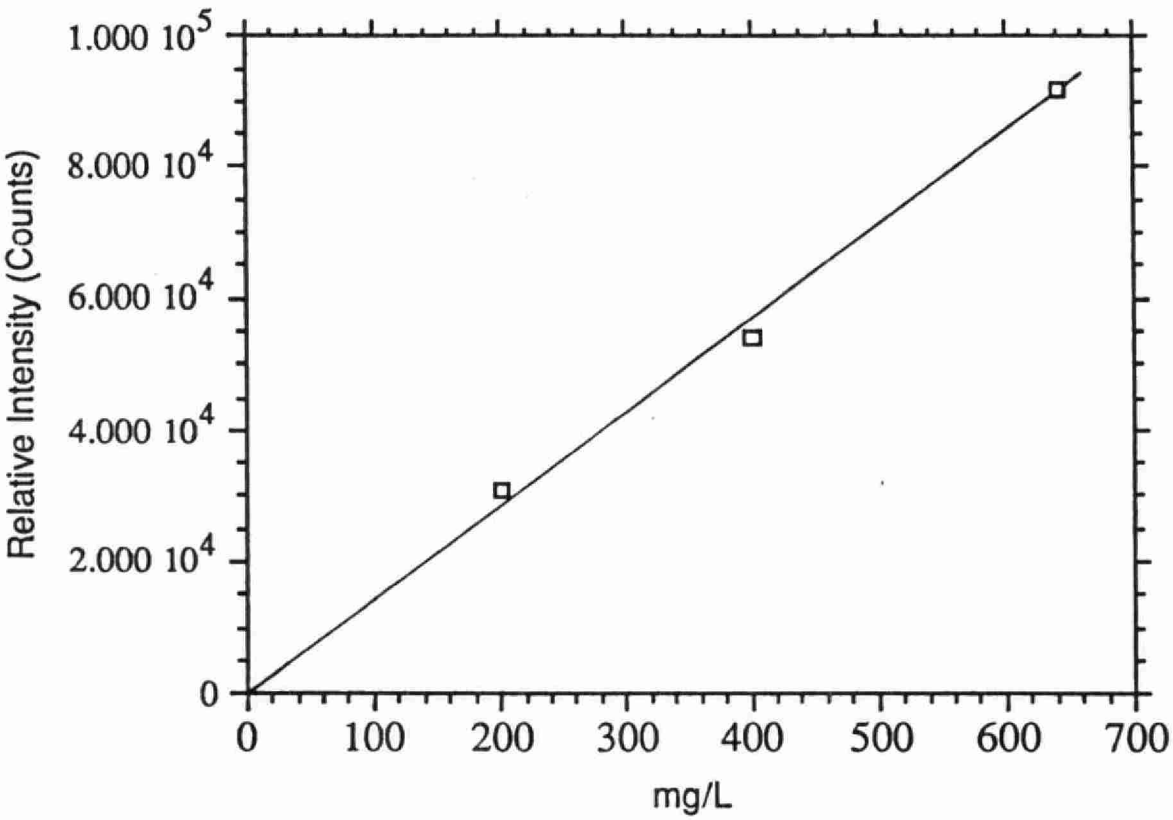
1.000 10^5
8.000 10^4
6.000 10^4
4.000 10^4
2.000 10^4
0
Relative Intensity (Counts)
0
100
200
300
400
500
600
700
mg/L

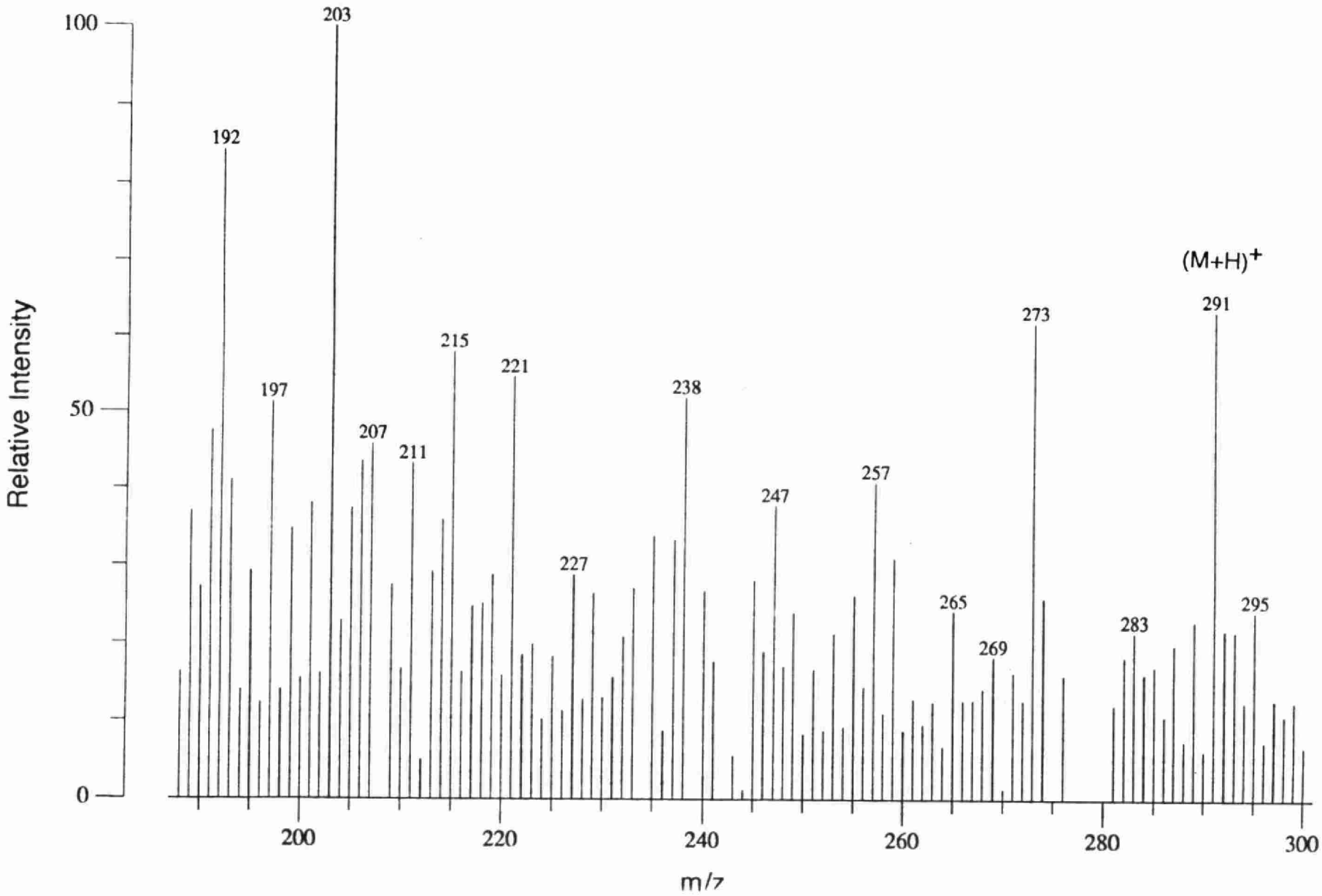
Relative Intensity
100
50
0
203
192
197
207
211
215
221
238
227
247
257
273
(M+H)+
291
265
269
283
295
200
220
240
260
280
300
m/z

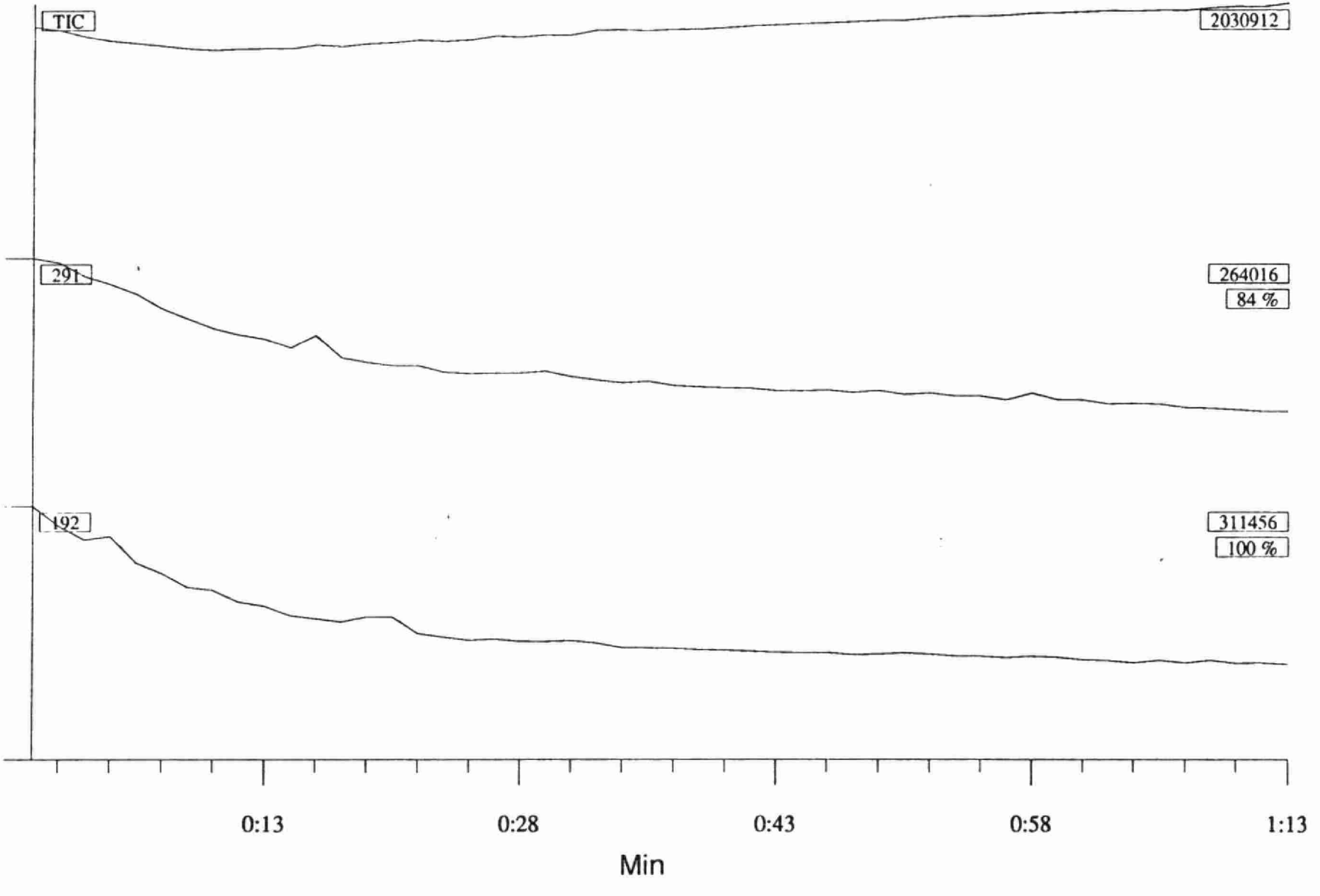
TIC
2030912
291
264016
84 %
192
311456
100 %
0:13
0:28
0:43
0:58
1:13
Min

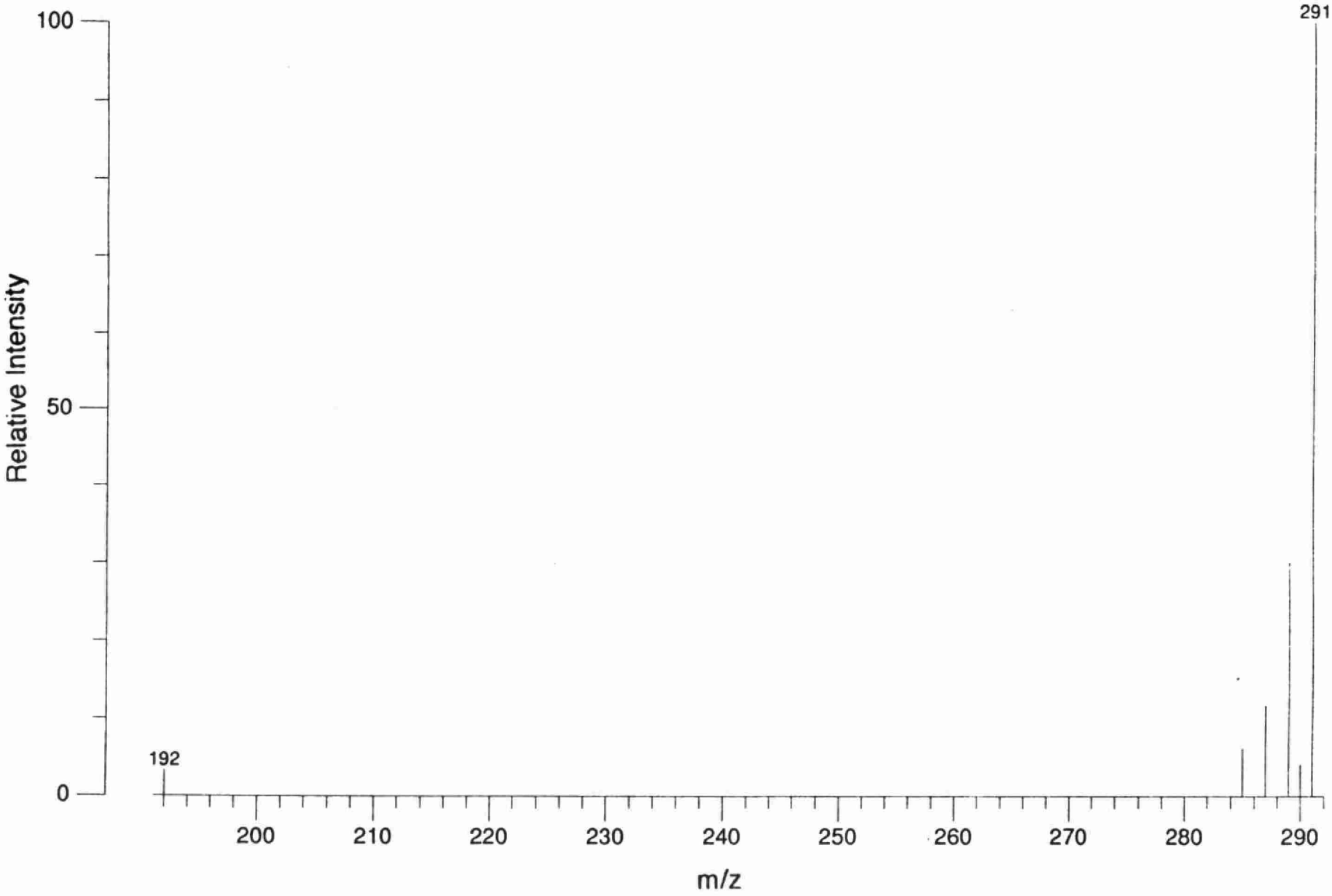
100
50
0
Relative Intensity
291
192
200
210
220
230
240
250
260
270
280
290
m/z

APPENDIX

The work reported in this Appendix, although is not directly related to Particle Beam - Mass Spectrometry, we carried out this work due to its importance in environmental analytical chemistry.using FAB-MS

Fast-atom Bombardment Mass Spectrometry of Sodium and Potassium Oxalates– Mass Spectrometric Evidence for the Existence of (Sodium-Oxalate)$^-$ and (Potassium-Oxalate)$^-$ Ion Pairs in Aqueous Solutions

ABSTRACT

Mass spectrometric evidence for the formation of (sodium-oxalate)$^-$ ($NaC_2O_4^-$) and (potassium-oxalate)$^-$ ($KC_2O_4^-$) ion pairs in aqueous solutions of potassium and sodium oxalates has been provided by analyzing different concentrations of sodium and potassium oxalate in water, containing 10% glycerol. This work suggests that FAB-MS can be used to reveal the behavior of ionic species in aqueous solutions. The $KC_2O_4^-$ and $NaC_2O_4^-$ ion pairs form clusters with neutral molecules of potassium and sodium oxalates and glycerol. No ion pair or cluster formation was observed when dry salts (without glycerol) were analyzed. This behavior differed from what has been observed for alkali halides under similar experimental conditions.

Keywords: *Mass spectrometry; fast-atom bombardment; (sodium-oxalate)$^-$ ion pair; (potassium-oxalate)$^-$ ion pair*

Ion association models are extensively used to explain the characteristics of aqueous environmental and biological solutions. [1-2] The ion association models used for the speciation and calculation of the supersaturation index of urine for calcium oxalate phases (the principal components of the kidney stones) consider ion pairing of urinary cations with oxalate. These ion pairs include (calcium-oxalate)^0 ($CaC_2O_4^0$), (magnesium-oxalate)^0 ($MgC_2O_4^0$), (proton-oxalate)$^-$ ($HC_2O_4^-$), (sodium-oxalate)$^-$ ($NaC_2O_4^-$) and (potassium-oxalate)$^-$ ($KC_2O_4^-$). [3] However, on the basis of conductivity measurements of sodium oxalate solutions, Berland et al. [4] assumed sodium oxalate to be a completely dissociated electrolyte.

In urine, where sodium concentration is very high, omission of the $NaC_2O_4^-$ ion pair (if it really does exist) in the equilibrium calculations of calcium oxalate phases will result in significantly higher supersaturation values of urine with respect to calcium oxalate monohydrate and dihydrate phases than is actually present. Correction for the existence of $KC_2O_4^-$ and $NaC_2O_4^-$ ion pairs in equilibrium calculations therefore becomes necessary to calculate the correct value of the supersaturation of kidney stone forming calcium oxalate phases in urine. Corrections for ion pairing of oxalate with sodium and potassium need to be also applied in the speciation calculations of environmental waste solutions as oxalate, being an industrial pollutant and naturally occurring ligand, is also ubiquitous in environmental solutions[5] along with cations sodium and potassium.

The presence of $KC_2O_4^-$ and $NaC_2O_4^-$ ion pairs in aqueous solutions containing potassium, sodium, and oxalate ions has been documented by solubility [6-7], potentiometry [8] and Raman spectroscopy [9]. Although a value of the stability constant ($k = [NaC_2O_4^-] / [Na^+] [C_2O_4^-] = 13.2$ dm^3 mol^{-1}) has been reported for the $NaC_2O_4^-$ ion pair [6], a value of $k = 10$ dm^3 mol^{-1} is normally expected for most sodium/potassium - anion)$^-$ ion pairs such as $KC_2O_4^-$, KSO_4^-,

$NaC_2O_4^-$ and $NaSO_4^-$. Caprioli [10], and Johnstone and Rose [11] have demonstrated that fast-atom bombardment mass spectrometry (FAB-MS) can provide an accurate knowledge of existing ionic-equilibria in liquid solutions. Caprioli [10] determined the dissociation constants of weak acids in aqueous solutions by FAB-MS method which compared well with the literature values while Johnstone and Rose [11] have reported that FAB-MS can be used routinely to examine complex formation between metal cations and macrocyclic ligands in solution. In view of the controversy raised by Berland et al. [4] we wanted to use FAB-MS to investigate the existence of $KC_2O_4^-$ and $NaC_2O_4^-$ ion pairs in solutions containing sodium/potassium and oxalate ions.

Experimental

Chemicals

Spectrophotometric grade glycerol was obtained from Aldrich Chemical Company, Inc., Milwaukee, WIS 53233. Analytical reagent grade sodium and potassium oxalate salts were from BDH Inc., Toronto.

Instrumentation and Procedures

A Kratos Concept IS double-focussing mass spectrometer (Kratos Analytical, Urmston, Manchester, UK) (E/B Configuration) using a fast atom bombardment (FAB) source, was used for mass spectrometric analyses. The instrument was controlled by a Kratos DS 90 Data General Eclipse based computer system. A Kratos Mach 3 data system running on a SUN SPARC station was used for further data work-up. For all studies, a nominal resolving power of 1000 was used. High resolution analysis of potassium oxalate solution was carried out using a resolution of 7500. I^- with m/z = 126.9045 was used as standard. The spectrometer was fitted

with an Ion Tech saddle field atom gun and xenon was used as the fast-atom beam. The fast-atom beam energy was 7.5 keV and the density corresponding to an emission current was about 1 mA. The source was operated at room temperature and 8 kV accelerating potential. The scan rate was 10 sec per decade. One microliter of solutions of different concentrations of sodium and potassium oxalate, prepared in 10 % glycerol, were placed on the probe tip for FAB-MS determination.

Results and Discussion

The representative FAB-MS spectra of sodium and potassium oxalate solutions are shown in Figs. 1 and 2 , respectively. The peaks due to $NaC_2O_4^-$ (m/z = 111) and $KC_2O_4^-$ (m/z = 127) ion-pairs are clearly seen in the FAB-MS spectra of sodium and potassium oxalate solutions. The base peak in all the spectra of dilute potassium / sodium oxalate solutions, was $(Gly-H)^-$ ion (m/z = 91, Gly is glycerol). In all the spectra of different concentrations of sodium/potassium oxalate in 10 % glycerol and 10 % pure glycerol, a number of low mass ions such as m/z 71, 59, 45, 17 were also present. These ions are formed as a result of gas-phase dissociation of $(Gly-H)^-$ ion. Cluster ions of $(Gly-H)^-$ anion with glycerol molecules such as $(Gly-H)^-(Gly)_n$, n= 0 - 5, were also present. Both oxalate ion pairs i. e., $NaC_2O_4^-$ and $KC_2O_4^-$, formed a series of clusters with glycerol, the most intense ones at m/z 203 and 219, respectively being for the $NaC_2O_4^-(Gly)$ and $KC_2O_4^-(Gly)$ ion pairs. In fact, the ions at m/z 203 and 219 formed as a result of association of ion pairs $NaC_2O_4^-$ and $KC_2O_4^-$ with Gly were the most intense peaks after the base peak at m/z 91 in all spectra of dilute solutions of sodium and potassium oxalate solutions. The $NaC_2O_4^-$ and $KC_2O_4^-$ ion pairs also form series of clusters with neutral

molecules of $Na_2C_2O_4$ ($NaC_2O_4^-$ $(Na_2C_2O_4)_n$, n = 0 - 3; m/z = 111, 245, 379, 513) and $K_2C_2O_4$ ($KC_2O_4^-$ $(K_2C_2O_4)_n$, n = 0 - 3; m/z = 127, 293, 459, 625).

In addition to $NaC_2O_4^-$ and $KC_2O_4^-$, ion pairs such as $HC_2O_4^-$, $M(Gly-H)^-$, $M_2(Gly-H)^-$ (M = Na or K), and $Gly(Gly-H)^-(Gly)_n$, n= 0 - 4 are also observed in oxalate solutions. The formation of these ion pairs can be suggested on the bais of following equilibria:

Gly	′	$(Gly-H)^- + H^+$	(i)
$(Gly-H)^- + Na^+$	′	$GlyNa^- + H^+$	(ii)
$GlyNa^- + Na^+$	′	$GlyNa_2^- + H^+$	(iii)
$H^+ + C_2O_4^{2-}$	′	$HC_2O_4^-$	(iv)
$Gly + (Gly-H)^-$	′	$Gly(Gly-H)^-$	(v)

It seems that the formation of $HC_2O_4^-$ ion pair, which has occurred as a result of pairing of H^+ with $C_2O_4^{2-}$, ions has driven the dissociation reaction of glycerol (reaction i) to the right side since the abundance of $(Gly-H)^-$ and $(Gly-H)^-(Gly)$ ions was higher in 10% glycerol solution containing potassium and sodium oxalate than in pure 10% glycerol. All the anions and anion-pairs discussed above formed clusters with neutral molecule of $Na_2C_2O_4$ (and $K_2C_2O_4$) and glycerol as follows: $(Gly-H)^-(Na_2C_2O_4)_n$, n = 0 - 4, m/z = 91, 225, 359, 493, 627; $Gly(Gly-H)^-(Na_2C_2O_4)_n$, n = 0 - 3, m/z = 183, 317, 451, 585; $Na(Gly-H)^-(Na_2C_2O_4)_n$, n = 0 - 3, m/z = 113, 247, 381, 515;.$Na_2(Gly-H)^-(Na_2C_2O_4)_n$, n= 0-2, m/z = 135, 269, 403.; $HC_2O_4^-$ $(Na_2C_2O_4)_n$, n = 0 - 4, m/z = 89, 223, 357, 491, 625; $(Gly-H)^-(Gly)_n$, n = 0 - 3, m/z = 91, 183, 275, 363; $Na(Gly-H)^-(Gly)_n$, n = 0 - 4, m/z = 113, 205, 297, 389, 481;.$Na_2(Gly-H)^-(Gly)_n$, n= 0-3, m/z = 137, 229, 321, 413.; $HC_2O_4^-$ $(Gly)_n$, n = 0 - 5, m/z = 89, 181, 273, 365, 457, 549.

$NaC_2O_4^-$ also showed cluster formation with glycerol and glycerol-sodium oxalate clusters as: $NaC_2O_4^-(Gly)_n$, n = 0 - 5; m/z = 111, 203, 295, 387, 479, 571; and $NaC_2O_4^-$-$Gly(Na_2C_2O_4)_n$, n = 0 - 4; m/z = 203, 337, 471, 605, 739. Other

clusters formed were: $NaC_2O_4^-$-Na(Gly-H)$^-$(Gly)$_n$, or $Na_2C_2O_4$-(Gly-H)$^-$(Gly)$_n$ n= 0 - 4; m/z = 225, 317, 409, 501, 593; and $HC_2O_4^-$(Gly$Na_2C_2O_4$)$_n$, n = 0 - 4; m/z = 89, 181, 315, 449, 583. Analogous cluster formation was also observed in case of potassium oxalate solutions (Fig. 2).

There are two possible mechanisms by which the ion pair and ion cluster formation can occur in FAB-MS analyses of solutions. According to mechanism 1, the ions and ion clusters can form by recombination of ions and neutral molecules in the gas phase. In mechanism 2 it is assumed that ions and ion clusters that are determined by FAB-MS analysis of solutions are already present in solution. In the latter case FAB-MS results should show a close relationship with ionic equilibria occurring in liquid solutions. These mechanisms of ions and ion-cluster formation in FAB-MS have been debated by many researchers. [12] In order to know whether the FAB-MS results, which are measured as the distribution of ions in gas phase, are closely related to ionic equilibria set up in the liquid phase (i.e., sodium and potassium oxalate solutions in 10% glycerol in the present case), we carried out FAB-MS analysis of sodium and potassium oxalate solutions at different concentrations.

The results of the FAB-MS analysis of $Na_2C_2O_4$ and $K_2C_2O_4$ solutions of different concentrations reported here seems to indicate that the abundances of ion-clusters and ion pairs determined by FAB-MS are closely related to possible solution equilibria. For example at low concentrations, such as 1.0 mmol dm^{-3} potassium oxalate, FAB-MS did not show any significant abundance of $KC_2O_4^-$ ion pair and clusters containing $KC_2O_4^-$ ion pair. This can be explained on the basis of equilibrium calculations of 1.0 mmol dm^{-3} potassium oxalate solution. Using a stability constant value of 10.0 dm^3 mol^{-1} for $KC_2O_4^-$ ion pair, we estimated that in 1.0 mmol dm^{-3} potassium oxalate solution, the concentration of $KC_2O_4^-$ ion pair is very small i.e., less than 0.01 mmol dm^{-3}, which could not be determined by FAB-

MS. We can argue here that if the ion pair formation was taking place in gas phase we should have seen the $KC_2O_4^-$ ion pair in 1.0 mmol dm^{-3} potassium oxalate solution since concentration of desorbed K^+ and $C_2O_4^{2-}$ ions may be high enough in the gas phase to form a $KC_2O_4^-$ ion pair.

At 10.0, 20.0, 40.0, 50.0 and 80.0 mmol dm^{-3} concentrations of potassium and/or sodium oxalate, the concentrations of $KC_2O_4^-$ or $NaC_2O_4^-$ ion pair is estimated to be at 0.5, 1.5, 4.5, 6.4 and 13.3 mmol dm^{-3}, respectively. Therefore, in $Na_2C_2O_4$ and $K_2C_2O_4$ solutions of 10.0 mmol dm^{-3} or higher (which contained approximately 0.5 mmol dm^{-3} concentration of ion pairs), the presence of $KC_2O_4^-$ or $NaC_2O_4^-$ ion pairs and their clusters should be seen in their FAB-MS spectra. This indeed was the case as FAB-MS spectra of all potassium and sodium oxalate solutions of concentrations 10.0 mmol dm^{-3} or greater showed significant abundances of $KC_2O_4^-$ or $NaC_2O_4^-$ ion pairs and their clusters.

The FAB-MS spectrum of 10.0 mmol dm^{-3} potassium oxalate depicted in Fig. 3 shows small peaks due to the $KC_2O_4^-$ ion pair at m/z = 127 and its cluster with $K_2C_2O_4$ at m/z = 293. The most intense peak, showing the presence of the $KC_2O_4^-$ ion pair in potassium oxalate solution was of the $KC_2O_4^-$(Gly) cluster at m/z = 219. This peak was not seen in the FAB-MS spectrum of 1.0 mmol dm^{-3} potassium oxalate solution in 10% glycerol. In fact, the peaks of ion clusters $NaC_2O_4^-$(Gly) and $KC_2O_4^-$(Gly) at m/z = 203 and 219, respectively, for $Na_2C_2O_4$ and $K_2C_2O_4$ solutions in glycerol can be taken as confirmatory peaks for $NaC_2O_4^-$ and $KC_2O_4^-$ ion pair formation as their intensities were much higher than peaks of other clusters containing sodium and potassium oxalate ion pairs. The abundances of the $NaC_2O_4^-$ $(Na_2C_2O_4)_n$, and $KC_2O_4^-$ $(K_2C_2O_4)_n$, clusters were very much dependent on the concentration of ion pairs in solution. For example, at 10.0 and 20.0 mmol dm^{-3}, the concentration of $KC_2O_4^-$ or $NaC_2O_4^-$ ion pairs was not enough to form clusters with neutral molecules of sodium and potassium

oxalate. However, as the concentrations of $NaC_2O_4^-$ and $KC_2O_4^-$ ion pairs increased in solution, the abundances of $NaC_2O_4^-$ $(Na_2C_2O_4)_n$, and $KC_2O_4^-$ $(K_2C_2O_4)_n$, ion clusters increased. This is illustrated in Figs. 4 and 5, respectively for sodium and potassium oxalate solutions. These results suggest that the abundances of $NaC_2O_4^-$ and $KC_2O_4^-$ ion pairs and their clusters are closely related to their concentrations in solution.

Fig. 6 shows the relative abundances of $GlyNa^-$, $GlyNa_2^-$, $HC_2O_4^-$, and $NaC_2O_4^-$ ion pairs as a function of sodium oxalate concentration. The increase in the relative abundances of these ion pairs with the increase in sodium oxalate concentration in sodium oxalate - 10% glycerol solutions is expected on the basis of solution equilibria (i) to (iv). This again suggest that FAB-MS results reported here are representative of solution equilibria occurring in sodium oxalate - 10% glycerol solutions. We would also like to point out that in Fig. 6 relative abundances of the $HC_2O_4^-$ ion pair are much higher than the relative abundances of $GlyNa^-$, $GlyNa_2^-$, and $NaC_2O_4^-$ ion pairs. This can be explained on the basis of the larger value of the stability constant of the $HC_2O_4^-$ ion pair estimated to be 15,000 $dm^3\ mol^{-1}$, compared with the stability constant of the $NaC_2O_4^-$ ion pair of about 10 $dm^3\ mol^{-1}$. The value of the stability constants of GlyNa- and $GlyNa_2^-$ ion pairs is not known. As expected, the relative abundances of the clusters of all these ion pairs with glycerol and sodium oxalate increased with the increase in sodium oxalate concentration.

The relative abundances of glycerol clusters with the sodium oxalate ion pair i.e., $NaC_2O_4^-(Gly)_n$, also increased with the increase in sodium oxalate concentration, especially, in dilute solutions as shown in Fig. 7. Fig. 8 shows the relative abundances of $(Gly\text{-}H)^-$ ions and its ion clusters with glycerol and $Na_2C_2O_4$. The peak of $(Gly\text{-}H)^-$ was remained the base peak in all the spectra of sodium and potassium oxalate solutions up to 80 mmol dm^{-3}, despite its strong

binding with $Na_2C_2O_4$ (or $K_2C_2O_4$) molecules to form $(Gly\text{-}H)^-Na_2C_2O_4$ cluster at m/z 225 relative abundance of which increased with the increase in $Na_2C_2O_4$ concentration. The large abundance of $(Gly\text{-}H)^-$ in the FAB-MS spectrum may be explained on the basis of equilibria (i) and (iv), reported earlier in this section. The relative abundance of the $(Gly\text{-}H)^-Gly$ cluster at m/z 183 however, decreased sharply as the concentration of sodium oxalate increased from 10 to 80 mmol dm^{-3}. Perhaps the formation of the $(Gly\text{-}H)^-Gly\text{-}Na_2C_2O_4$ cluster at m/z 317, relative abundance of which increased with the increase in the sodium oxalate concentration, caused the decrease in the abundance of $(Gly\text{-}H)^-Gly$. The relative abundances of $NaC_2O_4^-$-NaGly $(Gly)_n$, or $Na_2C_2O_4$-$(Gly\text{-}H)^-(Gly)_n$ n= 0 - 4; m/z = 225, 317, 409, 501 also increased with the increase in sodium oxalate concentration (Fig. 8).

In the FAB-MS spectrum of a very high concentration of potassium oxalate (10% glycerol saturated with potassium oxalate), $(Gly\text{-}H)^-$ was no longer the base peak. The relative abundance of all glycerol containing ion pairs and clusters was substantially lowered in this spectrum, as shown in Fig. 9. The gas phase ions of glycerol and clusters of $NaC_2O_4^-(Na_2C_2O_4)_n$ were relatively more abundant.

FAB-MS spectra of mixed solution of 40.0 mmol dm^{-3} each of sodium sulfate and potassium oxalate (Fig. 10) showed the presence of $NaSO_4^-$ and KSO_4^- ion pairs, in addition of $NaC_2O_4^-$ and $KC_2O_4^-$ ion pairs. The relative abundances of $NaSO_4^-$ and KSO_4^- ion pairs is quite similar to that of $NaC_2O_4^-$ and $KC_2O_4^-$ ion pairs, which was expected on the basis of the similar values of stability constants of these ion pairs. The peak due to $KC_2O_4^-$ ion pair was mixed with a glycerol (matrix) peak of similar mass and hence appears to be larger than KSO_4^- ion pair peak. FAB-MS investigation of mixed solutions of potassium sulfate and potassium oxalate at high resolution confirmed that the relative abundance of $KC_2O_4^-$ ion pair is quite similar to that of KSO_4^- ion pair. These results suggest that abundances of

various ion pairs and ion pair clusters determined by FAB-MS of mixed solutions of sodium sulfate and potassium oxalate are closely related to their concentrations in solution.

FAB-MS analysis of the solid potassium oxalate (without glycerol) did not show any ion pair or ion pair cluster formation. This suggested that $KC_2O_4^-$ ion pair and its clusters, determined in solutions, were not desorbed from the sputtered solid. It seems that FAB-MS results from potassium/sodium oxalates show different behavior than FAB-MS analyses of alkali halides[12,13]. In case of FAB-MS study of alkali halides, very similar cluster formation was observed from the sputtered solid and from solutions.

Although the results of low resolution FAB-MS analyses of potassium/sodium oxalate solutions and mixed solutions of sodium sulfate and potassium oxalate, reported above, are consistent with ion pair formation of $NaC_2O_4^-$ and $KC_2O_4^-$ ions, it was thought desirable to confirm the presence of some of these ion pairs by high resolution FAB-MS analysis. Analysis of a 80.0 mmol dm^{-3} solution of potassium was carried out by high resolution FAB-MS using I^- with m/z = 126.9045 as standard, confirmed the presence of $KC_2O_4^-$ ions at m/z = 126.9383 (calculated mass = 126.9434). The presence of $NaC_2O_4^-$, $HC_2O_4^-$, $NaSO_4^-$ and KSO_4^- ion pairs was also confirmed by high resolution FAB-MS.

In conclusion, the results reported in this paper have provided FAB-MS evidence for the existence of $NaC_2O_4^-$ and $KC_2O_4^-$ ions in solutions of sodium and potassium oxalate containing solutions. This contrasts with the assumption of Berland et.al. [4] who assumed sodium oxalate to be a completely dissociated electrolyte. The results are consistent with FAB-MS analysis carried by Caprioli [10], and Johnstone and Rose [11] who demonstrated that FAB-MS can reveal the existence of ionic-equilibrium of liquid solutions.

Acknowledgement

We thank NSERC for financial support in providing equipment grants for the purchase of Kratos Concept IS double-focussing mass spectrometer.

References

1 Sposito, G., *Soil Sci. Soc. Am. J.*, 1984, **48**, 531.

2 Werness, P.G., Brown, C.M., Smith, L.H., and Finlayson, B., *J. Urology*, 1985, **134**, 1242.

3 Singh, R. P., Gaur, S.S.,Sheehan, M. E., and Nanacollas, G. H., *J. Crystal Growth*, 1988, **87**, 318.

4 Berland, Y., Olmer, M., Gandvuillemin, M., Lundager Madsen, H. E., and Boistelle, R., *J. Crystal Growth*, 1988, **87**, 494.

5 Mesuere, K., and Fish, W., *Environ. Sci. Technol.*, 1992, **26**, 2357.

6 Singh, R. P., *Bull. Chem. Soc. Jpn.*, 1989, **52**, 2205.

7 Finlayson, B., and Roth, R. A., *Urology*, 1973, **1**, 142.

8 Daniele, P. G., Rigano, C., and Sammartano, S., *Thermochim. Acta*, 1981, **46**, 103.

9 Kanamori, K., Mihara M., and Kawai, K., *Bull. Chem. Soc. Jpn.*, 1979, **52**, 2205.

10 Caprioli, R. M., *Anal. Chem.*, 1983, **55**, 2387.

11 Johnstone, R. A. W., and Rose, M. E., *J. Chem. Soc., Chem. Commun.*, 1983, 1268.

12 Sunner, J., *J. Am. Soc. Mass Spectrom.*, 1993, **4**, 410.

13 Miller, J. M., and Theberge, R., *Org. Mass Spectrom.*, 1985, **20**, 600.

Figure Captions

Fig. 1 Fast-atom bombardment mass spectrum of 80 mmol dm^{-3} sodium oxalate in 10 % glycerol

Fig. 2 Fast-atom bombardment mass spectra of 50.0 mmol dm^{-3} potassium oxalate in 10 % glycerol

Fig. 3 Fast-atom bombardment mass spectra of 10.0 mmol dm^{-3} potassium oxalate in 10 % glycerol

Fig. 4 Plot of the ratios of relative abundances of $NaC_2O_4^-$ (m/z = 111) : $NaC_2O_4^-$ ($Na_2C_2O_4$) (m/z = 245) and $NaC_2O_4^-$ ($Na_2C_2O_4)_2$ (m/z = 379) : $NaC_2O_4^-$ ($Na_2C_2O_4$) against the concentration of sodium oxalate in solution

Fig. 5 Plot of the ratios of relative abundances of $KC_2O_4^-$ (m/z = 127) : $KC_2O_4^-$ ($K_2C_2O_4$) (m/z = 293) and $KC_2O_4^-$ ($K_2C_2O_4)_2$ (m/z = 459) : $KC_2O_4^-$ ($K_2C_2O_4$) against the concentration of potassium oxalate in solution

Fig. 6 Relative abundances of $HC_2O_4^-$ (m/z = 89), $GlyNa^-$ (m/z = 113), $NaC_2O_4^-$ (m/z = 111), and $GlyNa_2^-$ (m/z = 135) ion pairs as a function of sodium oxalate concentration

Fig. 7 Relative abundances of glycerol clusters with the sodium oxalate ion pair i.e., $NaC_2O_4^-(Gly)_n$, (n = 1 - 4; m/z = 89, 295, 387, and 479) as a function of sodium oxalate concentration

Fig. 8 Relative abundances of $(Gly\text{-}H)^-$ ions and its ion clusters with glycerol and $Na_2C_2O_4$ i.e., $(Gly\text{-}H)^-(Gly)_n$ (n = 0 - 2; m/z = 91, 183, 275), and $NaC_2O_4^-$-$NaGly(Gly)_n$, or $Na_2C_2O_4$-$(Gly\text{-}H)^-(Gly)_n$ n= 0 - 4; m/z = 225, 317, 409, 501 as a function of sodium oxalate concentration

Fig. 9 Fast-atom bombardment mass spectra of 10 % glycerol saturated in potassium oxalate

Fig 10 Fast-atom bombardment mass spectra of a mixture of 40.0 mmol dm^{-3} each of potassium oxalate and sodium sulfate in 10 % glycerol

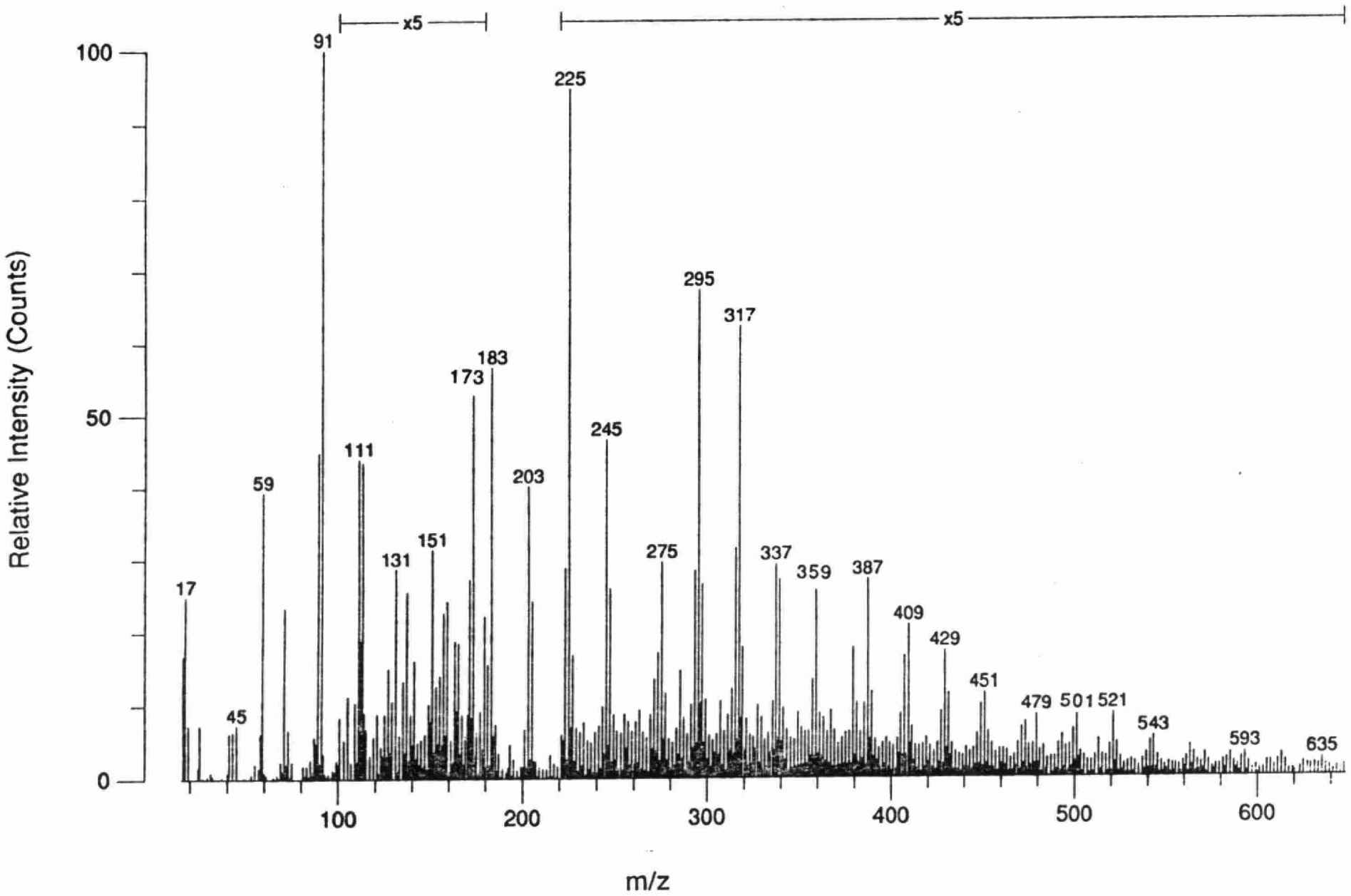
x5
x5
100
50
0
Relative Intensity (Counts)
91
225
295
317
183
173
111
245
203
59
151
131
275
337
359
387
409
429
451
479
501
521
543
593
635
17
45
100
200
300
400
500
600
m/z

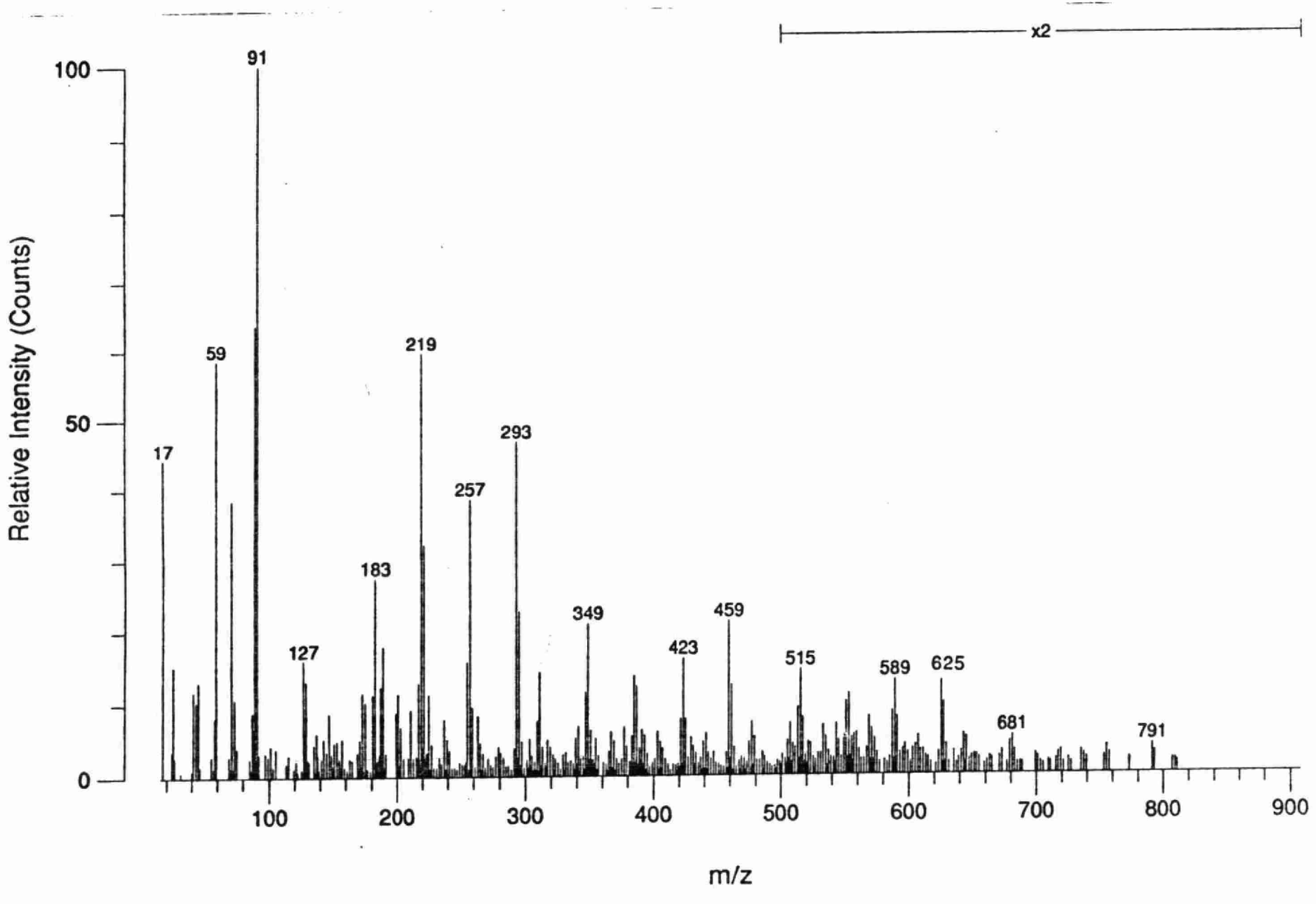
x2
100
50
0
Relative Intensity (Counts)
91
59
219
17
293
257
183
349
459
423
127
515
589
625
681
791
100
200
300
400
500
600
700
800
900
m/z

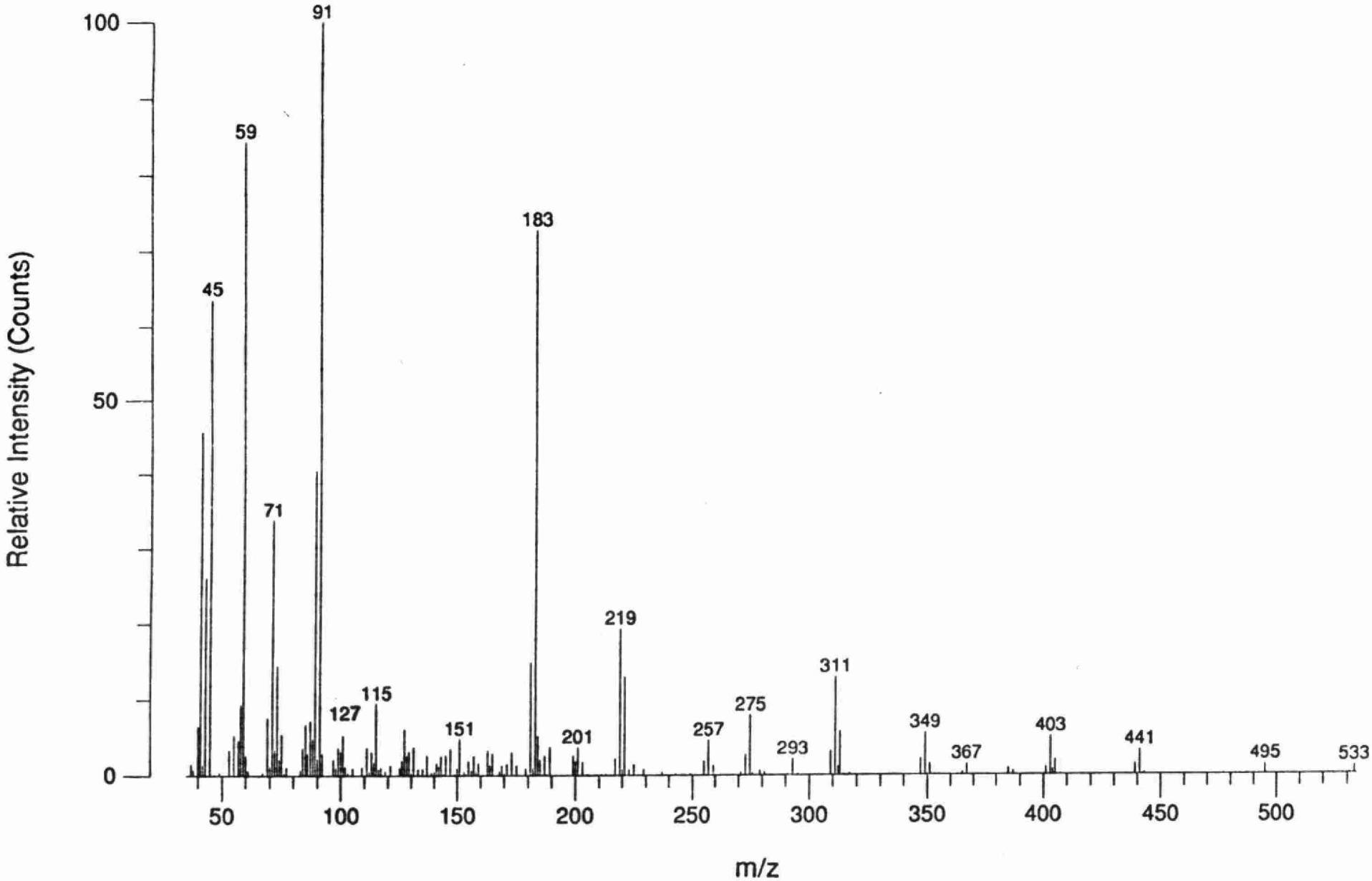
Relative Intensity (Counts)
100
50
0
91
59
183
45
71
219
311
115
127
275
151
257
293
349
403
201
367
441
495
533
50
100
150
200
250
300
350
400
450
500
m/z

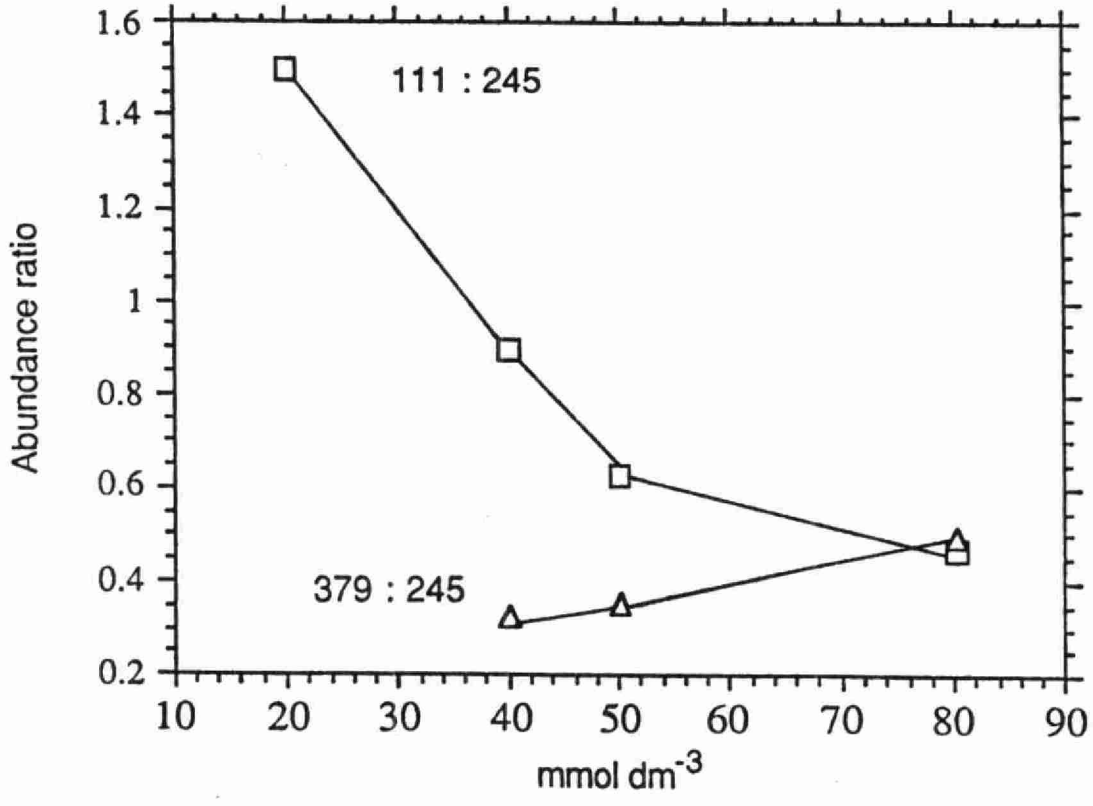
1.6
1.4
1.2
1
0.8
0.6
0.4
0.2
Abundance ratio
111 : 245
379 : 245
10
20
30
40
50
60
70
80
90
mmol dm-3

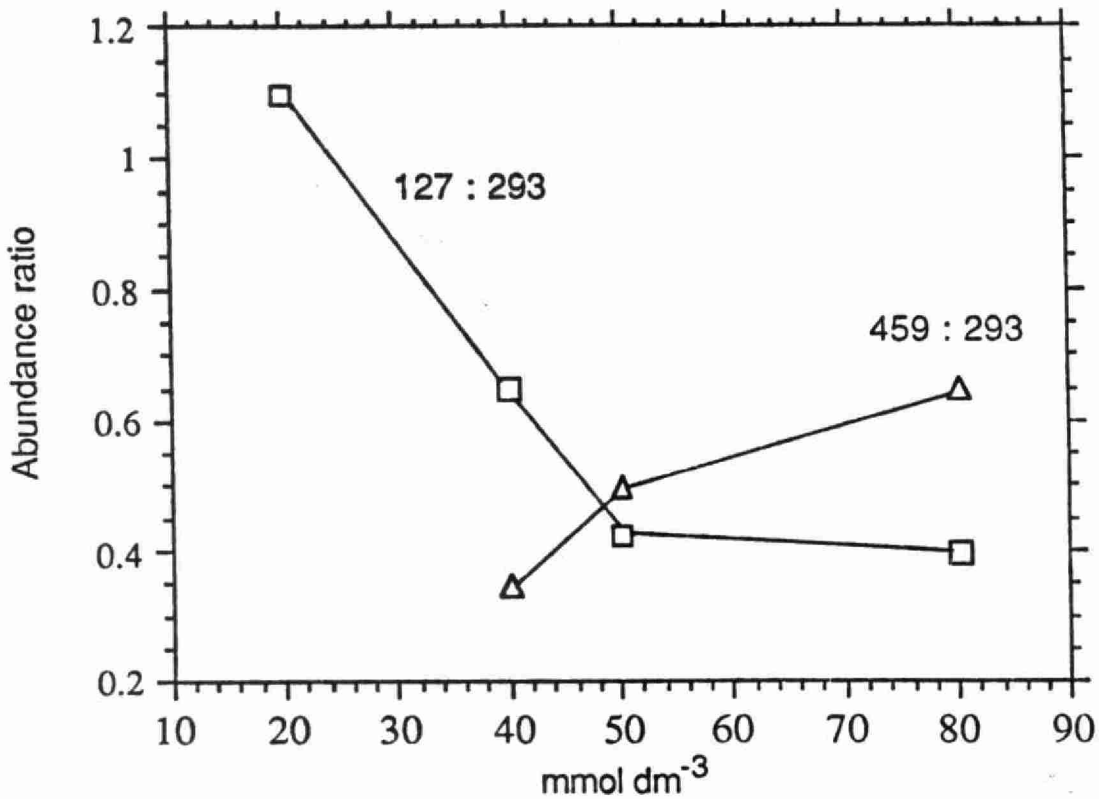
1.2
1
0.8
0.6
0.4
0.2
Abundance ratio
127 : 293
459 : 293
10
20
30
40
50
60
70
80
90
mmol dm-3

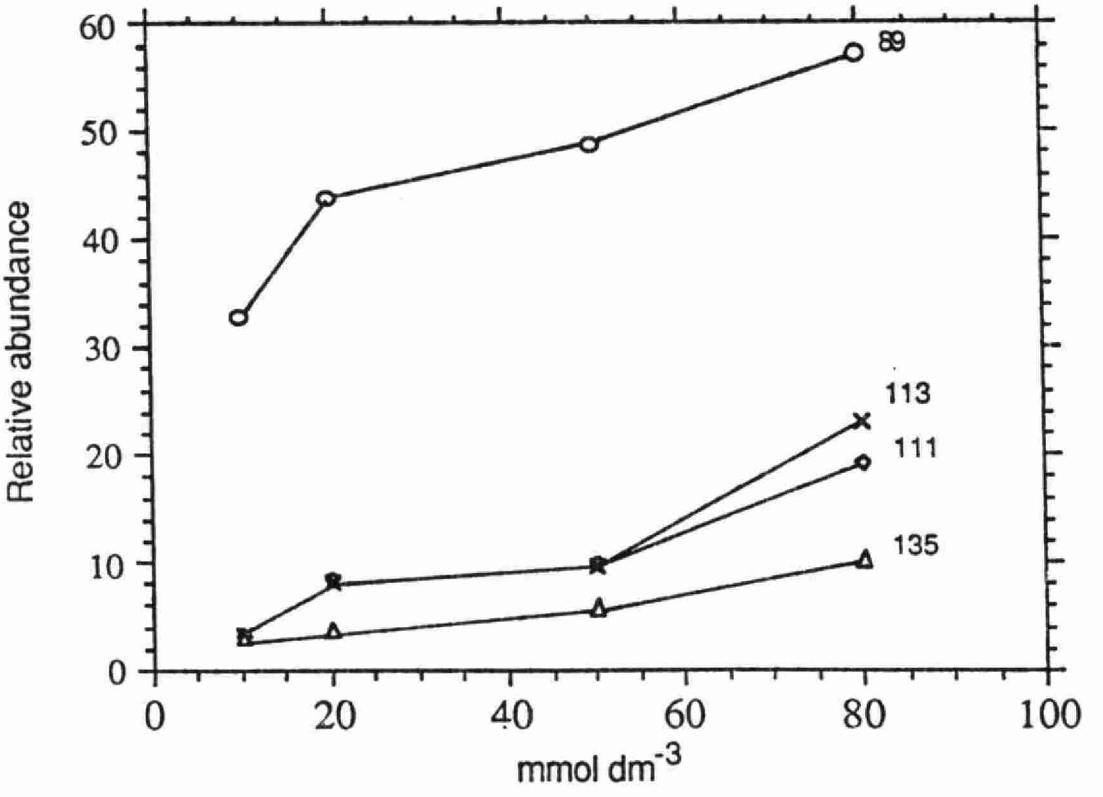
Relative abundance
60
50
40
30
20
10
0
0
20
40
60
80
100
mmol dm-3
89
113
111
135

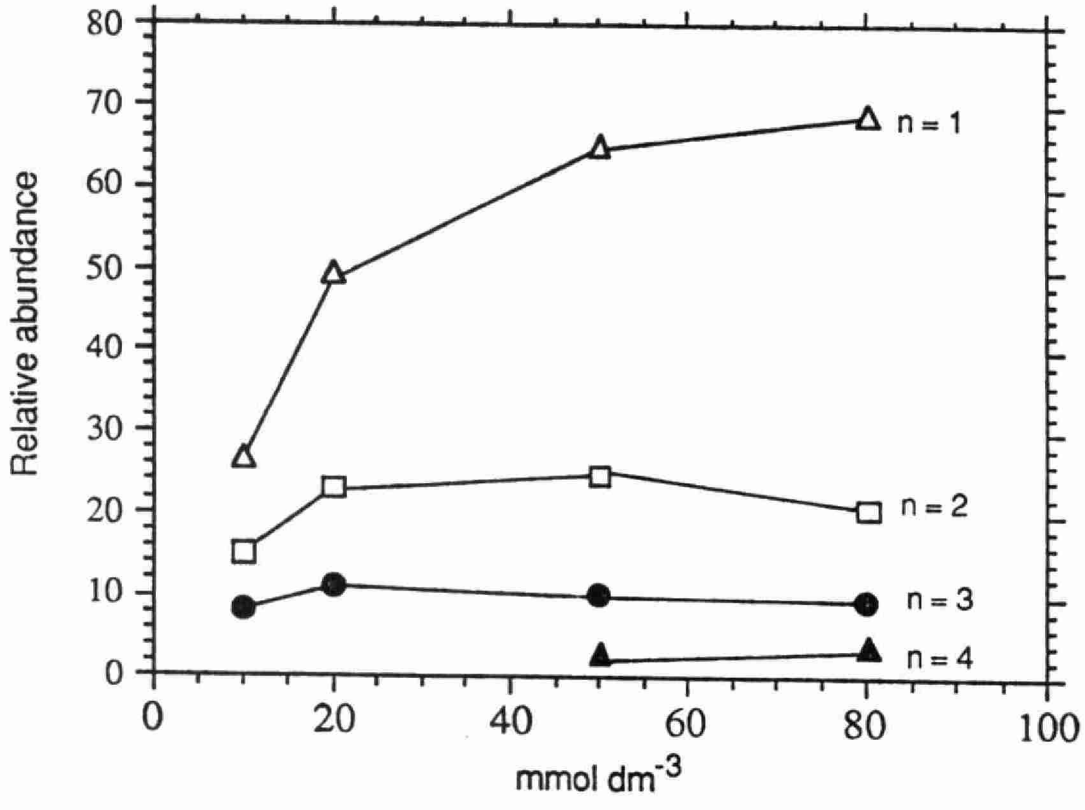
Relative abundance
80
70
60
50
40
30
20
10
0
0
20
40
60
80
100
mmol dm-3
n = 1
n = 2
n = 3
n = 4

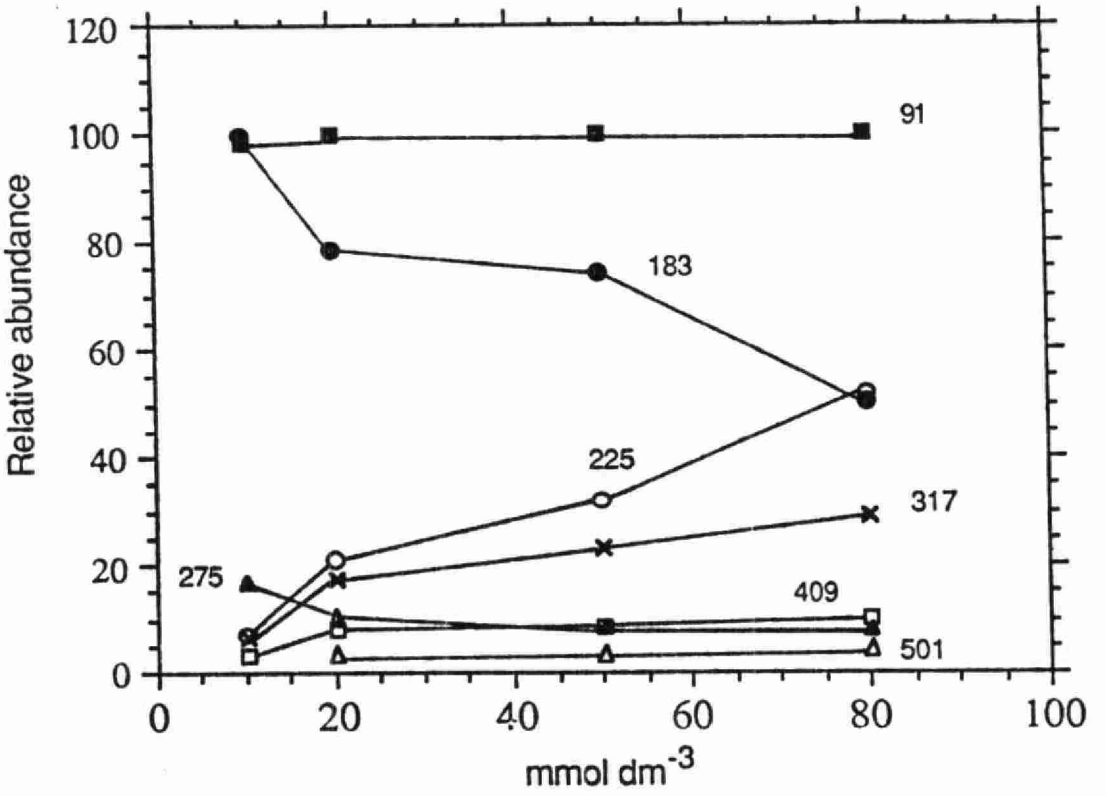
Relative abundance
120
100
80
60
40
20
0
0
20
40
60
80
100
mmol dm-3
91
183
225
317
275
409
501

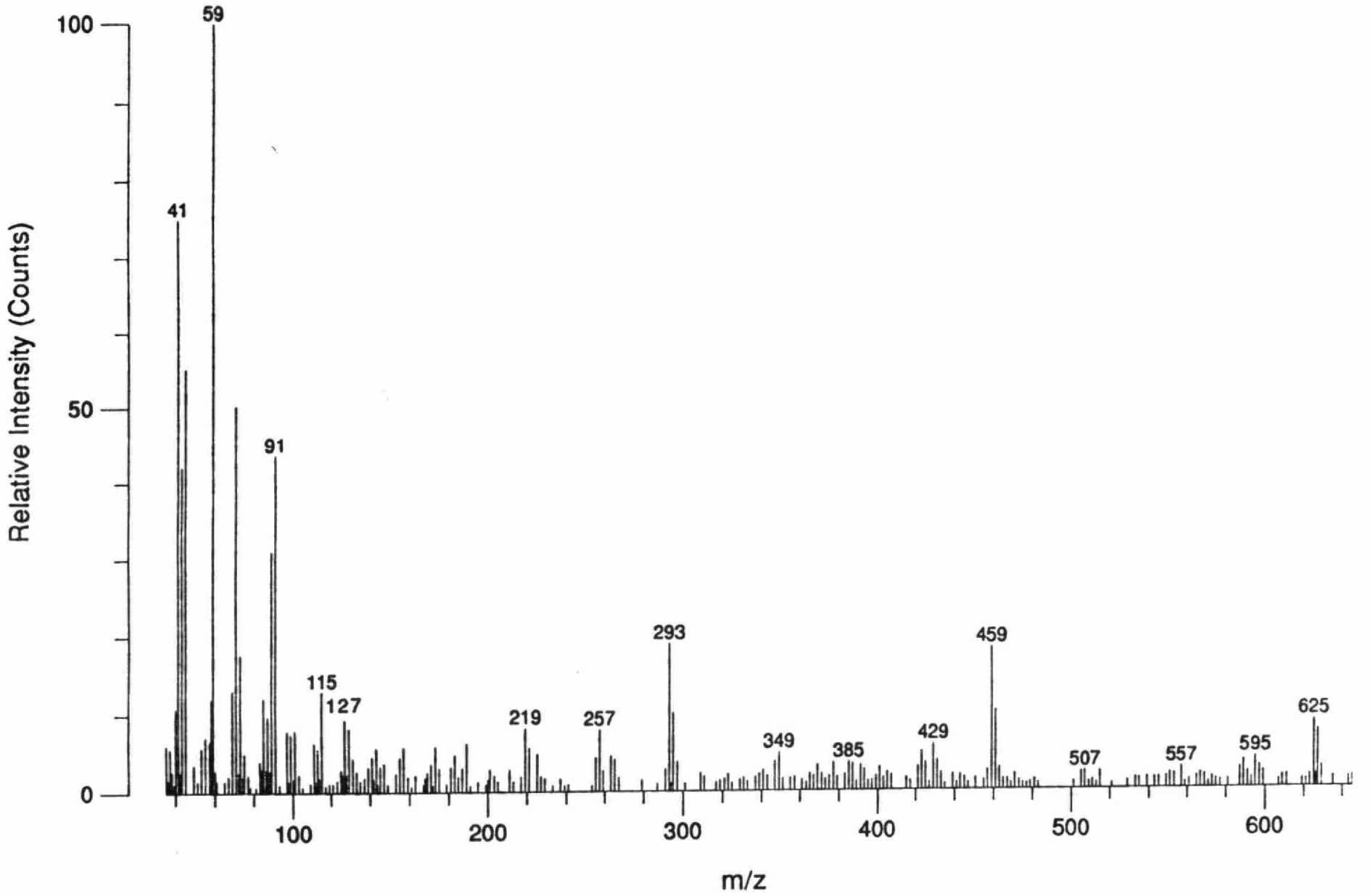
Relative Intensity (Counts)
100
50
0
59
41
91
115
127
219
257
293
349
385
429
459
507
557
595
625
100
200
300
400
500
600
m/z

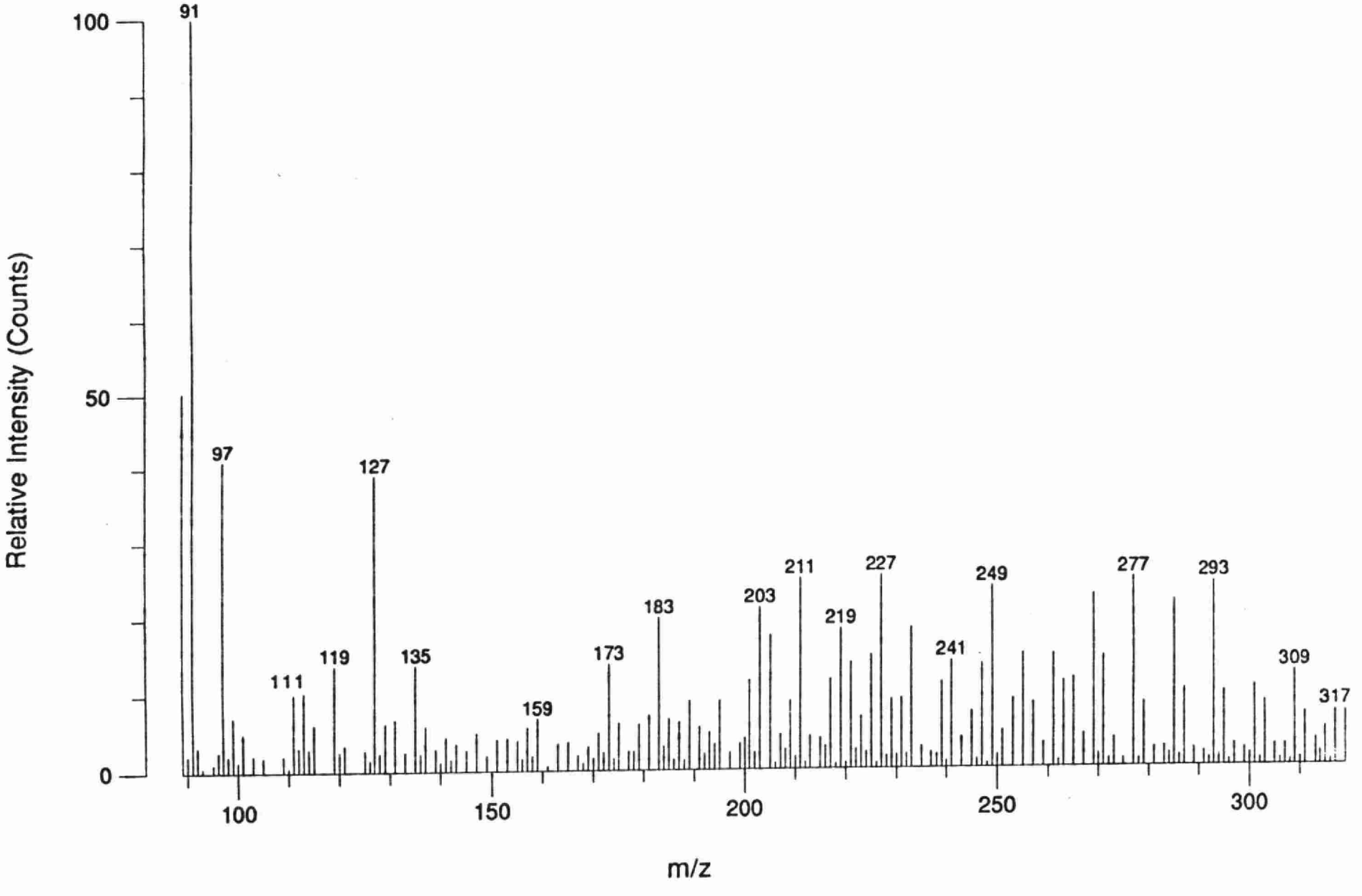
Relative Intensity (Counts)
100
50
0
91
97
127
111
119
135
159
173
183
203
211
219
227
241
249
277
293
309
317
100
150
200
250
300
m/z